Titre: Title:	Comportement dynamique non linéaire des coques cylindriques anisotropiques non uniformes soumises à un écoulement supersonique
Auteur: Author:	Redouane Ramzi
Date:	2012
Type:	Mémoire ou thèse / Dissertation or Thesis
Référence: Citation:	Ramzi, R. (2012). Comportement dynamique non linéaire des coques cylindriques anisotropiques non uniformes soumises à un écoulement supersonique [Thèse de doctorat, École Polytechnique de Montréal]. PolyPublie. https://publications.polymtl.ca/1025/

UNIVERSITÉ DE MONTRÉAL

COMPORTEMENT DYNAMIQUE NON LINÉAIRE DES COQUES CYLINDRIQUES ANISOTROPIQUES NON UNIFORMES SOUMISES À UN ÉCOULEMENT SUPERSONIQUE

REDOUANE RAMZI

DÉPARTEMENT DE GÉNIE MÉCANIQUE

ÉCOLE POLYTECHNIQUE DE MONTRÉAL

THÈSE PRÉSENTÉE EN VUE DE L'OBTENTION

DU DIPLÔME DE PHILOSOPHIAE DOCTOR

(GÉNIE MÉCANIQUE)

DÉCEMBRE 2012

UNIVERSITÉ DE MONTRÉAL

ÉCOLE POLYTECHNIQUE DE MONTRÉAL

Cette thèse intitulée :

COMPORTEMENT DYNAMIQUE NON LINÉAIRE DES COQUES CYLINDRIQUES ANISOTROPIQUES NON UNIFORMES SOUMISES À UN ÉCOULEMENT SUPERSONIQUE

présentée par : RAMZI Redouane

en vue de l'obtention du diplôme de : Philosophiae Doctor

a été dûment acceptée par le jury d'examen constitué de :

M. BALAZINSKI Marek, Ph.D., président

M. LAKIS Aouni A., Ph.D., membre et directeur de recherche

M. KAHAWITA René, Ph.D., membre

M. NEJAD ENSAN Manouchehr, Ph.D., P.Eng., membre

DÉDICACE

À mes très chers parents

À mes frères et sœurs

REMERCIEMENTS

Je voudrais exprimer mes profondes gratitudes et appréciations à mon directeur de recherche,

Dr. Aouni Lakis, de sa précieuse orientation, de ses encouragements, et conseils sur les attitudes de recherche tout au long de mes études supérieures, et aussi pour l'occasion qu'il m'a donnée pour la préparation de mon diplôme de doctorat au sein de l'École Polytechnique.

Je présente mes remerciements spéciaux aux membres du comité du jury de ma thèse,

Dr. Marek Balazinski,

Dr. Aouni A. Lakis,

Dr. René Kahawita,

Dr. Manouchehr Nejad Ensan,

Dr. Gérald J. Zagury,

pour le temps consacré à l'évaluation de mon travail de recherche et aussi à ses suggestions.

Je tiens à exprimer ma gratitude à nombreux membres de ma famille qui ont continué à me soutenir et m'encourager. Je ne serai jamais en mesure de rembourser vos actes innombrables de gentillesse et d'amour, ni de vos sacrifices personnels. Je suis particulièrement reconnaissant à mon père et ma mère qui ont consacré plus de temps pour moi que toute autre personne.

RÉSUMÉ

L'analyse des coques minces soumises à un écoulement d'air supersonique a été le sujet de plusieurs recherches. La plupart de ces études traite de l'analyse linéaire des coques cylindriques ouvertes avec ou sans écoulement supersonique. Peu de travaux ont été faits pour l'analyse non linéaire (géométrique et/ou du fluide) des coques cylindriques fermées soumises à l'écoulement supersonique.

On propose dans cette thèse le développement d'un modèle qui est capable d'analyser linéairement et non linéairement des coques minces, élastiques, anisotropes, fermées et soumises à des pressions internes et d'écoulement d'air supersonique externe. La dynamique non linéaire et l'instabilité de flottement des coques cylindriques circulaires fermées sont aussi analysées. La méthode développée est une combinaison de la méthode des éléments finis, de la théorie des coques minces et de la théorie aérodynamique du fluide. Les coques fermées, sujet de l'étude, sont principalement simplement supportées et les autres conditions frontières arbitraires sont aussi traitées.

La première partie de ce travail traite l'analyse non linéaire structurale (grande amplitude de vibration) des coques cylindriques vides et fermées. La coque est divisée en plusieurs éléments finis de type coque cylindrique fermée et les fonctions de déplacements linéaires sont dérivées de la théorie de coque cylindrique mince de Sanders. Les coefficients modaux sont dérivés de la théorie non linéaire de Sandres-Koiter pour les coques cylindriques minces en termes des fonctions de déplacements linéaires développées. Les matrices de rigidité non linéaires du second et troisième ordre sont déterminées à partir de la méthode des éléments finis. Les équations non linéaires sont résolues par la méthode numérique de Runge-Kutta d'ordre quatre. Les fréquences linéaires et non linéaires sont alors déterminées en fonction de l'amplitude du mouvement de la coque pour plusieurs cas. Les résultats obtenus sont en bonne concordance avec ceux des autres auteurs.

Dans la seconde partie de cette thèse, on présente un modèle pour l'analyse de flottement des coques cylindriques, soumises à un écoulement supersonique externe. L'équation linéaire de la théorie aérodynamique de Piston nous a permet d'exprimer directement la pression exercée par le fluide comme une fonction des déplacements en tout point de la structure. L'intégration

analytique de la pression nous donne des matrices exprimant l'interaction fluide-structure dans l'écoulement supersonique. Plusieurs figures présentées dans cette partie illustrent la théorie et le comportement dynamique des coques cylindriques, soumises à un fluide en écoulement supersonique. Une bonne concordance des résultats a été obtenue avec d'autres théories et expériences.

La troisième partie de cette recherche présente un modèle pour prédire l'influence des non-linéarités associées aux grandes amplitudes de vibration de parois de la coque et à l'écoulement supersonique du fluide des coques cylindriques minces, soumises à des pressions internes et de la compression axiale. Avec les matrices de masse et de rigidité linéaires et non linéaires de la coque vide ainsi qu'avec les matrices de rigidité et d'amortissements linéaires et non linéaires du fluide en écoulement supersonique, nous développons dans cette partie des matrices linéaires et non linéaires pour l'écoulement supersonique d'air. En dérivant une expression non linéaire pour la pression aérodynamique en fonction des déplacements nodaux ainsi que de la combinaison des effets non linéaires de l'écoulement supersonique du fluide et la grande amplitude de vibration de la structure, l'équation non linéaire obtenue est résolue par la méthode numérique de Runge-Kutta d'ordre quatre. Les fréquences linéaires et non linéaires sont alors déterminées en fonction de l'amplitude de vibration de la coque et l'épaisseur des parois des coques pour plusieurs cas.

Cette méthode combine les avantages de la méthode des éléments finis qui traite des coques complexes et la précision de la formulation basée sur des fonctions de déplacements dérivées de la théorie des coques et aussi la théorie aérodynamique de Piston qui donne l'expression de la pression aérodynamique à chaque point de la structure étudiée. On a donc ici un modèle puissant pour prédire les caractéristiques de flottement linéaires et non linéaires des coques cylindriques soumises à l'écoulement supersonique du fluide.

ABSTRACT

Analysis of thin shells subjected to supersonic airflow has been the subject of several researches. Most of these studies treat the linear analysis of open cylindrical shells (curved plates) with or without supersonic flow. Few works have been done for nonlinear analysis (geometric and/or fluid) of closed cylindrical shells subjected to supersonic flow. We propose here in this thesis to develop a model that is able to linear and nonlinear analysis of thin elastic anisotropic closed shells, and subjected to internal pressure and external supersonic airflow. Nonlinear dynamics and flutter instability of closed circular cylindrical shells are also analyzed. The model developed is a combination of finite element method, thin shell theory and aerodynamic fluid theory. Closed shells are mainly simply supported; other arbitrary boundary conditions are also treated. The first part of this work studies the nonlinear structural analysis (large amplitude of vibration) of empty closed cylindrical shells. The shell is divided into several closed cylindrical finite element and the functions of motion are derived from linear theory of thin cylindrical shells of Sanders. The modal coefficients are derived from the nonlinear theory of Sandres-Koiter for thin cylindrical shells in terms of linear displacement functions developed. The nonlinear stiffness matrices of second and third order are determined from the finite element method. The nonlinear equations are solved by fourth order Runge-Kutta numerical method. The linear and nonlinear frequencies are then determined as a function of the movement amplitude of the shell for several cases. The results obtained are in good agreement with those of other authors. In the second part of this thesis, we present a model for the flutter analysis of cylindrical shells, subjected to an external supersonic flow. The linear equation of aerodynamics Piston theory allows us to express directly the pressure exerted by the fluid as a function of the displacements at any point of the structure. The analytical integration of the pressure gives us matrices expressing the fluid-structure interaction in supersonic flow. Several figures presented in this section illustrate the theory and the dynamic behavior of cylindrical shells subjected to supersonic fluid flow. A good agreement was obtained with other theories and experiments .The third part of this research presents a model to predict the influence of nonlinearities associated with large amplitude of vibration of the shell walls and the supersonic fluid flow of thin cylindrical shells taking into account the internal pressure and axial compression. With linear and nonlinear mass and stiffness matrices of the empty shell as well as the linear and nonlinear stiffness and damping fluid matrices, we develop

consequently the linear and nonlinear matrices for supersonic airflow. By deriving an expression for the non-linear depending on the aerodynamic pressure nodal displacements, as well as the combination of non-linear effects of the supersonic flow of the fluid and the large amplitude of vibration of the structure, the non-linear equation obtained is resolved by the fourth order Runge-Kutta numerical method. The linear and nonlinear frequencies are then determined as a function of the amplitude of vibration of and the thickness of the shells for several cases. This method combines the advantages of the finite element method treating a complex shells and accuracy of the formulation based on displacement functions derived from shell theory and also aerodynamic Piston theory which gives an expression of aerodynamic pressure at each point of the structure studied. So here we have a powerful model to predict the linear and nonlinear characteristics during flutter phenomena of cylindrical shells subjected to supersonic fluid flow.

TABLE DES MATIÈRES

DÉDICACE III

REMERCIEMENTS IV

RÉSUMÉ V

ABSTRACT VII

TABLE DES MATIÈRES IX

LISTE DES TABLEAUX XIII

LISTE DES FIGURES XIV

LISTE DES SIGLES ET ABRÉVIATIONS XVI

INTRODUCTION 1

CHAPITRE 1: REVUE DE LITTÉRATURE 3

1.1 Revue de littérature 3

1.2 Plan de la thèse 7

CHAPITRE 2: ARTICLE 1- EFFECT OF GEOMETRIC NON-LINEARITIES ON NON-LINEAR VIBRATIONS OF CLOSED CYLINDRICAL SHELLS 9

2.1 Abstract 9

2.2 Introduction 9

2.3 Linear Part 11

2.4 Non-linear Part 15

2.5 Numerical resolution 19

2.6 Discussion of Results 21

2.7 Conclusion 26

2.8 Appendix 27

2.9 References 29

CHAPITRE 3: ARTICLE 2- EFFECTS OF GEOMETRIC NONLINEAIRITIES ON CYLINDRICAL SHELLS SUBJECTED TO A SUPERSONIC FLOW 31

3.1 Abstract 31

3.2 Nomenclature 31

3.3 Introduction 33

3.4 Structural Model 36

3.4.1 Linear Part 36

3.4.2 Nonlinear Part 39

3.5 Stress Matrix 43

3.6 Aerodynamic Model 44

3.7 Nonlinear Analysis 46

3.8 Calculation and Discussion 48

3.8.1 Convergence of the Method 48

3.8.2 Onset of Flutter Predictions for Cylindrical Sheels in Supersonic Flow 49

3.8.3 Behavior of nonlinearity flutter for a pressurized cylindrical shell 50

3.8.4 Effect of Freestream Static Pressure in Post-Flutter 51

3.8.5 Effect of internal stresses in the flutter stage of cylindrical shells subjected to supersonic flow 52

3.8.6 Effect of length-radius ratios of cylindrical shells on the supersonic flutter 53

3.8.7 Effect of Shell Boundary Conditions 54

3.8.8 Effect of supersonic flow on the nonlinear behavior of cylindrical shells 56

3.8.9 Effect of circumferential wave number 56

3.9 Conclusion 57

3.10 Appendix 59

3.11 References 62

CHAPITRE 4 : ARTICLE 3 - EFFECT OF GEOMETRIC AND FLUID FLOW NONLINEARITIES ON CYLINDRICAL SHELLS SUBJECTED TO A SUPERSONIC FLOW

4.1 Abstract 64

4.2 Nomenclature 64

4.3 Introduction 67

4.4 Structural model development 69

4.4.1 Masse and stiffness matrices for linear structural model 69

4.4.2 Stiffness matrices for nonlinear structural model 72

4.5 Initial stress matrix 77

4.6 Aerodynamic model development 78

4.7 Nonlinear numerical analysis 80

4.8 Calculation and discussion 83

4.8.1 Convergence of the method for differents modes 83

4.8.2 Onset of flutter predictions for cylindrical shells subjected to a supersonic flow 84

4.8.3 Validation of model 85

4.8.4 Effect of circumferential wave mode 86

4.8.5 Effect of internal pressure 87

4.8.6 Effect of supersonic flow regimes in flutter of circular cylindrical shells 88

4.8.7 Nonlinear flutter behavior for different longitudinal modes 89

4.9 Conclusion 90

4.10 Appendix 92

4.11 References 96

CHAPITRE 5: DISCUSSION GÉNERALE..... 98

CONCLUSIONS ET RECOMMANDATIONS..... 99

BIBLIOGRAPHIE ..... ….101

LISTE DES TABLEAUX

Tableau 1.1: Catégories d'analyse de flottement des coques 3

Tableau 3.1: Critical freestream static pressure for different shells boundary conditions, p_x=0.0 psi.....55

LISTE DES FIGURES

Figure 2.1: Cylindrical finite element geometry 11

Figure 2.2: Finite element discretization and nodal displacement 13

Figure 2.3: Influence of large amplitude on nonlinear frequency 21

Figure 2.4: Influence of large amplitude on nonlinear frequency ratio for n=10 and m=1 22

Figure 2.5: Influence of longitudinal modes on nonlinear vibration at large amplitude 23

Figure 2.6: Influence of various boundary conditions on nonlinear behavior of cylindrical shells 24

Figure 2.7: A comparison with the results of Evensen and Ganapathi (ξ = 0.5, ε = 0.01 and 1.0); -.-.- , Present study; ——— , Evensen [8]; - - - - , Ganapathi [15]. 24

Figure 2.8: A comparison with the results of Evensen (ξ = 2.0, ε = 0.01 and 1.0) ——— ; Present analysis; - - - - , Evensen [8] 25

Figure 2.9: The amplitude-frequency relation. - - - - -, Present analysis ——; Ganapathi [15] 26

Figure 3.1: Cylindrical shell and finite element geometries 35

Figure 3.2: Finite element discretization and nodal displacement 37

Figure 3.3: Natural frequency vs Number of elements 49

Figure 3.4: a) Real part and b) imaginary part of eigenvalues of the system vs freestream static pressure p_∞, n = 23, pm = 0.5 psi, p_x = 0.0 psi. 50

Figure 3.5: Flutter frequency vs mean amplitude of first mode 51

Figure 3.6: Amplitude of flutter vs frequency flutter for different regions of flutter 52

Figure 3.7: Effect of internal pressure during flutter 53

Figure 3.8: Flutter amplitude vs frequency flutter for different L/R 54

Figure 3.9: Flutter amplitude vs flutter frequency for different shell boundary conditions 55

Figure 3.10: Effect of supersonic flow in nonlinear behavior of cylindrical shells M = 3, p_∞ = 0.5 psi, p_m = 0.0 psi, n = 23 56

Figure 3.11: Flutter amplitude versus frequency flutter of cylindrical shells at different circumferential wave numbers 57

Figure 4.1: Finite element discretization and nodal displacement 70

Figure 4.2: Naturel frequency vs Number of elements 84

Figure 4.3: a) Real part and b) Imaginary part of eigenvalues of the system vs freestream static pressure p_∞, n = 23, p_m = 0.5 psi, p_x = 0.0 psi. 85

Figure 4.4: Flutter frequency vs amplitude, p_{ec} = 0.66 psi. 86

Figure 4.5: Amplitude flutter vs frequency flutter at n = 23 and n = 24 87

Figure 4.6: Effect of internal stress during the flutter, n = 25, p_{ec} =0.75 psi 88

Figure 4.7: Flutter amplitude vs frequency flutter for different L/R 89

Figure 4.8: Flutter amplitude vs flutter frequency for different longitudinal modes 90

LISTE DES SIGLES ET ABRÉVIATIONS

HOT	Highly optimized tolerance
NASP	National Aerospace Plante
HSCT	High-Speed Civil Transport
RLV	Reusable Launch Vehicle
JSF	Joint Strike Fighter
QSP	Quiet Supersonic Plateform
DARPA	Defense Advanced Research Projects Agency
LCO	Oscillation de cycle limite
MEF	Méthode d'élément finis
2-D	Bidimensionnel
3-D	Tridimensionnel
DOF	Degré de liberté
QUAD	Quadrique

INTRODUCTION

La première observation de flottement peut être retracée au milieu des années 1940 où les roquettes allemandes V-2 ont rencontré des problèmes de flottement qui ont abouti à secouer les parois en métal lorsque les roquettes ont volé à une vitesse supersonique. Les défaillances structurelles dues au flottement ont été largement prises en compte dans les avions, les navettes spatiales, les missiles, les roquettes et les ponts à cause de la vitesse élevée d'écoulement d'air.

Le phénomène de flottement d'une coque est généralement auto-excité par des oscillations auto-entretenues de la partie externe d'un véhicule volant lorsqu'il est exposé à un écoulement d'air le long de sa surface. L'origine de ce genre d'instabilité structurelle est l'interaction entre l'écoulement de fluide et le solide. L'effet de la pression aérodynamique appliquée sur la structure conduit à la coalescence de la fréquence entre certains modes de vibration de la coque qui représentent un symbole spécifique de flottement, ce qui résulte que la résonance de ces modes en coalescence amplifie l'amplitude de vibration de la coque.

L'étude de flottement de la coque tombe dans le domaine de l'aéroélasticité (Bisplinghoff et al.) dans le sens qu'elle est un résultat des interactions entre les forces d'inerties, aérodynamiques et élastiques. En plus du flottement de la coque, il existe un autre comportement en flottement appelé le flottement d'aile, qui s'adresse au battement des ailes en raison de la pression aérodynamique sur les deux côtés de la structure. Le flottement de la coque se produit dans des structures comme les panneaux de la structure d'aéronefs et des panneaux spatiaux minces qui subissent de la pression d'air en écoulement. Les théories fondamentales et la compréhension physique de flottement des coques peuvent être trouvées dans de nombreux livres tels que Dowell, Librescu et quelques articles scientifiques dans la littérature.

La prévention ou la prédiction du flottement a longtemps été reconnue comme un critère essentiel dans la conception des véhicules de vol à haute vitesse, comme High-Speed Civil Transport (HSCT), National Aerospace Plante (NASP), X-33 Advanced Technology Demonstrator, Reusable Launch Vehicle (RLV), Joint Strike Fighter (JSF), X-38 Spacecraft, le program Hyper-X de X-43 et récemment le programme Quiet Supersonic Plateform (QSP) parrainé par la DARPA. Les recherches approfondies sur des analyses et des expériences de flottement ont fourni des séries d'outils pour les concepteurs. Aujourd'hui, grâce aux progrès impressionnants du matériel informatique et des logiciels, les concepteurs se dirigent de plus en plus vers les outils

analytiques-numériques et, par conséquent, la forte demande des méthodes de calcul numérique plus puissant, précis et efficace pour l'analyse de flottement a lancé des activités de recherche résurgentes.

Devant le passage de transsonique à supersonique et de supersonique à hypersonique, l'amélioration de la vitesse de vol devient un but ultime pour la conception des structures aérospatiales. On note aussi que pour l'analyse de flottement de la coque d'un véhicule volant à une vitesse hypersonique, la plupart des expériences et expertises accumulées par des générations d'aéroélasticiens sur les analyses de flottement supersonique des coques cylindriques comme l'étude approfondie présentée dans cette thèse peuvent être exploitées. Les facteurs majeurs tels que les choix de la théorie de l'aérodynamique, linéaire/non linéaire du modèle structural dynamique, l'approche analytique/numérique à appliquer, les considérations des effets de paramètres du système et l'analyse des vibrations aéroélastiques hypersoniques restent les mêmes que pour l'analyse de flottement supersonique. L'analyse linéaire du comportement dynamique des coques cylindriques vides ou soumises à l'écoulement supersonique reste limité et ne correspond pas aux résultats expérimentaux ce qui nous oriente vers l'étude non linéaire afin d'expliquer et de prédire des phénomènes aéroélastiques.

Le but de cette présente étude est de développer un logiciel basé sur une formulation modale d'éléments finis, capable de faire l'analyse linéaire et non linéaire du comportement de flottement des coques minces sous un écoulement d'air supersonique. Une telle formulation modale est destinée à être un outil de conception pratique pour les coques cylindriques de véhicules supersoniques afin d'obtenir le coût (temps de calcul) réduit efficace sans perdre de précision et assez simple pour l'application sans recours à des manipulations mathématiques sophistiquées et aussi de prendre en compte autant que possible les considérations de la conception réelle, par exemple l'application de pression interne et de chargement axial qui a été incorporée dans l'algorithme. Il est également prévu que ce logiciel aidera à l'analyse de fatigue et de la conception du contrôleur de la suppression de flottement durant le développement de véhicules supersoniques. La revue de littérature qui suit sert un bref résumé de la recherche pertinente et expose également la nécessité du travail effectué dans le reste de cette thèse de recherche.

CHAPITRE 1 : REVUE DE LITTÉRATURE ET PLAN DE LA THÈSE

1.1 Revue de littérature

Les études théoriques et expérimentales de flottement des coques ont commencé en 1950. Les recherches et les résultats menés dans ce stade précoce ont été résumés par Fung (1960) and Johns (1965). Après, les auteurs ont groupé une littérature théorique sur le flottement des coques dans des catégories basiques en se basant sur les théories structurales et aérodynamiques utilisées dans l'article de Dowell (1970), comme montré dans le Tableau 1.1. Le tableau est pris à partir de l'article récent de Mei et al (1999). Les types d'analyse cités dans le tableau sont aussi attribués par Gray et Mei (1993), en considérant la théorie d'analyse de flottement de la coque proposée par McIntosh et al (1977). Une étude bibliographique sur le sujet spécifique d'analyse de flottement de la coque a été donnée par Reed (1997) avec le support du programme NASP. Il y a aussi des articles de revue concernant certains types d'analyse de flottement listés dans le tableau 1.1, les articles de revue concernant l'application de la méthode des éléments finis pour l'analyse de flottement du panneau par Bismarck-Nasr (1999) et la revue de méthodes analytiques variées incluant l'approche d'éléments finis pour les analyses non linéaires de flottement supersonique du panneau donnée par Zhou (1999).

Tableau 1.1 : Catégories d'analyse de flottement des coques

Théorie structurale	Théorie aérodynamique	Nombre de mach
Linéaire	Piston linéaire	$\sqrt{2}<M<5$
Linéaire	Écoulement potentiel linéarisé	$1<M<5$
Non linéaire	Piston linéaire	$\sqrt{2}<M<5$
Non linéaire	Écoulement potentiel linéarisé	$1<M<5$
Non linéaire	Piston non linéaire	$M>5$
Non linéaire	Équation d'Euler ou Navier –Stokes	Transsonique, Supersonique and Hypersonique

à cause de la simplicité mathématique de la théorie structurale linéaire, la majorité des analyses de flottement préliminaire appartient à l'analyse linéaire de flottement de la coque. Parmi ces travaux, on trouve : Hedgepeth (1963), Dugundji (1966) and Cunningham (1989). Comme indiqué clairement dans l'article de Dowell (1967), l'analyse de flottement du panneau utilisant la théorie linéaire est incapable de prendre en compte les non-linéarités structurales. La théorie structurale linéaire indique qu'il existe une pression dynamique critique à partir de laquelle le mouvement de la coque devient instable et se développe exponentiellement avec le temps. En réalité, quand l'amplitude de vibration de la coque devient grande, le panneau s'étend aussi. Cette tension dans le plan introduit des forces significatives de traction de membrane (Woinowsky-Krieger (1959)) de sorte que la flexion de la coque est retenue dans une plage limitée, qui est appelée oscillation de cycle limité (LCO). L'analyse linéaire de flottement de coques est utilisée seulement pour prédire les limites de flottement. D'autres chercheurs comme Eisley (1956), Houboult (1958), Fung (1958), and Bolotin (1963) ont utilisé la théorie structurale non linéaire pour la détermination des limites de flottement. Plusieurs analyses non linéaires de flottement du panneau peuvent être trouvées dans une vaste quantité de littérature, mais celles de flottement de coques cylindriques fermées sont rares. La théorie de large déflexion de Von Karman est largement utilisée pour tenir compte de la non-linéarité géométrique, qui a été appliquée avec succès au problème de flottement non linéaire du panneau. En dépit de la cohérence comparative sur laquelle la théorie structurale non linéaire a été utilisée, différentes théories aérodynamiques linéaires ont été employées, la plus populaire adoptée est la théorie de Piston de premier ordre quasi-stationnaire, qui est appliquée pour la vitesse d'écoulement de nombre de Mach $\sqrt{2}$. Dowell (1967) a appliqué la théorie aérodynamique d'écoulement potentielle linéarisée pour étudier le comportement de LCO des plaques dans un écoulement d'air avec le nombre de Mach proche de 1. La théorie aérodynamique quasi-statique d'Ackret, connue comme la théorie statique de la bande (Cunningham), a été appliquée à l'analyse de flottement supersonique non linéaire par Fralich (1965). Généralement, l'analyse linéaire de flottement est utilisée pour la prédiction de limites de stabilité à travers l'analyse propre tandis que l'analyse non linéaire de flottement a besoin d'un traitement spécial. La plupart des approches d'analyse incluent l'intégration numérique directe, la méthode de balance harmonique et la méthode de perturbation. La première application de l'intégration numérique directe est due à Dowell (1967) dans l'étude des oscillations non linéaires pour des plaques simplement supportées dans le plan en flottement.

Ventres (1970) a recherché le comportement non linéaire de flottement des plaques encastrées par l'intégration numérique directe. Les procédures de cette approche incluent la première application de la méthode de Galerkin dans le domaine spatial pour les équations différentielles partielles non linéaires du mouvement pour donner un ensemble d'équations différentielles ordinaires couplées dépendant du temps, donc l'intégration numérique temporelle est effectuée pour simuler la réponse de flottement. La méthode de Raleigh-Ritz, qui exige que les modes supposés satisfont seulement les conditions limites géométriques, est une autre approche pour l'expansion spatiale approximée pour la déflexion de la plaque. La méthode de balance harmonique a été aussi appliquée avec succès pour l'analyse non linéaire de flottement par certains chercheurs (1965-1987).

Cette méthode, comparée à l'intégration numérique directe, nécessite moins de temps de calcul mais elle est extrêmement fastidieuse à mettre en œuvre. La méthode de perturbation a été introduite pour l'analyse non linéaire de flottement par Morino (1976); un bon compromis est trouvé entre les méthodes de perturbation et celles de la méthode de balance par Kuo (1972). En général, pour les deux méthodes de perturbation et de balance harmonique, la déflexion du panneau est représentée en termes de deux à six modes normaux.

Certaines limitations intrinsèques présentent des obstacles à l'application des approches analytiques mentionnées précédemment à des analyses plus vastes. Par exemple, la méthode de Galerkin ou la méthode de Rayleigh-Ritz exige des hypothèses raisonnables par rapport aux fonctions de la forme de mode normal, qui doivent satisfaire les conditions limites du panneau. Généralement, les panneaux avec des conditions de support simple, comme les limites simplement supportées ou encastrées, sont faciles à traiter. Pour les conditions de support complexe, même pour la combinaison des conditions de support simple, les fonctions de déplacement situables peuvent ne pas existées ou sont trop compliquées à manipuler. Les propriétés matérielles anisotropiques des matériaux composites ont une large application d'ingénierie, donc il est difficile pour analyser le flottement non linéaire utilisant les méthodes analytiques. Compte tenu de ces problèmes, les chercheurs ont eu recours à des méthodes numériques comme la méthode des éléments finis (MEF) dont son utilisation pour l'analyse linéaire de flottement du panneau a été initialisée par Olson (1967), suivie par plusieurs chercheurs (1970-1977). L'application de la MEF pour le flottement non linéaire du panneau a commencé en 1977 par Mei dans l'étude de flottement de panneau 2D avec la négligence de

l'inertie de membrane. La MEF pour l'analyse non linéaire de flottement peut être en plus classifiée en deux catégories :

La formulation d'éléments finis dans le domaine fréquentiel et la formulation dans le domaine temporel. La formulation du domaine fréquentiel est bien développée et largement appliquée pour résoudre les limites de flottement (analyse propre) et l'étude des oscillations harmoniques LCO. Mei et Rogers (1976) ont incorporé le module de l'analyse de flottement supersonique pour le panneau 2D dans le code de Nastran. Rao and Rao (1980) ont recherché le flottement supersonique des panneaux 2D restreints dans les bornes. Mei et Weidman (1977) ont été les premiers qui ont étudié le LCO du panneau 3D, les effets d'amortissement, les rapports d'aspect, les forces initiales dans le plan et les conditions limites ont été examinées aussi. Le flottement des panneaux 3D a été étudié par Mei et Wang (1982) et Hang and Yang (1983) ont utilisé les éléments finis de plaque triangulaire pour étudier des harmoniques LCO. En comparaison, la formulation du domaine du temps qui implique l'intégration numérique est moins documentée dans l'analyse non linéaire de flottement des panneaux. Les principaux obstacles pour l'implantation de la formulation dans le domaine temporel sont (Green and Killey (1972) et Robinson (1990)) : i) le grand nombre de degrés de liberté (DOF) de système, ii) les matrices de rigidité non linéaires pour chaque élément doit être à chaque pas de temps et iii) le pas de temps de l'intégration est extrêmement petit.

D'autres groupes de chercheurs ont focalisé leurs études sur le flottement non linéaire du panneau considérant la non-linéarité aérodynamique donnée par Chandiramani et Librescu (1996). Le flottement dans l'écoulement supersonique des panneaux en composites cisaillés et déformés a été recherché. La théorie de déformation de cisaillement et les charges aérodynamiques basées sur la théorie de Piston de troisième ordre ont été utilisées. Les équations de flottement du panneau ont été dérivées en utilisant la méthode de Galerkin. La méthode de continuation de la longueur de l'arc a été utilisée pour déterminer l'état d'équilibre statique et ses stabilités dynamiques ont été ensuite examinées. Les effets des petites imperfections géométriques du panneau, la direction de l'écoulement d'air et la compression uniforme dans le plan sur les limites de flottement ont été recherchés. Il a été conclu que la théorie de déformation de cisaillement et la théorie aérodynamique non linéaire sont nécessaires pour la détermination des limites de flottement des panneaux en composite modérément épaisses. Le mouvement de post-flottement de ces panneaux en composite a aussi été étudié par l'application d'une technique de prédicateur-

correcteur de Newton-Raphson pour la solution périodique et l'intégration numérique pour les solutions quasi-périodiques de flottement.

1.2 Plan de la thèse

La thèse inclut cinq chapitres qui répondent à la structuration d'une thèse présentée sous forme d'articles, où chaque article contient résumé, introduction, revue de la littérature, méthode suivie, résultats, discussion et liste des références. Après ces articles, on donne une discussion générale et une conclusion en illustrant la réussite des objectifs visés dans ce projet de thèse. Les articles suivants ont été soumis pour publication au cours de l'étude doctorale.

R. Ramzi, A. Lakis. Effect of Geometric Non-linearities on Non-linear Vibrations of Closed Cylindrical Shells, accepté pour publication dans: International Journal of Structural Stability and Dynamics.

R. Ramzi, A. Lakis. Effects of Geometric Nonlinearities on Cylindrical Shells Subjected to a Supersonic Flow, accepté pour publication dans: Computers & Fluids.

R. Ramzi, A. Lakis. Effect of Geometric and Fluid Flow Nonlinearities on Cylindrical Shells Subjected to a Supersonic Flow, accepté pour publication dans: International Journal of Numerical Methods and Applications.

Le premier chapitre présente une revue de littérature pertinente dans le sujet et un plan de thèse proposé dans ce mémoire.

Dans le chapitre 2, qui correspond au 1er article, une formulation d'éléments finis détaillée est donnée, ainsi que l'équation du mouvement dérivé basée sur le principe de travail virtuel. La théorie des coques minces de Sanders-Koiter est utilisée pour aborder la non-linéarité structurale et la méthode des éléments finis pour discrétiser la coque cylindrique. Une transformation modale est effectuée sur l'équation de mouvement du système assemblé. Les procédures d'évaluation des matrices de rigidité non linéaires sont présentées aussi.

Dans le chapitre 3, qui correspond au 2^{e} article, les équations gouvernant le mouvement en coordonnées modales sont transformées en une représentation d'état d'espace afin de faciliter la mise en œuvre de l'intégration numérique directe. La méthode d'intégration de Runge-Kutta d'ordre quatre est aussi appliquée pour trouver des résultats de l'analyse des coques cylindriques soumises à l'écoulement supersonique.

Le chapitre 4, qui correspond au 3e article, présente des résultats numériques et des discussions d'une analyse non linéaire géométrique des coques cylindriques et aussi de l'écoulement du fluide. Les amplitudes de vibration sont comparées aux résultats existants des méthodes analytiques et numériques à des fins de vérification.

Une discussion générale vient de montrer la validation de la méthodologie suivie et les résultats obtenus par la comparaison avec différentes études des recherches publiées par d'autres chercheurs pour chaque article considéré dans cette thèse et ceci est le sujet du 5e chapitre.

À la fin de cette thèse, une conclusion générale et des recommandations ont été données pour récapituler tous les sujets abordés dans cette thèse et le travail futur prévu.

CHAPITRE 2: ARTICLE 1 - EFFECT OF GEOMETRIC NON-LINEARITIES ON NON-LINEAR VIBRATIONS OF CLOSED CYLINDRICAL SHELLS

Submitted, 22 march 2012 to the International Journal of Structural Stability and Dynamics

Redouane Ramzi and Aouni Lakis

2.1 Abstract

Geometrically non-linear free vibrations of closed isotropic cylindrical shells are investigated through an analytical-numerical model. The method developed is a combination of Sanders-Koiter nonlinear shell theory and the finite element method. The cylindrical shell is subdivided into cylindrical finite elements and the displacement functions are derived from exact solutions of Sander's equations for thin cylindrical shells. Expressions for the mass, linear and non-linear stiffness matrices are determined by exact analytical integration. Various boundary conditions of shell and in-plane effects are considered. Non-linear responses are analyzed using the Runge-Kutta numerical method. The non-linear frequency ratio is determined with respect to the amplitude thickness ratio of the motion for different study cases. Detailed numerical results are presented for various parameters for a closed isotropic shell. The results indicate either hardening or softening types of non-linear behaviors, depending on the structure data.

The results of this approach show good agreement with pertinent results published by many authors considering several cases of shells. This research clarifies the current disagreement about types of cylindrical shells with geometric non-linearities.

2.2 Introduction

In recent development work for the aerospace, spatial, oil and nuclear industries, the study of thin-walled cylindrical shells is of great importance in structural design to obtain the desired performance, rigidity, lightness, strength and stability characteristics of a structure in different conditions. This challenge has led to several published studies based on thin shell theories such us Sanders-Koiter, Donnell's shallow-shell, Flũgge-Lur'e-Byrne and Novozhilov theories. The resonant frequency in non-linear vibration is a function of its amplitude through the frequency-amplitude relationship which indicates whether the non-linearity is hardening or softening. The

first study on non-linear vibrations of circular cylindrical shells was undertaken by Reissner[1] in 1955. Donnell's shallow-shell theory for a single half-wave of the vibration mode was applied to the case of simply supported shells, and the results showed that the non-linearity could be either of the hardening or softening type. Cummings [2] has remarked that the governing equations used by Reissner depend on the area of integration. Chu [3] made a similar analysis but for a closed cylindrical shell, and found that the non-linearity characteristic was of the hardening type. Evensen [4] experimentally tested some shells that were subjected to large vibration amplitudes and observed that the non-linearity was of the softening type. After this he re-examined Chu [3] and Nowinski's [5] analysis. Olson [6] also observed a slight softening non-linearity during experimental studies of a thin seamless shell made of copper. Evensen and Fulton [7] studied the non-linear dynamic response of thin circular cylindrical shells, and they concluded that the non-linearity may be either hardening or softening depending upon the ratio of the number of axial waves to the number of circumferential waves. Evensen [8] analyzed the free and forced non-linear vibrations of thin circular rings using two vibration modes (driven and companion modes), and applying Galerkin's procedure for resolution of the equations of motion. Evenseen [9] also studied infinitely long cylindrical shells using the harmonic balance method. The non-linear free vibration of circular cylindrical shells was examined by Alturi [10] using Donnell's equations given by Chu [3], and Dowell and Ventres [11]. The Galerkin technique was used to reduce the problem to a system of coupled non-linear ordinary differential equations for the modal amplitudes. The result was a non-linear hardening type. Chen and Babcock [12] analyzed the large vibration amplitudes of a simply-supported thin-walled cylindrical shell using the perturbation method to study the influence of the companion mode on the non-linear forced response of a circular cylindrical shell. The results indicate that the non-linearity may be either softening or hardening depending on the mode. To account for geometric non-linearity, small arbitrary initial imperfections, and using the strain-displacement relations of the Sanders-Koiter non-linear theory, Radwan and Genin [13-14] derived a set of non-linear modal equations for thin shells of arbitrary geometry using the modal expansion method. The results obtained indicated a hardening type non-linearity. Using a QUAD-4 shear flexible developed shell element model (FEM), the free non-linear vibrations of thin circular cylindrical shells have been studied by Ganapathi and Vardan [15]. The non-linear governing equations were solved using a Welson numerical integration scheme; modified Newton-Raphson iterations have been employed.

The approach presented in this article involves two steps:

Using linear strain-displacement and stress-strain relationships which are inserted into Sander's equations of equilibrium, we determine the displacement functions by solving the linear equation system. We then determine the mass and linear stiffness matrices for a finite element and assemble the matrices for the complete shell.

Using strain-displacement relationships from the Sanders-Koiter non-linear theory, the modal coefficients are obtained from the displacement functions. The second and third order non-linear stiffness matrices for a finite element are then calculated by precise analytical integration with respect to modal coefficients.

The finite element proposed was a closed cylindrical segment (Figure 1) with four degrees of freedom at each node: axial, radial, circumferential, and rotational.

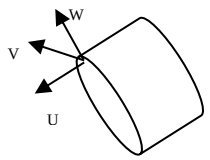

Figure 2.1: Cylindrical finite element geometry

This approach is more accurate than usual finite element methods. Other advantages offered by this method include:

Arbitrary boundary conditions can be used - High and low frequencies may be obtained with high accuracy - Precise results are obtained in cases with low and high circumferential wave numbers - Valid for a large amplitude of vibration that can reach 5 times the wall thickness of the closed cylindrical shell - More accurate than the usual finite element methods - Computation time is very short -Structured and simple method.

2.3 Linear Part

The equations of motion of an anisotropic cylindrical shell in terms of U, V, and W (axial, tangential and radial displacements) (Figure 2) are written as follows:

$$L_J(U, W, V, P_{ij}) = 0 \qquad (1)$$

Where $L_{J(J=1,2,3)}$ are three linear partial differential equations (given in Appendix) and p_{ij} are elements of the elasticity matrix for anisotropic shells which is given by:

$$[P]=\begin{bmatrix} p_{11} & p_{12} & 0 & p_{14} & p_{15} & 0 \\ p_{21} & p_{22} & 0 & p_{24} & p_{25} & 0 \\ 0 & 0 & p_{33} & 0 & 0 & p_{36} \\ p_{41} & p_{42} & 0 & p_{44} & p_{45} & 0 \\ p_{51} & p_{52} & 0 & p_{54} & p_{55} & 0 \\ 0 & 0 & p_{63} & 0 & 0 & p_{66} \end{bmatrix} \tag{2}$$

For the isotropic case,

$$[P]=\begin{bmatrix} D & \upsilon D & 0 & 0 & 0 & 0 \\ \upsilon D & D & 0 & 0 & 0 & 0 \\ 0 & 0 & \frac{D(1-\upsilon)}{2} & 0 & 0 & 0 \\ 0 & 0 & 0 & K & \upsilon K & 0 \\ 0 & 0 & 0 & \upsilon K & K & 0 \\ 0 & 0 & 0 & 0 & 0 & \frac{K(1-\upsilon)}{2} \end{bmatrix}$$

where,

$$K=\frac{Eh^3}{12(1-\upsilon^2)} \text{ Bending stiffness, } \quad D=\frac{Eh}{1-\upsilon^2} \text{ Membrane stiffness} \tag{3}$$

The displacement functions associated with the circumferential wave number are assumed in the normal manner, as:

$$\begin{aligned} U(x,\theta) &= Ae^{\frac{\lambda x}{R}}\cos(n\theta) \\ W(x,\theta) &= Be^{\frac{\lambda x}{R}}\cos(n\theta) \\ V(x,\theta) &= Ce^{\frac{\lambda x}{R}}\sin(n\theta) \end{aligned} \tag{4}$$

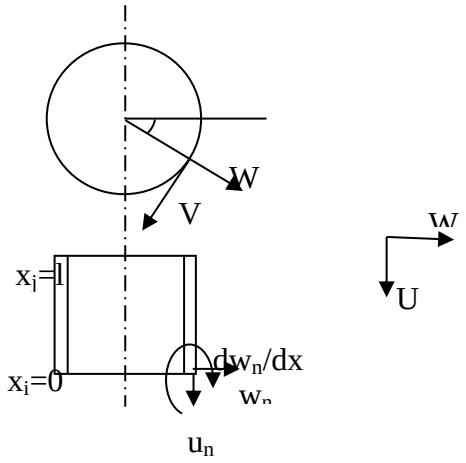

Figure 2.2: Finite element discretization and nodal displacement

where n is the circumferential mode,

Note that this approach treats closed cylindrical shells based on the circumferential wave number, not on the longitudinal wave number.

Substituting (4) into the equations of motion (1), a system of three homogeneous equations, linear functions of constants A, B, C, are obtained. For the solution to be non-trivial, the determinant of this system must be equal to zero. This brings us to the following characteristic equation:

$$Det\left(\left[H\right]\right) = f_8\lambda^8 + f_6\lambda^6 + f_4\lambda^4 + f_2\lambda^2 + f_0 \tag{5}$$

The values of coefficients f_i in this eighth-degree polynomial are given in Appendix.

Each root of this equation yields a solution to the linear equations of motion (1). The complete solution is obtained by adding the eight solutions independently with constants A_i, B_i and C_i

(i = 1, 2,…., 8). These constants are not independent. We can therefore express A_i and B_i as a function of C_i, as follows:

$$\begin{aligned} A_i &= \alpha_i C_i \\ B_i &= \beta_i C_i \end{aligned} \tag{6}$$

The values of α_i and β_i can be obtained from system (1) by introducing relation (6). To determine eight C_i constants, it is necessary to formulate eight boundary conditions for the finite elements. The axial, tangential and radial displacements will be specified for each node. The following relation defines the element displacement vector at the boundaries:

$$\begin{Bmatrix}\delta_i \\ \delta_j\end{Bmatrix} = \begin{Bmatrix} u_i & v_i & w_i & u_j & v_j & w_j \end{Bmatrix}^T \tag{7}$$

$$\begin{Bmatrix}\delta_i \\ \delta_j\end{Bmatrix} = [A]\{C\} \tag{8}$$

where the elements of matrix [A] are given in Appendix.

Multiplying Eq. (8) by $[A]^{-1}$ and substituting the result into Eq. (4), we obtain:

$$\begin{Bmatrix} U(x,\theta) \\ V(x,\theta) \\ W(x,\theta) \end{Bmatrix} = [N] \begin{Bmatrix}\delta_i \\ \delta_j\end{Bmatrix} \tag{9}$$

where [N] represents the shape function matrix given in this form:

$$[N] = [T][R]\left[A^{-1}\right] \tag{10}$$

and [T], [R], [A] are described in Appendix.

The constitutive relation between the stress and deformation vector of a cylindrical shell is given as:

$$\{\sigma\} = [P][B] \begin{Bmatrix}\delta_i \\ \delta_j\end{Bmatrix} \tag{11}$$

The mass and stiffness matrices for each element are derived using the classic finite element procedure and can then be expressed as:

$$\begin{aligned} [m] &= \rho h \iint [N]^T [N] dA \\ [k_L] &= \iint [B]^T [P][B] dA \end{aligned} \tag{12}$$

Where ρ is the density of the shell, h its thickness and $dA = Rdxd\theta$. The matrices [m] and [k] are obtained analytically by carrying out the necessary matrix operations over x and θ in the equation. The global matrices $[M_s]$ and $[K_s]$ may be obtained, respectively, by assembling the mass and stiffness matrices for each individual finite element.

2.4 Non-linear part

The coefficients of the modal equations are obtained using the Lagrange method in the same way developed by Radwan and Genin [13], paying attention to geometric non-linearities. Following this, the second and third non-linear stiffness matrices corresponding to geometric non-linearities are computed and superimposed on the linear system.

Shell displacements (u,v,w) are expressed as sums of generalized product coordinates $q_i(t)$ and spatial functions U, V, W (see Eq.(4)).

$$\begin{aligned} u &= \sum_i q_i(t) U_i(x,\theta) \\ v &= \sum_i q_i(t) V_i(x,\theta) \\ w &= \sum_i q_i(t) W_i(x,\theta) \end{aligned} \tag{13}$$

The deformation vector is written as a function of the generalized coordinates by separating the linear part from the non-linear part.

$$\{\varepsilon\} = \{\varepsilon_L\} + \{\varepsilon_{NL}\} = \{\varepsilon_{xx}, \varepsilon_{\theta\theta}, 2\varepsilon_{x\theta}, \kappa_{xx}, \kappa_{\theta\theta}, 2\kappa_{x\theta}\}^T \tag{14}$$

Where subscripts ``L`` and ``NL`` mean ``linear`` and ``non-linear``, respectively, and ε_L and ε_{NL} are defined in Appendix.

The Lagrange's equations of motion in generalized coordinates $q_i(t)$ are found using Hamilton's principle and Eq. (13):

$$\frac{d}{dt}\left(\frac{\partial T}{\partial \dot{q}_i}\right) - \frac{\partial T}{\partial q_i} + \frac{\partial V}{\partial q_i} = Q_i \tag{15}$$

where T is the total kinetic energy, V is the total elastic strain energy of deformation and the Q_i's are the generalized forces. In this case study; $Q_i = 0$ (free vibration).

Using the vector deformation given by (14), the developed formulation for total kinetic and strain energy and inserting these into the Lagrange equation (15), the following non-linear modal equations are obtained after a long development of equations:

$$\sum_r m_{pr}\ddot{\delta}_r + \sum_r k_{pr}^{(L)}\delta_r + \sum_r \sum_s k_{prs}^{(NL2)}\delta_r\delta_s + \sum_r \sum_s \sum_q k_{prsq}^{(NL3)}\delta_r\delta_s\delta_q = 0 \qquad (16)$$

$$p = 1, 2, ...$$

Where m_{pr}, $k_{pr}^{(L)}$ are terms of the mass and linear stiffness matrices given by Eq. (12). The terms $k_{prs}^{(NL2)}$ and $k_{prsq}^{(NL3)}$ represent the second and third-order non-linear stiffness and are given by the following integrals for the case of an isotropic closed cylindrical shell:

$$K_{prs}^{(NL2)} = \iint \left\{ p_{11}A_{prs} + p_{22}B_{prs} + p_{12}(D_{prs} + E_{prs}) + p_{33}C_{prs} \right\} dA \qquad (17)$$

and

$$K_{prsq}^{(NL3)} = \iint \left\{ p_{11}A_{prsq} + p_{22}B_{prsq} + p_{12}(D_{prsq} + E_{prsq}) + p_{33}C_{prsq} \right\} dA \qquad (18)$$

Where $dA = Rdxd\theta$, p_{ij} are the terms of the elasticity matrix [P], and the terms A_{prs},B_{prs},C_{prs},D_{prs},E_{prs} and A_{prsq},B_{prsq},C_{prsq},D_{prsq},E_{prsq} represent the coefficients of the modal equations. These coefficients are given by the following equations:

$$\begin{aligned}
A_{prs} &= a_p A_{rs} + a_r A_{sp} + a_s A_{pr} & \qquad A_{prsq} &= 2A_{pq} A_{rs} \\
B_{prs} &= b_p B_{rs} + b_r A_{sp} + b_s B_{pr} & \qquad B_{prsq} &= 2B_{pq} B_{rs} \\
C_{prs} &= c_p C_{rs} + c_r C_{sp} + c_s C_{pr} & \qquad C_{prsq} &= 2C_{pq} C_{rs} \\
D_{prs} &= a_r B_{sp} + a_s B_{pr} + b_p A_{rs} & \qquad D_{prsq} &= 2A_{pq} B_{rs} \\
E_{prs} &= b_r A_{sp} + b_s A_{pr} + a_s B_{rs} & \qquad E_{prsq} &= 2B_{pq} A_{rs}
\end{aligned} \qquad (19)$$

with;

$$a_p = U_{p,x}, \qquad b_p = 1/R\,(V_{p,\theta} + W_p), \qquad c_p = 1/2\,(U_{p,\theta}/R + V_{p,x})$$

$$A_{pq} = 1/8\,R2\,(R\,V_{p,x} - U_{p,\theta}) \,.\, (R\,V_{q,x} - U_{q,\theta}) + 1/2\,W_{p,x}W_{q,x} \qquad (20)$$

$$B_{pq} = 1/8\,R2\,(R\,V_{p,x} - U_{p,\theta}) \,.\, (R\,V_{q,x} - U_{q,\theta}) + 1/2\,R2\,(W_{p,\theta} - V_p) \,.\, (W_{q,\theta} - V_q)$$

$$C_{pq} = 1/4\,R\,(W_{p,x}W_{q,\theta} - W_{q,x}W_{p,\theta}) - 1/4\,R\,(V_p W_{q,x} + V_q W_{p,x})$$

where U, V and W are spatial functions determined by Eq. (4).

In Eqs. (16 - 20), the subscripts ‘p,q’, ’p,r,s’ and ‘p,r,s,q’ represent the coupling between two, three and four modes, respectively.

Let us illustrate the development of the expression for the (p,q) term of matrices A_{pq} and A_{pqrs}.

The expression A_{pq} is given by:

$$A_{pq} = a_{pq} e^{\left(\lambda_p + \lambda_q\right) x/R} \tag{21}$$

and A_{pqrs} is :

$$A_{prsq} = \sum_{r=1}^{8} \sum_{s=1}^{8} a_{rs} a_{pq} \varepsilon_{rs} e^{(\lambda_p + \lambda_r + \lambda_s + \lambda_q) x/R} \tag{22}$$

ε_{rs} is the term (r,s) of matrix [E], where [E] represents a matrix of constants defined by $\left[E\right] = \left[A^{-1}\right]^T \left[A\right]$, and

$$a_{pq} = \frac{1}{2R^2}\left[\frac{1}{4} a_{pq}^{(1)} \sin^2\left(n\theta\right) + a_{pq}^{(2)} \cos^2\left(n\theta\right)\right] \tag{23}$$

with

$$a_{pq}^{(1)} = \left(\beta_p \lambda_p + n\alpha_p\right)\left(\beta_q \lambda_q + n\alpha_q\right) \tag{24}$$

$$a_{pq}^{(2)} = \lambda_p \lambda_q \tag{25}$$

Similarly, the matrices $[B_{pq}]$… $[E_{prsq}]$ can be written as a function of α, β, λ, x and θ. The (p, q) terms of these matrices are described in Appendix. For details of the basis of the presented method, consult Ref. [13].

After integration, we obtain:

$$\left[k_{prs}^{(NL2)}\right] = \left[A^{-1}\right]^T \left[J^{(NL2)}\right]\left[A^{-1}\right] \tag{26}$$

$$\left[k_{prsq}^{(NL3)}\right] = \frac{\pi}{8R^2}\left[A^{-1}\right]^T \left[J^{(NL3)}\right]\left[A^{-1}\right] \tag{27}$$

The (p,q) term in matrix $\left[J_{p,q}^{(NL2)} \right]$ and $\left[J_{p,q}^{(NL3)} \right]$ are written as:

$$J^{(NL2)}(p,q) = \begin{cases} \sum_{l=1}^{8}\sum_{s=1}^{8} \dfrac{\varepsilon_{sr}}{\left(\lambda_p + \lambda_q + \lambda_r\right)} G1(p,q)\left[e^{\left(\lambda_p+\lambda_q+\lambda_r\right)\frac{\ell}{R}} - 1 \right] \\ if\ \lambda_p + \lambda_q + \lambda_r \neq 0 \\ \sum_{k=1}^{8}\sum_{l=1}^{8} \varepsilon_{sr} G1(p,q) \dfrac{\ell}{R} \\ if\ \lambda_p + \lambda_q + \lambda_r = 0 \end{cases} \tag{28}$$

and

$$J^{(NL3)}(p,q) = \begin{cases} \sum_{k=1}^{8}\sum_{l=1}^{8} \dfrac{\varepsilon_{sr}}{\left(\lambda_p + \lambda_q + \lambda_r + \lambda_s\right)} G2(p,q)\left[e^{\left(\lambda_p+\lambda_q+\lambda_r+\lambda_s\right)\frac{\ell}{R}} - 1 \right] \\ if\ \lambda_p + \lambda_q + \lambda_r + \lambda_s \neq 0 \\ \sum_{k=1}^{8}\sum_{l=1}^{8} \varepsilon_{sr} G2(p,q) \dfrac{\ell}{R} \\ if\ \lambda_p + \lambda_q + \lambda_r + \lambda_s = 0 \end{cases} \tag{29}$$

where G1(p,q) and G2(p,q) are coefficients in conjunction with α, β, λ and elements pij in matrix [P]. The general expressions of G1(p,q) and G2(p,q) are given by :

$$\begin{aligned} \mathrm{G1}_{(\mathrm{p,q})} &= p_{11} II_1 \left[a_p^{(1)} A^{-1} a_{rs}^{(1)} + a_r^{(1)} A^{-1} a_{sp}^{(1)} + a_s^{(1)} A^{-1} a_{pr}^{(1)} \right] \\ &+ p_{11} II_2 \left[a_p^{(1)} A^{-1} a_{rs}^{(2)} + a_r^{(1)} A^{-1} a_{sp}^{(2)} + a_s^{(1)} A^{-1} a_{pr}^{(2)} \right] \\ &+ p_{22} II_1 \left[b_p^{(1)} A^{-1} b_{rs}^{(2)} + b_r^{(1)} A^{-1} b_{sp}^{(2)} + b_s^{(1)} A^{-1} b_{pr}^{(2)} \right] \\ &+ p_{33} II_1 \left[c_p^{(1)} A^{-1} c_{rs}^{(1)} + c_r^{(1)} A^{-1} c_{sp}^{(1)} + c_s^{(1)} A^{-1} c_{pr}^{(1)} \right] \\ &+ p_{12} II_1 + \left[a_r^{(1)} A^{-1} b_{sp}^{(1)} + a_s^{(1)} A^{-1} a_{pr}^{(1)} + b_p^{(1)} A^{-1} a_{rs}^{(1)} \right] \\ &+ p_{12} II_2 \left[b_p^{(1)} A^{-1} a_{rs}^{(2)} \right] \\ &+ p_{12} II_1 \left[b_r^{(1)} A^{-1} a_{sp}^{(1)} + b_s^{(1)} A^{-1} a_{pr}^{(1)} + a_p^{(1)} A^{-1} b_{rs}^{(1)} \right] \\ &+ p_{12} II_2 \left[b_r^{(1)} A^{-1} a_{sp}^{(2)} + b_s^{(1)} A^{-1} a_{pr}^{(2)} \right] \end{aligned} \tag{30}$$

where,

$$II_1 = \frac{\sin^3(2\pi n)}{3} \qquad II_2 = \frac{\sin(2\pi n)(2+\cos^2(2\pi n))}{3n} \tag{31}$$

and

$$
\begin{aligned}
G2_{(p,q)} = {} & \frac{3}{16}\left(p_{11}+p_{22}+2p_{12}\right)a_{pl}^{(1)}a_{kq}^{(1)} + 3\left(p_{11}a_{pl}^{(2)}a_{kq}^{(2)} + p_{22}b_{pl}^{(1)}b_{kq}^{(1)}\right) \\
& + p_{12}\left(a_{pl}^{(2)}b_{kq}^{(1)} + b_{pl}^{(1)}a_{kq}^{(2)}\right) + \frac{1}{4}\left(p_{11}+p_{12}\right)\left(a_{pl}^{(2)}a_{kq}^{(1)} + a_{pl}^{(1)}a_{kq}^{(2)}\right) \\
& + \frac{3}{4}\left(p_{12}+p_{22}\right)\left(a_{pl}^{(1)}b_{kq}^{(1)} + b_{pl}^{(1)}a_{kq}^{(1)}\right) \\
& + \frac{1}{4}p_{33}\left(c_{pl}^{(1)}c_{kq}^{(1)} + c_{pl}^{(2)}c_{kq}^{(2)} + c_{pl}^{(2)}c_{kq}^{(1)} + c_{pl}^{(1)}c_{kq}^{(2)}\right)
\end{aligned}
\tag{32}
$$

where the terms $a^{(1)}$ and $a^{(2)}$ are given by Eqs. (24-25). Terms $b^{(1)}$…, $c^{(1)}$…and $c^{(2)}$ are coefficients appearing in expressions for the elements of matrices $[B_{pq}]$ and $[C_{pq}]$ defined in Eqs (20). These coefficients are given in Appendix.

2.5 Numerical resolution

The mass and stiffness matrices, both linear and non-linear, given in Eqs. (12-26-27) are only determined for one element. After subdividing the shell into several elements, the global mass and stiffness matrices are obtained by assembling the matrices for each element.

Assembly is done in such a way that all the equations of motion and the continuity of displacements at each node are satisfied. These matrices are designated as [M], $[K^{(L)}]$, $[K^{(NL2)}]$ and $[K^{(NL3)}]$ respectively.

$$
[M]\{\ddot{\delta}\} + \left[K^{(L)}\right]\{\delta\} + \left[K^{(NL2)}\right]\{\delta^2\} + \left[K^{(NL3)}\right]\{\delta^3\} = \{0\} \tag{33}
$$

Where δ is the displacement vector and $[M]$, $\left[K^{(L)}\right]$, $\left[K^{(NL2)}\right]$ and $\left[K^{(NL3)}\right]$ are respectively the mass, linear and second and third-order non-linear stiffness matrices of the system.

In practice, very specific conditions are applied to the shell boundaries. Thus, these square matrices are reduced to square matrices of order NREDUC=NDF*(N+1)-J, where J represents the number of constraints applied. The system of equations then becomes:

$$
\left[M^{(r)}\right]\left\{\ddot{\delta}^{(r)}\right\} + \left[K_L^{(r)}\right]\left\{\delta^{(r)}\right\} + \left[K_{NL2}^{(r)}\right]\left\{\delta^{(r)2}\right\} + \left[K_{NL3}^{(r)}\right]\left\{\delta^{(r)3}\right\} = \{0\} \tag{34}
$$

Where the subscript ‘‘r’’ means, ‘‘reduced’’.

Let us set:

$$\left\{\delta^{(r)}\right\} = [\Phi]\{q\} \tag{35}$$

where $[\Phi]$ represents the square matrix for eigenvectors of the linear system and $\{q\}$ is a time-related vector. Substituting Eq. (33) into system (32) and pre-multiplying the whole equation by $[\Phi]^T$, we obtain;

$$[\Phi]^T\left[M^{(r)}\right][\Phi][\ddot{q}]+[\Phi]^T\left[K_L^{(r)}\right][\Phi]\{q\}+[\Phi]^T\left[K_{NL2}^{(r)}\right]\times\left([\Phi]\{q\}\right)^2+[\Phi]^T\left[K_{NL3}^{(r)}\right]\left([\Phi]\{q\}\right)^3=0 \tag{36}$$

The products of matrix $[\Phi]^T\left[M^{(r)}\right][\Phi]$ and $[\Phi]^T\left[K_L^{(r)}\right][\Phi]$ represent diagonal matrices, written as $\left[M^{(D)}\right]$ and $\left[K_L^{(D)}\right]$ respectively. By neglecting the cross-product terms in $\left([\Phi]\{q\}\right)^2$ and $\left([\Phi]\{q\}\right)^3$ of Eq. (34), we obtain:

$$m_{pp}\ddot{q}_p + k_{pp}^{(L)}q_p + \sum_{s=1}^{NREDUC} k_{ps}^{(NL2)}q_s^2 + \sum_{s=1}^{NREDUC} k_{ps}^{(NL3)}q_s^2 = 0 \tag{37}$$

Thus there are ‘‘NREDUC’’ simultaneous equations in the form of Eq. (35).

$$\text{Setting} \quad q_p(t) = A_p f_p(\tau) \qquad \text{with } f_p(0)=1 \text{ and } \dot{f}_p(0)=0 \tag{38}$$

Eq. (35) becomes, after the A_i simplification and dividing by m_{pp},

$$\ddot{f}_{pp} + \frac{k_{pp}^{(L)}}{m_{pp}} f_p + \frac{k_{pp}^{(NL2)}}{m_{pp}} t\left(A_p/t\right) f_p^3 + \frac{k_{pp}^{(NL3)}}{m_{pp}} t^2\left(A_p/t\right)^2 f_p^3 = 0 \tag{39}$$

where t represents the shell thickness. The coefficient k_{pp}/m_{pp} represents the p linear vibration frequency of system. The solution $f_p(\tau)$ of these ordinary non-linear differential equations which satisfies the initial conditions (36) is approximated by a fourth-order Runge-Kutta numerical method. The linear and non-linear natural angular frequencies are evaluated using a systematic search for the $f_p(\tau)$ roots as a function of time. The ω_{NL}/ω_L ratio is expressed as a function of the non-dimensional ratio A_p/t where A_p is the vibration amplitude.

2.6 Discussion of Results

The single mode response of an empty, closed isotropic cylindrical shell corresponding to m=1 and n=4, is shown in Figure 2.3. The calculation has been performed for a simply supported cylindrical shell with the following dimensions and material properties: t=0.0254 cm, R=2.54 cm, L=40 cm, E=200 GPa, ν=0.3, ρ=7800 kg/m^3. It illustrates a non-linearity of the hardening type for a low number of circumferential waves. The presented results are compared with Refs. [22-23]. Ref. [22] was obtained based on Donnell's simplified non-linear method considering only lateral displacement. Raju and Rao used the finite element method based on an energy formulation.

It is observed that the variation ratio between the non-linear and linear frequency W_{nl}/W_l increases as the ratio A/t increases although these variations are small for A/t below 1.0. The difference between results obtained by the present theory and those of Refs. [22-23] might be due to the fact that Nowinski [22] neglected in-plane inertia and took into account only lateral displacement. Raju and Roa [23] expressed the displacement components along the shell generator in polynomial form.

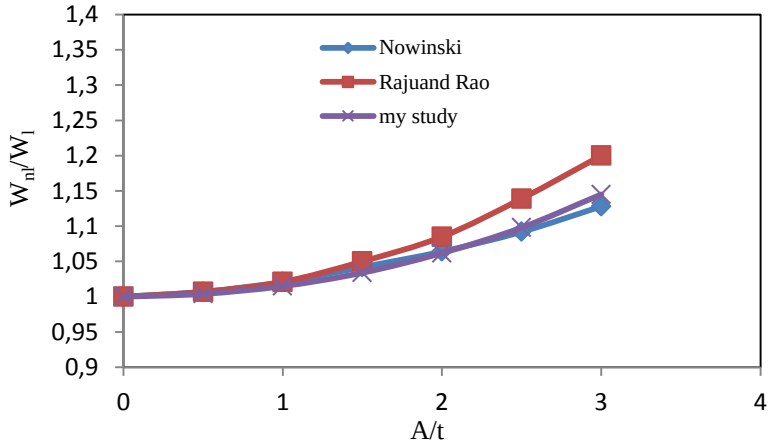

Figure 2.3: Influence of large amplitude on non-linear frequency

In Figure 2.4, the non-linear frequency response as a function of the amplitude of vibration for the non-linear free vibration case for Olsen's shell (n=10, m=1, ξ=0.1635, ε=0.003025, ν=0.365) is compared with theoretical and experimental results obtained previously by several authors in order to validate the present work. This case concerned an empty isotropic cylindrical shell with

simply-supported ends. The geometrical and material characteristics of the cylindrical shell considered by Olson [6] are: L=0.39 m, R= 0.203 m, t = 0.11176×10^{-3} m, E = 124×10^{9} Pa,

ν =0.35 and ρ = 8930 kg/m3. Good agreement can be seen, which allows us to confirm that the new approach presented in this paper can be used in analyzing the influence of large amplitude vibrations on simply-supported closed cylindrical shells.

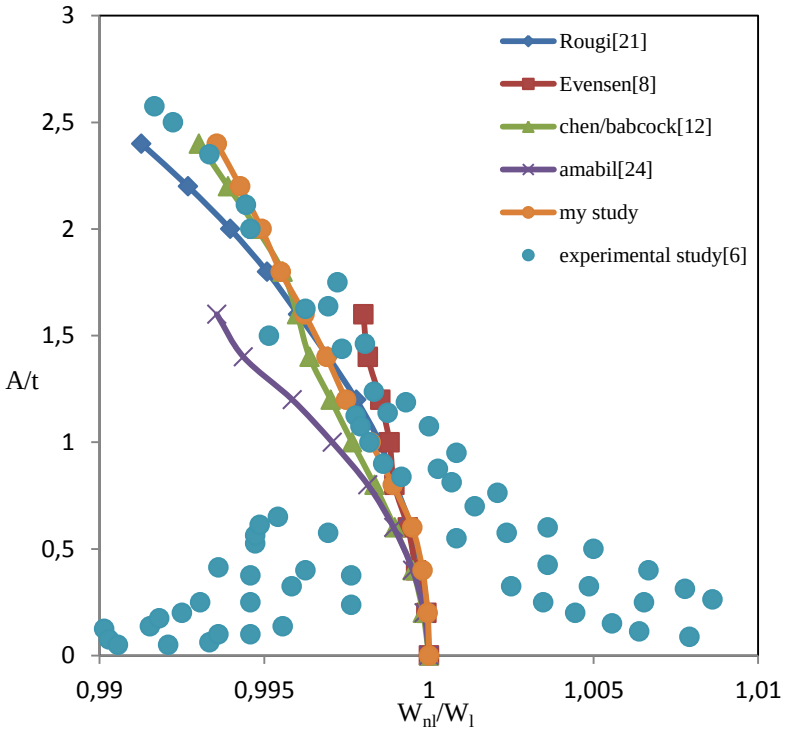

Figure 2.4: Influence of large amplitude on non-linear frequency ratio for n=10 and m=1

In Figure 2.5, the effect of the axial longitudinal mode on non-linear behavior of the cylindrical shell under large-amplitude vibration for circumferential wave number n = 10, is investigated. Here, the closed shell is simply supported and has the following data: E = 200 GPa, v=0.3, ρ = 7800 kg/m3, R = 2.54 cm, L = 40 cm, t = 0.0254 cm. Results show that the non-linearity is the softening type for m=1 and the hardening type for other longitudinal axial modes. A more pronounced non-linearity is seen at mode m = 7.

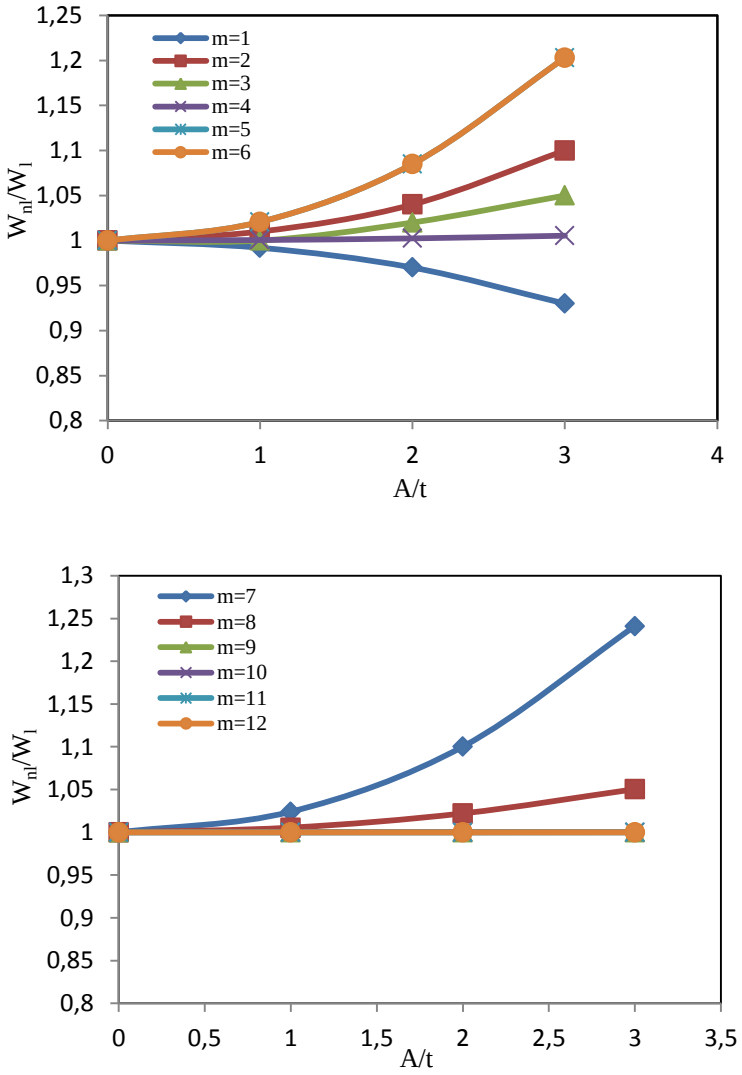

Figure 2.5: Influence of longitudinal modes on non-linear vibration at large amplitude

An advantage of the presented model is that it allows the study of various boundary conditions. This is clearly shown in Figure 2.6, which presents the effect of boundary conditions on non-linear free vibration. The shell tested has the same data as Figure 2.5.

The non-linearity is the hardening type for the shell with free-free boundary conditions, however the softening type is observed for other boundary conditions, and more pronounced in clamped-clamped and simply supported – simply supported. The effect is small for a cylindrical shell under clamped-simply supported and clamped-free boundary conditions.

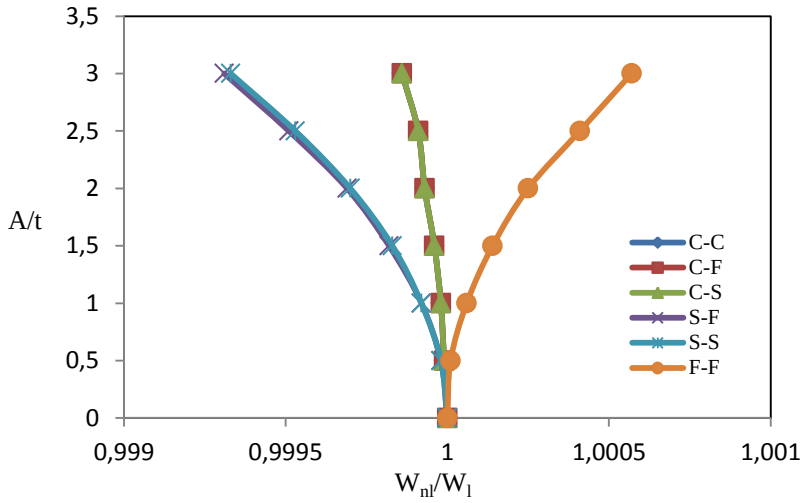

Figure 2.6: Influence of various boundary conditions on nonlinear behavior of cylindrical shells

As a next step; a detailed parametric study was carried out for the simply-supported shell, and results from the presented method were compared with those of available analytical models. Two values of aspect ratio $\xi = m\pi R/nL$ and three values of parameter $\varepsilon = (n^2h/R)^2$ were considered. They are; $\xi = 0.5$ and $\varepsilon = 0.01$, 1.0; m and n are the axial half wave and circumferential wave numbers and L and R are the length and radius of the cylindrical shell respectively.

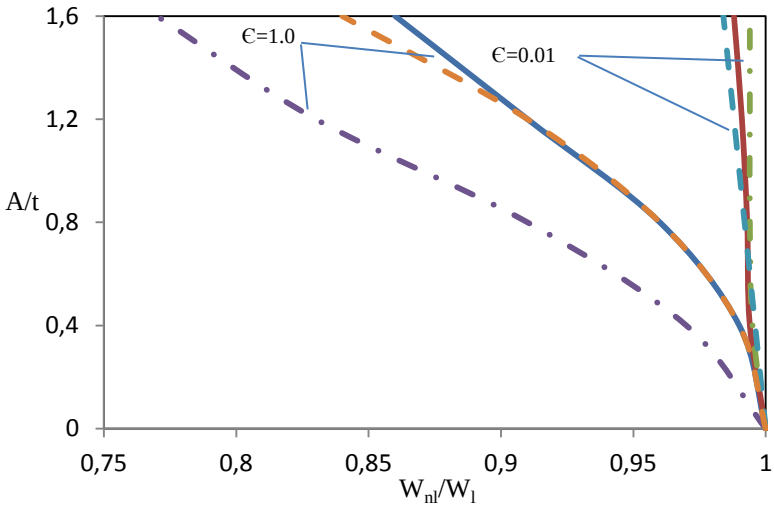

Figure 2.7: A comparison with the results of Evensen and Ganapathi ($\xi = 0.5$, $\varepsilon = 0.01$ and 1.0);

-·-·- , Present study; ____ , Evensen [8]; - - - - , Ganapathi [15].

In Figure 2.7, the results of our study show that the non-linearity is the softening type for small values of ξ (for example ξ = 0.5), and as ε increases the vibrations become more and more non-linear. It can be concluded that the strength of the non-linearity depends on the value of the parameter ε. For comparison purposes, Evensen's and Ganapathi's results [8-15] have been plotted in Figure 2.7. The result obtained using the present method represents a good compromise. Furthermore, in Figure 2.8 a hardening behavior of non-linearity vibrations is observed for large values of ξ (ξ = 2.0 as shown in Figure 2.8). Similar observations are revealed using the Evensen analysis [8]; the non-linearity trend becomes stronger for large values of ε. The numerical results obtained in this section for ξ = 0.5 and ξ = 2.0 are also in good agreement with results reported in Ref. [25].

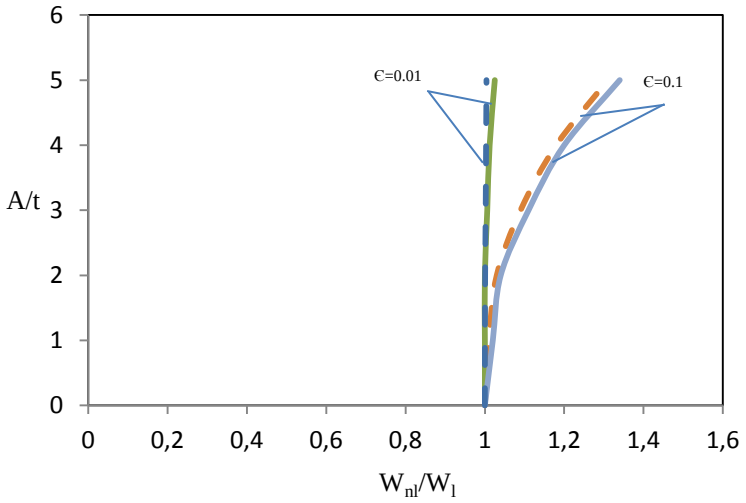

Figure 2.8: A comparison with the results of Evensen (ξ = 2.0, ε = 0.01 and 1.0). —— ; Present analysis; - - -, Evensen [8]

To study the influence of in-plane boundary conditions on non-linear vibrations of a cylindrical shell, the case of a simply-supported shell with axial displacement is restrained (u = w = v = 0). Figure 2.9 presents the results obtained in comparison with Ganapathi analysis 15, for various values of ξ and ε. Analysis of Figures [2.7-9] reveals that the trends of non-linearity behavior does not change, which is confirmed by Ganapathi's [15] results for an isotropic cylindrical shell.

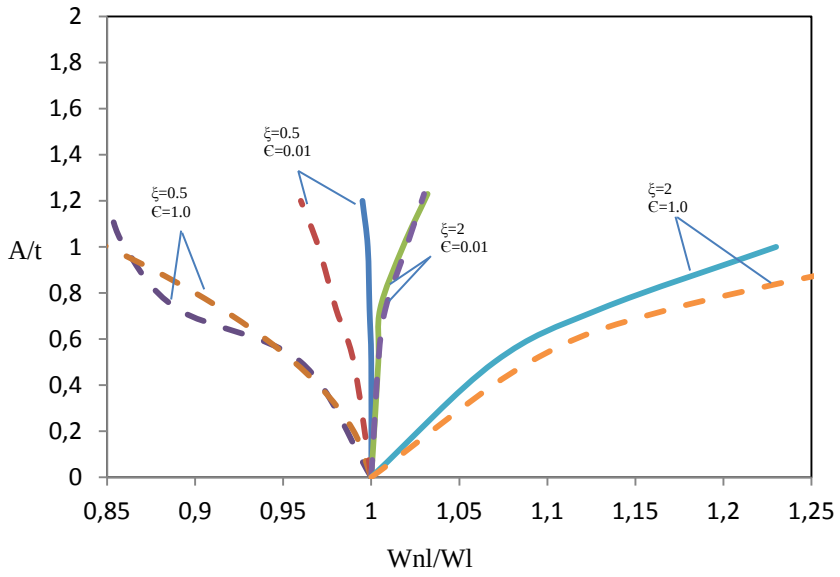

Figure 2.9: The amplitude-frequency relation. - - - - - , Present analysis —— ; Ganapathi [15]

2.7 Conclusion

The non-linear free vibrations of thin-walled cylindrical shells were analyzed using an approach based on non-linear Sanders-Koiter shell theory and a hybrid finite element method. The second and third order stiffness matrices for an empty closed cylindrical element were considered. This study was performed for various shells examined in the literature for both low and high circumferential wave numbers. A precise prediction of non-linearity trends under high-amplitude vibration can be provided using the presented method. The effects of various boundary conditions and axial modes on non-linear vibration behaviors have also been treated. In all cases, the degree of non-linearity is dependent upon thickness, radius, length, circumferential and axial wave numbers. However, the type of non-linearity is determined by the aspect ratio ξ. The results obtained for non-linearities are in good agreement with available studies for ξ = 0.5, 2.0. and ε = 0.01, 0.1, 1.0. In-plane boundary conditions have no effect the nature of non-linearity. Results for low and high wave numbers compare closely with previous studies based on different non-linear shell theories and numerical methods for non-linear equation resolution. The presented method allows a large field study of geometric and material parameters under various conditions in which these structures may be used.

2.8 Appendix

Sander's linear equations for thin cylindrical shells in terms of axial, tangential and circumferential displacements are:

$$L_1(U,V,W,P_{ij}) = P_{11}\frac{\partial^2 U}{\partial x^2} + \frac{P_{12}}{R}\frac{\partial^2 U}{\partial x^2}\left(\frac{\partial^2 V}{\partial x\partial\theta} + \frac{\partial W}{\partial x}\right) - P_{14}\frac{\partial^3 W}{\partial x^3} + \frac{P_{15}}{R^2}\left(\frac{\partial^3 W}{\partial x\partial\theta^2} + \frac{\partial^2 V}{\partial x\partial\theta}\right) + \left(\frac{P_{33}}{R} - \frac{P_{63}}{2R^2}\right)\left(\frac{\partial^2 V}{\partial x\partial\theta} + \frac{1}{R}\frac{\partial^2 U}{\partial\theta^2}\right)$$
$$+\left(\frac{P_{36}}{R^2} - \frac{P_{66}}{2R^3}\right)\left(-2\frac{\partial^3 W}{\partial x\partial\theta^2} + \frac{3}{2}\frac{\partial^2 V}{\partial x\partial\theta} - \frac{1}{2R}\frac{\partial^2 U}{\partial\theta^2}\right)$$

$$L_2(U,V,W,P_{ij}) = \left(\frac{P_{21}}{R} - \frac{P_{51}}{R^2}\right)\frac{\partial^2 U}{\partial x\partial\theta} + \frac{1}{R}\left(\frac{P_{22}}{R} + \frac{P_{52}}{R^2}\right)\left(\frac{\partial^2 V}{\partial\theta^2} + \frac{\partial W}{\partial\theta}\right) - \left(\frac{P_{24}}{R} + \frac{P_{54}}{R^2}\right)\frac{\partial^3 W}{\partial x^2\partial\theta} + \frac{1}{R^2}\left(\frac{P_{25}}{R} + \frac{P_{55}}{R^2}\right)\left(-\frac{\partial^3 W}{\partial\theta^3} + \frac{\partial^2 V}{\partial\theta^2}\right)$$
$$+\left(P_{33} + \frac{3P_{63}}{2R}\right)\left(\frac{\partial^2 V}{\partial x^2} + \frac{\partial^2 U}{R\partial x\partial\theta}\right) + \frac{1}{R}\left(P_{36} + \frac{3P_{66}}{2R}\right)\left(-2\frac{\partial^3 W}{\partial x^2\partial\theta} + \frac{3}{2}\frac{\partial^2 V}{\partial x^2} - \frac{1}{2R}\frac{\partial^2 U}{\partial x\partial\theta}\right)$$

$$L_3(U,V,W,P_{ij}) = P_{41}\frac{\partial^3 U}{\partial x^3} + \frac{P_{42}}{R}\left(\frac{\partial^3 V}{\partial x^2\partial\theta} + \frac{\partial^2 W}{\partial x^2}\right) - P_{44}\frac{\partial^4 W}{\partial x^4} + \frac{P_{45}}{R^2}\left(-\frac{\partial^4 W}{\partial x^2\partial\theta^2} + \frac{\partial^3 V}{\partial x^2\partial\theta}\right) + \frac{2P_{63}}{R}\left(\frac{1}{R}\frac{\partial^3 U}{\partial x\partial\theta^2} + \frac{\partial^3 V}{\partial x^2\partial\theta}\right)$$
$$+\frac{2P_{66}}{R^2}\left(-2\frac{\partial^4 W}{\partial x^2\partial\theta^2} + \frac{3}{2}\frac{\partial^3 V}{\partial x^2\partial\theta} - \frac{1}{2R}\frac{\partial^3 U}{\partial x\partial\theta^2}\right) + \frac{P_{51}}{R^2}\frac{\partial^3 U}{\partial x\partial\theta^2} + \frac{P_{52}}{R^3}\left(\frac{\partial^3 V}{\partial\theta^3} + \frac{\partial^2 W}{\partial\theta^2}\right) + \frac{P_{55}}{R^4}\left(-\frac{\partial^4 W}{\partial\theta^4} + \frac{\partial^3 V}{\partial\theta^3}\right)$$
$$-\frac{P_{21}}{R}\frac{\partial U}{\partial x} - \frac{P_{54}}{R^2}\frac{\partial^4 W}{\partial x^2\partial\theta^2} + \frac{P_{22}}{R^2}\left(\frac{\partial V}{\partial\theta} + W\right) + \frac{P_{24}}{R^2}\frac{\partial^2 W}{\partial\theta^2} - \frac{P_{25}}{R^3}\left(-\frac{\partial^2 W}{\partial\theta^2} + \frac{\partial V}{\partial\theta}\right)$$

The coefficients of characteristic Eq. (5) are given by:

$$f_1 = p_{33} - p_{36}/R + p_{66}/4R^2$$
$$f_3 = p_{12} + p_{33} + (p_{15} + p_{36})/R - 3p_{66}/4R^2$$
$$f_5 = (p_{15} + 2p_{36} - p_{66}/R)/R$$
$$f_7 = p_{22} + p_{55}/R^2 + 2p_{25}/R$$
$$f_9 = p_{33} + 3p_{36}/R + 9p_{66}/4R^2$$
$$f_{11} = (2p_{36} + p_{24} + 3p_{66}/R + p_{54}/R)/R$$

$$f_8 = \left(f_9/r^2\right)\left(p_{11}p_{44} - p_{14}^2\right)$$
$$f_6 = \left(n^2/r^2\right)\left[f_9\left(f_1p_{44} + 2p_{11}p_{45} + 4p_{11}p_{66} - 2f_5rp_{14}\right) + f_7\left(p_{11}p_{44} - p_{14}^2\right) - r^2f_{11}^2p_{11} - f_3^2p_{44} + 2rf_3f_{11}p_{14}\right] +$$
$$\left(2/r\right)f_9\left(p_{11}p_{24} - p_{14}p_{12}\right)$$
$$f_4 = \left(n^4/r^2\right)\left[f_1f_7\,p_{44} + f_9p_{11}p_{55} + \left(2p_{45} + 4p_{66}\right)\left(f_1f_9 + f_7p_{11} - f_3^2\right) + \left(p_{25} + \left(1/r\right)p_{55}\right).\left(2f_3p_{14} - 2f_{11}p_{11}r\right) +$$
$$f_{11}r^2\left(2f_3f_5 - f_1f_{11}\right) - rf_5\left(2f_7p_{14} + rf_5f_9\right)\right] + \left(n^2/r\right).\left[2\left(p_{25} + rp_{22}\right)\left(\left(f_3/r\right)p_{14} - f_{11}p_{11}\right) -$$
$$2p_{12}\left(f_5f_9r + f_7p_{14} - f_3f_{11}r\right) - 2p_{24}\left(f_3^2 - f_1f_9 - f_7p_{11}\right) + 2\,f_9p_{11}p_{25}\right] + f_9\left(p_{11}p_{22} - p_{12}^2\right)$$
$$f_2 = \left(n^6/r^2\right)f_7\left(2p_{45} + 4p_{66}\right) + p_{55}\left(f_1f_9 + f_7p_{11} - f_3^2\right) - r^2f_5^2f_7 +$$
$$\left(p_{25} + \left(1/r\right)p_{55}\right).\left(-2rf_1f_{11} + 2rf_3f_5 - p_{11}p_{25} - \left(1/r\right)p_{11}p_{55}\right)\Big] +$$
$$\left(n^4/r\right)\Big[2f_1f_7p_{24} + 2p_{25}\left(f_1f_9 + f_7\,p_{11} - f_3^2\right) - 2p_{12}\left(rf_5f_7 - f_3p_{25} - \left(f_3/r\right)p_{55}\right)\Big] -$$
$$2\left(p_{25} + rp_{22}\right)\left(f_1f_{11} + \left(1/r\right)p_{11}p_{25} + \left(1/r^2\right)p_{11}p_{55} - f_3f_5\right)\Big] +$$
$$n^2\Big[p_{22}\left(f_1f_9 + f_7p_{11} - f_3^2\right) - \left(1/r\right)\left(p_{25} + rp_{22}\right)\left(\left(1/r\right)p_{11}p_{25} + p_{11}p_{22} - 2f_3p_{12}\right) - f_7p_{12}^2\Big]$$
$$f_0 = n^4f_1f_7\left[p_{22} + \left(2/r\right)n^2p_{25} + \left(n^4/r^2\right)p_{55}\right] - n^2f_1\left[\left(n^3/r\right)\left(p_{25} + \left(1/r\right)p_{55}\right) + \left(n/r\right)\left(p_{25} + rp_{22}\right)\right]^2$$

Matrices $[T]_{3\times3}$, $[R]_{3\times8}$, and $[A]_{8\times8}$ are defined as:

$$[T]=\begin{bmatrix}\cos(n\theta) & 0 & 0\\ 0 & \cos(n\theta) & 0\\ 0 & 0 & \sin(n\theta)\end{bmatrix}$$

$$R(1,i)=\alpha_i e^{\lambda_i x/R} \quad , \quad R(2,i)=e^{\lambda_i x/R} \quad , \quad R(3,i)=\beta_i e^{\lambda_i x/R} \qquad i=1,2,...,8$$

$$A(1,i)=\alpha_i, \quad A(2,i)=1, \quad A(3,i)=\frac{\lambda_i}{R}, \quad A(4,i)=\beta_i, \quad A(5,i)=\alpha_i e^{\lambda_i l/R}$$

$$A(6,i)=e^{\lambda_i l/R}, \quad A(7,i)=\frac{\lambda_i}{R}e^{\lambda_i l/R}, \quad A(8,i)=\beta_i e^{\lambda_i l/R} \qquad i=1,2,...8$$

Expressions $\{\varepsilon_L\}$ and $\{\varepsilon_{NL}\}$ for cylindrical shells are given by:

$$\{\varepsilon_L\}=\begin{Bmatrix}\frac{\partial U}{\partial x}\\ \frac{1}{R}\left(\frac{\partial V}{\partial \theta}+W\right)\\ \frac{\partial V}{\partial x}+\frac{1}{R}\frac{\partial U}{\partial \theta}\\ -\frac{\partial^2 W}{\partial x^2}\\ -\frac{1}{R^2}\left(\frac{\partial^2 W}{\partial \theta^2}-\frac{\partial V}{\partial \theta}\right)\\ -\frac{2}{R}\frac{\partial^2 W}{\partial x\partial \theta}+\frac{3}{2R}\frac{\partial V}{\partial x}-\frac{1}{2R^2}\frac{\partial U}{\partial \theta}\end{Bmatrix}$$

and

$$\{\varepsilon_{NL}\}=\begin{Bmatrix}\frac{1}{2}\left(\frac{\partial W}{\partial x}\right)^2+\frac{1}{8}\left(\frac{\partial V}{\partial x}-\frac{1}{R}\frac{\partial U}{\partial \theta}\right)^2\\ \frac{1}{2R^2}\left(V-\frac{\partial W}{\partial \theta}\right)^2+\frac{1}{8}\left(\frac{\partial V}{\partial x}-\frac{1}{R}\frac{\partial U}{\partial \theta}\right)^2\\ \frac{1}{2R}\left(\frac{\partial W}{\partial x}\frac{\partial W}{\partial \theta}-V\frac{\partial W}{\partial x}\right)\\ 0\\ 0\\ 0\end{Bmatrix}$$

Matrices $\left[B_{pq}\right]$ and $\left[C_{pq}\right]$

$$B_{pq}=b_{pq}e^{(\lambda_p+\lambda_q)x/R} \qquad C_{pq}=c_{pq}e^{(\lambda_p+\lambda_q)x/R}$$

where

$$b_{pq}=\frac{1}{2R^2}\left[\frac{1}{4}a_{pq}^{(1)}+b_{pq}^{(1)}\right]\sin^2(n\theta) \qquad c_{pq}=-\frac{1}{4R^2}\left[c_{pq}^{(1)}+c_{pq}^{(2)}\right]\sin(n\theta)\cos(n\theta)$$

with

$$a_{pq}^{(1)}=\left(\beta_p\lambda_p+n\alpha_p\right)\left(\beta_q\lambda_q+n\alpha_q\right) \qquad b_{pq}^{(1)}=\left(n+\beta_p\right)\left(n+\beta_q\right)$$

$$c_{pq}^{(1)}=n\left(\lambda_p+\lambda_q\right) \qquad p,q=1,...,8$$

2.9 References

1. E. Reissner, Non-linear Effects in Vibrations of Cylindrical Shells, Ramo-Wooldridge Corporate Report. (1995) AM5-6.

2. B.E. Cummings, Some non-linear vibration and response problems of cylindrical panels and shells, Graduate aeronautical Laboratories, California Institute of technology, Pasadona. (1962) SM 62-32 (AFOSR 3123).

3. H.N. Chu, Influence of large amplitudes on flexural vibrations of thin circular cylindrical shells, Journal of aerospace Sciences. 28 (1961) 602-609.

4. D.A. Evensen, Some observations on the non-linear vibration of thin cylindrical shells, American Institute of Aeronautics and Astronautics Journal. 1(1966) 2857-2858.

5. J. Nowinski, Non-linear transverse vibrations of orthotropic cylindrical shells, American Institute of Aeronautics and Astronautics. 1 (1963) 617-620.

6. M.D. Olson, Some experimental observations on the non-linear vibration of cylindrical shell, American Institute of Aeronautics and Astronautics 3 (1965) 1775-1777.

7. D.A. Evensen and R.E. Fulton, Some studies on the non-linear dynamic response of shell-type structures, Proceedings of an International Conference on Dynamic Stability of Structures, Evanston, IL 237-254, Oxford & New York: Pergamon Press (1966).

8. D.A. Evensen, Nonlinear flexural vibrations of thin-walled circular cylinders, Nasa Technical Note, Langley Research Center, (1967) NASA- TN D-4090 .

9. D.A. Evensen, Non-linear vibrations of an infinitely long cylindrical shell, American Institute of Aeronautics and Astronautics Journal. 6 (1968) 1401-1403.

10. S. Atluri, A perturbation analysis of non-linear free flexural vibrations of a circular cylindrical shell, International Journal of Solids and Structures. 8(1972) 549-569.

11. E.H. Dowell and C.S. Ventres, Modal equations for the non-linear flexural vibrations of a cylindrical shell, International Journal of Solids and Structures. 4 (1968) 975-991.

12. J.C. Chen and C.D. Babcock, Non-linear vibration of cylindrical shells, American Institute of Aeronautics and Astronautics Journal, 13 (1975) 868-876.

13. H. Radwan and J. Genin, Non-linear modal equations for thin elastic shells, International Journal of Non-linear Mechanics. 10 (1975) 15-29.

14. H.R. Radwan and J. Genin, Non-linear vibrations of thin cylinders. Journal of Applied Mechanics, 43(1976) 370-372.

15. M. Ganapathi and T.K. Varadan, Large amplitude vibrations of circular cylindrical shells, Journal of sound and vibration. 192 (1996), 1-14.

16. H.V Ramani, An analytical investigation of large amplitude free flexural vibration of thin circular cylindrical shells, M.S. Dissertation (1985), Indian Institute of Technology, Madras, India.

17. A.A. Lakis and M.P. Paidoussis, Dynamic Analysis of Axially Non-Uniform Thin Cylindrical Shells, Journal of Mechanical Engineering Science. 14(1) (1972) 49-71.

18. A. Selmane, and A.A. Lakis, Non-Linear Dynamic Analysis of orthotropic Open Cylindrical Shells Subjected to a Flowing Fluid, Journal of Sound and Vibration. 202(1) (1997) 67-93.

19. J.L. Sanders, An Improved First-Approximation Theory for Thin Shell. (1959) NASA R-24.

20. M.H. Toorani, and A.A. Lakis, General equations of Anisotropic Plates and Shells Including Transverse shear Deformations, Rotary Inertia and Initial Curvature Effects, Journal of Sound and Vibration. 237(4) (2000) 561-651.

21. R. Rougui, and F. Moussaoui, R. Benamar, Geometrically non- linear free and forced vibrations of simply supported circular cylindrical shells: A semi-analytical approach, International Journal of Non-linear Mechanics. 42 (2007) 1102-1115.

22. J.L. Nowinski, Non-linear transverse vibrations of orthotropic cylindrical shells, AIAA . 1 (1963) 617-620.

23. K.K, Raju, G.V. Rao, Large amplitude asymmetric vibrations of some thin elastic shells, Int. J. Non-linear Mech. 10 (1975) 15-29.

24. M. Amabili, F. Pellicano, M.P. Paidoussis, Non-linear vibrations of simply supported circular cylindrical shells coupled to quiescent fluid, J. Fluids Struct. 12 (1998) 883-918.

CHAPITE 3: ARTICLE 2 - EFFECTS OF GEOMETRIC NONLINEAIRITIES ON CYLINDRICAL SHELLS SUBJECTED TO A SUPERSONIC FLOW

Submitted, 15 June 2012 to Computers and Fluids

Redouane Ramzi and Aouni Lakis

3.1 Abstract

A nonlinear analysis is presented for cylindrical shells subjected to supersonic flow using Sanders-Koiter nonlinear shell theory for large amplitude of vibrations and linear piston theory for modeling the fluid/structure interaction. Internal pressure and axial loads are taken into account. A hybrid finite element is developed and applied for discretizing the system. Linear and nonlinear mass, stiffness and damping matrices are found. The governing equation of the system is resolved using the Runge Kutta numerical method. The flutter amplitude of vibration versus the flutter frequency is obtained. Several parameters that are critical in the design of aeronautic structures are investigated here. Results show that the system loses stability due to coupled mode flutter; however a softening type of nonlinearity in all cases studied occurs beyond the flutter. The results are in good agreement with existing theoretical and experimental results for flutter frequency and amplitude published in the literature.

3.2 Nomenclature

a_∞	Freestream speed of sound
A_i	Motion amplitude
[A]	Matrix defined in Appendix
[B]	Defined by Equation 11
$[C_f]$	Aerodynamic damping matrix of fluid
a_p, b_p, c_p	Modal coefficients determined by equation 20
a_{pq}, b_{pq}, c_{pq}	Coefficients determined by equations in Appendix
$a^{(i)}_{pq}, b^{(i)}_{pq}, c^{(i)}_{pq}$	Coefficients determined by equations in Appendix
A_{pq}, B_{pq}, C_{pq}	Modal coefficients determined by equations in Appendix
$A_{prs}, B_{prs}, C_{prs}, D_{prs}, E_{prs}$	Modal coefficients determined by equation 19
$A_{prsq}, B_{prsq}, C_{prsq}, D_{prsq}, E_{prsq}$	Modal coefficients determined by equation (19, 22)

D	Membrane stiffness, defined by Equation 3
$\{\varepsilon\}$	Deformation vector giving in Appendix
E	Young's modulus
[E]	Matrix defined by Equation 23
$\{F_p\}$	Force vector due to the aerodynamic pressure field
h	Shell thickness
K	Bending stiffness of shell, defined by Equation 3
$[K_s]$	Global stiffness matrix for a shell
[k]	Stiffness matrix for a shell element
$[k_f]$	Local aerodynamic stiffness matrix
$[k_I]$	Initial stiffness matrix for a shell element
$[K_f]$	Global aerodynamic damping matrix
$[K_I]$	Global initial stiffness matrix for a shell
$[K^{NL2}]$	Nonlinear stiffness matrix of second order
$[K^{NL3}]$	Nonlinear stiffness matrix of third order
L	Shell length
M	Mach number
$[M_s]$	Global mass matrix for a shell
n	Circumferential number
[m]	Mass matrix for a shell element
N	Cylindrical shell number
$N_x, N_\theta, N_{x\theta}$	Stress resultant for a circular cylindrical shell
$\overline{N}_x$, $\overline{N}_\theta$	Stress resultant due to shell internal pressure and axial compression
[N]	Defined by Equation 10
p_a	Aerodynamic pressure
p_∞	Freestream static pressure
p_m, p_x	Shell internal pressure and axial compression
[P]	Elasticity matrix
Q_x, Q_θ	Transverse stress resultant for a circular cylindrical shell
R	Shell radius
$[R_f]$	Matrix defined in Appendix

U	Axial displacement
U_i	Potential energy due to initial strain
V	Circumferential displacement
W	Radial displacement
x	Longitudinal coordinate
δ_i, δ_j	Displacement at node i and j
λ_j	Complex roots of the characteristic equation
υ	Poisson's ratio
γ	Adiabatic exponent
θ	Circumferential coordinate
ρ	Shell density
ρ_f	Fluid density
ω	Oscillation frequency
$\emptyset_{xx}$, $\emptyset_{x\theta}$, $\emptyset_n$	Elastic rotations for a circular cylindrical shell
$\{\sigma\}$	Stress vector

3.3 Introduction

The aeroelastic stability of closed cylindrical shells in supersonic flow is of keen interest for designers of skin panels of missiles, the space shuttle, and military aerospace vehicles. The first event of flutter instability on these structures appears to have been on the V-2 rocket. Among authors who focus their studies on developing linear models to investigate shell stability in supersonic flow, we find: Dowell, Olson and Fung, Barr and Stearman, and Ganapathi et al. However, a major difference occurs between experimental results and those from linear studies for prediction of flutter and the behavior of structures during flutter. A nonlinear study therefore becomes necessary to explain the behavior observed in the experiments. Very few studies have addressed the nonlinear aeroelastic stability of cylindrical shells subjected to supersonic flow.

In 1955, Librescu [1,2] was the first to study the stability of circular cylindrical finite shallow shells. He used Donnell's nonlinear shallow shell theory and piston theory for calculating the supersonic flow pressure, taking into account only simple mode expansion. No results on limit cycle amplitudes were given. A simplified form of Donnell's nonlinear shallow shell theory is applied by Olson and Fung [3] for simply-supported shells considering a simple two-mode

expansion including an axisymmetric term. The supersonic flow/structure interaction was modeled using linear piston theory. Evensen and Olson [5] considered the companion mode and four-degree-of-freedom mode expansion, which allows the study of travelling-wave flutter. The same behavior of travelling waves is predicted and measured for large-amplitude forced vibration of shells. Following this study, linear theoretical and experimental studies of supersonic flutter of circular cylindrical shells including geometric imperfections were published by Carter and Stearman [6] and Barr and Stearman [7,8]. They also developed a linear piston theory to calculate the supersonic flow pressure for Mach numbers superior to 1.6. Vol'mir and Medvedeva [9], studied the nonlinear supersonic flutter of circular cylindrical shells, considering the initial deflection and axial loads. They used a combination of Donnell's nonlinear shallow shell theory and linear piston theory; the finite difference numerical method was applied to search the solutions.

Amabili and Pellicano [10] investigated the aeroelastic stability of simply-supported, circular cylindrical shells in supersonic flow using Donnell's nonlinear shallow-shell theory describing large amplitude and linear piston theory to modulate the fluid flow/structure interaction. Their study takes into account structural damping and employs the Galerkin Method for descretizing the system. Results show that the system loses stability by standing wave flutter through supercritical bifurcation, however a very small increment in the free streamstatic pressure can produce a travelling wave flutter.

Horn et al [11] conducted an experimental study of the stability of circular cylindrical shells in axial air-flow of both subsonic and supersonic regimes. Divergence was found for subsonic flow and flutter for supersonic flow. Another experimental study of supersonic flutter of pressurized and axially compressed circular cylindrical shells was performed at the NASA Ames Research Center, California, in 1962 and 1964 [12].

The approach presented in this paper is summarized in three points:

- Using linear strain-displacement and stress-strain relationships which are inserted into Sander's equations of equilibrium, we determine the displacement functions by solving the linear equation system. We then determine the mass and linear stiffness matrices for a finite element and assemble the matrices for the complete shell.

- Using strain-displacement relationships from Sanders-Koiter nonlinear theory, the modal coefficients are obtained from the displacement functions. The second and third-order nonlinear stiffness matrices for a finite element are then calculated by precise analytical integration with respect to modal coefficients.

- Linear piston theory is applied for modeling and determining the supersonic flow pressure and describing the structure/fluid interaction.

The equations of cylindrical shells are used to obtain the displacement functions instead of using the more common arbitrary polynomial forms. The finite element proposed is a closed cylindrical segment (Figure 3.1) with four degrees of freedom at each node: axial, radial, circumferential, and rotational.

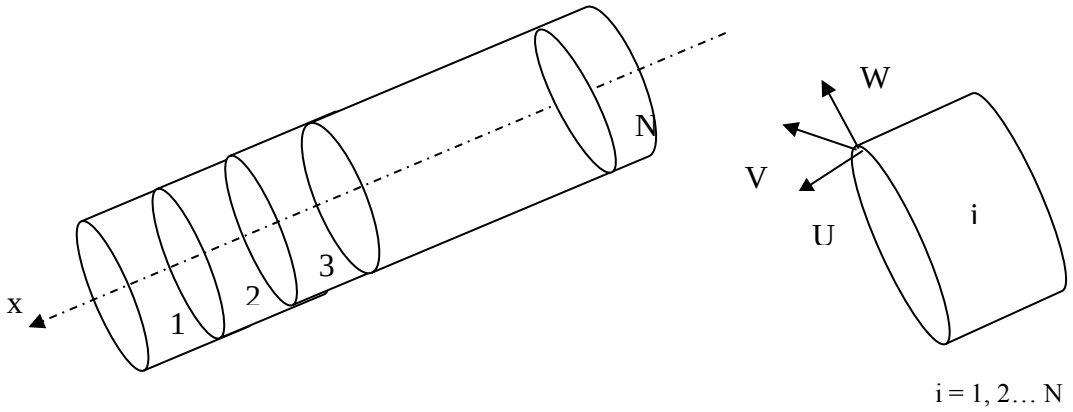

Figure 3.1: Cylindrical shell and finite element geometries

The approach developed here is more accurate than usual finite element methods. Different arbitrary boundary conditions can be used, and high and low frequencies may be obtained with high accuracy. Precise results are obtained with low and high circumferential wave numbers. Large amplitude vibration can be examined. The presented approach also enables short computation time and higher precision of results due to use of exactitude piston theory, which yields the pressure created by supersonic air flow at each point in the structure.

3.4 Structural Model

3.4.1 Linear Part

The equations of motion of an anisotropic cylindrical shell in terms of U, V and W (axial, tangential and radial displacements) (Figure 3.2) are written as follows:

$$L_J(U,W,V,P_{ij}) = 0 \tag{1}$$

Where $L_J(J=1,2,3)$ are three linear partial differential equations (given in Appendix) and p_{ij} are elements of the elasticity matrix for anisotropic shells which is given by:

$$[P] = \begin{bmatrix} p_{11} & p_{12} & 0 & p_{14} & p_{15} & 0 \\ p_{21} & p_{22} & 0 & p_{24} & p_{25} & 0 \\ 0 & 0 & p_{33} & 0 & 0 & p_{36} \\ p_{41} & p_{42} & 0 & p_{44} & p_{45} & 0 \\ p_{51} & p_{52} & 0 & p_{54} & p_{55} & 0 \\ 0 & 0 & p_{63} & 0 & 0 & p_{66} \end{bmatrix}$$

For the isotropic case,

$$[P] = \begin{bmatrix} D & \upsilon D & 0 & 0 & 0 & 0 \\ \upsilon D & D & 0 & 0 & 0 & 0 \\ 0 & 0 & \frac{D(1-\upsilon)}{2} & 0 & 0 & 0 \\ 0 & 0 & 0 & K & \upsilon K & 0 \\ 0 & 0 & 0 & \upsilon K & K & 0 \\ 0 & 0 & 0 & 0 & 0 & \frac{K(1-\upsilon)}{2} \end{bmatrix} \tag{2}$$

where,

$$K = \frac{Eh^3}{12(1-\upsilon^2)} \quad \text{Bending stiffness,} \qquad D = \frac{Eh}{1-\upsilon^2} \quad \text{Membrane stiffness} \tag{3}$$

The displacement functions associated with the circumferential wave number are assumed in the normal manner, as:

$$\begin{aligned} U(x,\theta) &= Ae^{\frac{\lambda x}{R}}\cos(n\theta) \\ W(x,\theta) &= Be^{\frac{\lambda x}{R}}\cos(n\theta) \\ V(x,\theta) &= Ce^{\frac{\lambda x}{R}}\sin(n\theta) \end{aligned} \tag{4}$$

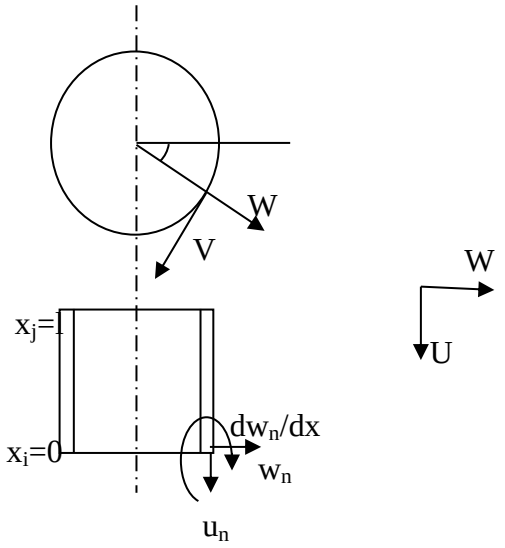

Figure 3.2: Finite element discretization and nodal displacement

where n is the circumferential mode,

Note that this approach treats closed cylindrical shells based on the circumferential wave number, not on the longitudinal wave number.

Substituting (4) into the equations of motion (1), a system of three homogeneous equations, linear functions of constants A, B, C, is obtained. For the solution to be non-trivial, the determinant of this system must be equal to zero. This brings us to the following characteristic equation:

$$Det\left(\left[H\right]\right) = f_8\lambda^8 + f_6\lambda^6 + f_4\lambda^4 + f_2\lambda^2 + f_0 \qquad (5)$$

The values of coefficients f_i in this eighth-degree polynomial are given in Appendix.

Each root of this equation yields a solution to the linear equations of motion (1). The complete solution is obtained by adding the eight solutions independently with constants A_i, B_i and C_i (i = 1,2,….,8). These constants are not independent. We can therefore express A_i and B_i as a function of C_i, as follows:

$$A_i = \alpha_i C_i$$
$$B_i = \beta_i C_i \qquad (6)$$

The values of α_i and β_i can be obtained from system (1) by introducing relation (6). To determine eight C_i constants, it is necessary to formulate eight boundary conditions for the finite elements. The axial, tangential and radial displacements will be specified for each node. The following relation defines the element displacement vector at the boundaries:

$$\begin{Bmatrix}\delta_i\\ \delta_j\end{Bmatrix} = \{u_i \;\; v_i \;\; w_i \;\; u_j \;\; v_j \;\; w_j\}^T \tag{7}$$

$$\begin{Bmatrix}\delta_i\\ \delta_j\end{Bmatrix} = [A]\{C\} \tag{8}$$

where the elements of matrix [A] are given in Appendix.

Multiplying Equation (8) by $[A]^{-1}$ and substituting the result into Equation (4), we obtain

$$\begin{Bmatrix}U(x,\theta)\\ V(x,\theta)\\ W(x,\theta)\end{Bmatrix} = [N]\begin{Bmatrix}\delta_i\\ \delta_j\end{Bmatrix} \tag{9}$$

where [N] represents the shape function matrix given in this form:

$$[N] = [T][R]\left[A^{-1}\right] \tag{10}$$

and [T], [R], [A] are described in Appendix.

The constitutive relation between the stress and deformation vector of a cylindrical shell is given as:

$$\{\sigma\} = [P][B]\begin{Bmatrix}\delta_i\\ \delta_j\end{Bmatrix} \tag{11}$$

The mass and stiffness matrices for each element are derived using the classic finite element procedure and can then be expressed as:

$$\begin{aligned}[m] &= \rho h \iint [N]^T [N]\, dA\\ [k] &= \iint [B]^T [P][B]\, dA\end{aligned} \tag{12}$$

Where ρ is the density of the shell, h its thickness and $dA = Rdxd\theta$. The matrices [m] and [k] are obtained analytically by carrying out the necessary matrix operations over x and θ in the

equation. The global matrices $[M_s]$ and $[K_s]$ may be obtained, respectively, by assembling the mass and stiffness matrices for each individual finite element.

3.4.2. Nonlinear Part

The coefficients of the modal equations are obtained using the Lagrange method in the same way developed by Radwan and Genin [13], paying attention to geometric nonlinearities. Following this, the second and third nonlinear stiffness matrices corresponding to geometric nonlinearities are computed and superimposed on the linear system.

Shell displacements (u, v, w) are expressed as sums of generalized product coordinates $q_i(t)$ and spatial functions U, V, W (see Eq. (4)).

$$\begin{aligned} u &= \sum_i q_i(t) U_i(x,\theta) \\ v &= \sum_i q_i(t) V_i(x,\theta) \\ w &= \sum_i q_i(t) W_i(x,\theta) \end{aligned} \tag{13}$$

The deformation vector is written as a function of the generalized coordinates by separating the linear part from the nonlinear part.

$$\{\varepsilon\} = \{\varepsilon_L\} + \{\varepsilon_{NL}\} = \{\varepsilon_{xx}, \varepsilon_{\theta\theta}, 2\varepsilon_{x\theta}, \kappa_{xx}, \kappa_{\theta\theta}, 2\kappa_{x\theta}\}^T \tag{14}$$

Where subscripts ``L`` and ``NL`` mean ``linear`` and ``nonlinear``, respectively, and ε_L and ε_{NL} are defined in Appendix.

The Lagrange's equations of motion in generalized coordinates $q_i(t)$ are found using Hamilton's principle and Equation (13):

$$\frac{d}{dt}\left(\frac{\partial T}{\partial \dot{q}_i}\right) - \frac{\partial T}{\partial q_i} + \frac{\partial V}{\partial q_i} = Q_i \tag{15}$$

where T is the total kinetic energy, V is the total elastic strain energy of deformation and the Q_i's are the generalized forces.

Using the vector deformation given by (14), the developed formulation for total kinetic and strain energy and inserting these into the Lagrange equation (15), the following nonlinear modal equations are obtained after a long development of equations:

$$\sum_r m_{pr}\ddot{\delta}_r + \sum_r k_{pr}^{(L)}\delta_r + \sum_r \sum_s k_{prs}^{(NL2)}\delta_r\delta_s + \sum_r \sum_s \sum_q k_{prsq}^{(NL3)}\delta_r\delta_s\delta_q = 0 \qquad p = 1, 2, ... \tag{16}$$

Where m_{pr}, $k_{pr}^{(L)}$ are terms of the mass and linear stiffness matrices given by Equation (12). The terms $k_{prs}^{(NL2)}$ and $k_{prsq}^{(NL3)}$ represent the second and third-order nonlinear stiffness and are given by the following integrals for the case of an isotropic closed cylindrical shell:

$$K_{prs}^{(NL2)} = \iint \left\{ p_{11}A_{prs} + p_{22}B_{prs} + p_{12}(D_{prs} + E_{prs}) + p_{33}C_{prs} \right\} dA \tag{17}$$

and

$$K_{prsq}^{(NL3)} = \iint \left\{ p_{11}A_{prsq} + p_{22}B_{prsq} + p_{12}(D_{prsq} + E_{prsq}) + p_{33}C_{prsq} \right\} dA \tag{18}$$

Where $dA = Rdxd\theta$, p_{ij} are the terms of the elasticity matrix [P], and the terms A_{prs}, B_{prs}, C_{prs}, D_{prs}, E_{prs} and A_{prsq}, B_{prsq}, C_{prsq}, D_{prsq}, E_{prsq} represent the coefficients of the modal equations. These coefficients are given by the following equations:

$$\begin{aligned}
A_{prs} &= a_p A_{rs} + a_r A_{sp} + a_s A_{pr} & \qquad A_{prsq} &= 2A_{pq} A_{rs} \\
B_{prs} &= b_p B_{rs} + b_r A_{sp} + b_s B_{pr} & \qquad B_{prsq} &= 2B_{pq} B_{rs} \\
C_{prs} &= c_p C_{rs} + c_r C_{sp} + c_s C_{pr} & \qquad C_{prsq} &= 2C_{pq} C_{rs} \\
D_{prs} &= a_r B_{sp} + a_s B_{pr} + b_p A_{rs} & \qquad D_{prsq} &= 2A_{pq} B_{rs} \\
E_{prs} &= b_r A_{sp} + b_s A_{pr} + a_s B_{rs} & \qquad E_{prsq} &= 2B_{pq} A_{rs}
\end{aligned} \tag{19}$$

with

$$a_p = U_{p,x}, \qquad b_p = 1/R\,(V_{p,\theta} + W_p), \qquad c_p = 1/2\,(U_{p,\theta}/R + V_{p,x})$$

$$\begin{aligned}
A_{pq} &= 1/8\,R^2\,(R\,V_{p,x} - U_{p,\theta})\,.\,(R\,V_{q,x} - U_{q,\theta}) + 1/2\,W_{p,x}W_{q,x} \\
B_{pq} &= 1/8\,R^2\,(R\,V_{p,x} - U_{p,\theta})\,.\,(R\,V_{q,x} - U_{q,\theta}) + 1/2\,R^2\,(W_{p,\theta} - V_p)\,.\,(W_{q,\theta} - V_q) \\
C_{pq} &= 1/4\,R\,(W_{p,x}W_{q,\theta} - W_{q,x}W_{p,\theta}) - 1/4\,R\,(V_p W_{q,x} + V_q W_{p,x})
\end{aligned} \tag{20}$$

Where U, V and W are spatial functions determined by Equation (4).

In Equations (16) - (20), the subscripts ‘p,q’, ’p,r,s’ and ‘p,r,s,q’ represent the coupling between two, three and four modes, respectively.

Let us illustrate the development of the expression for the (p,q) term of matrices A_{pq} and A_{pqrs}. The expression A_{pq} is given by:

$$A_{pq} = a_{pq} e^{\left(\lambda_p + \lambda_q\right) x/R} \tag{21}$$

and A_{pqrs} is :

$$A_{prsq} = \sum_{r=1}^{8} \sum_{s=1}^{8} a_{rs} a_{pq} \varepsilon_{rs} e^{(\lambda_p + \lambda_r + \lambda_s + \lambda_q) x/R} \tag{22}$$

ε_{rs} is the term (r,s) of matrix [E], where [E] represents a matrix of constants defined by $[E] = \left[A^{-1}\right]^T [A]$ (23) , and

$$a_{pq} = \frac{1}{2R^2}\left[\frac{1}{4} a_{pq}^{(1)} \sin^2\left(n\theta\right) + a_{pq}^{(2)} \cos^2\left(n\theta\right)\right] \tag{24}$$

with

$$a_{pq}^{(1)} = \left(\beta_p \lambda_p + n\alpha_p\right)\left(\beta_q \lambda_q + n\alpha_q\right) \tag{25}$$

$$a_{pq}^{(2)} = \lambda_p \lambda_q \tag{26}$$

Similarly, the matrices $[B_{pq}]$… $[E_{prsq}]$ can be written as a function of α, β, λ, x and θ. The (p, q) terms of these matrices are described in Appendix. For details of the basis of the presented method, consult reference [13].

After integration, we obtain:

$$\left[k_{prs}^{(NL2)}\right] = \left[A^{-1}\right]^T \left[J^{(NL2)}\right]\left[A^{-1}\right] \tag{27}$$

$$\left[k_{prsq}^{(NL3)}\right] = \frac{\pi}{8R^2}\left[A^{-1}\right]^T \left[J^{(NL3)}\right]\left[A^{-1}\right] \tag{28}$$

The (p,q) terms in matrix $\left[J_{p,q}^{(NL2)}\right]$ and $\left[J_{p,q}^{(NL3)}\right]$ are written as:

$$J^{(NL2)}(p,q)=\begin{cases}\displaystyle\sum_{l=1}^{8}\sum_{s=1}^{8}\frac{\varepsilon_{sr}}{\left(\lambda_p+\lambda_q+\lambda_r\right)}G1(p,q)\left[e^{\left(\lambda_p+\lambda_q+\lambda_r\right)\frac{\ell}{R}}-1\right]\\ if\ \lambda_p+\lambda_q+\lambda_r\neq 0\\ \displaystyle\sum_{k=1}^{8}\sum_{l=1}^{8}\varepsilon_{sr}G1(p,q)\frac{\ell}{R}\\ if\ \lambda_p+\lambda_q+\lambda_r=0\end{cases} \tag{29}$$

and

$$J^{(NL3)}(p,q)=\begin{cases}\displaystyle\sum_{k=1}^{8}\sum_{l=1}^{8}\frac{\varepsilon_{sr}}{\left(\lambda_p+\lambda_q+\lambda_r+\lambda_s\right)}G2(p,q)\left[e^{\left(\lambda_p+\lambda_q+\lambda_r+\lambda_s\right)\frac{\ell}{R}}-1\right]\\ if\ \lambda_p+\lambda_q+\lambda_r+\lambda_s\neq 0\\ \displaystyle\sum_{k=1}^{8}\sum_{l=1}^{8}\varepsilon_{sr}G2(p,q)\frac{\ell}{R}\\ if\ \lambda_p+\lambda_q+\lambda_r+\lambda_s=0\end{cases} \tag{30}$$

where G1(p,q) and G2(p,q) are coefficients in conjunction with α, β, λ and elements p_{ij} in matrix [P]. The general expressions of G1(p,q) and G2(p,q) are given by :

$$\begin{aligned}\mathrm{G1(p,q)} = {} & p_{11}II_1\left[a_p^{(1)}A^{-1}a_{rs}^{(1)}+a_r^{(1)}A^{-1}a_{sp}^{(1)}+a_s^{(1)}A^{-1}a_{pr}^{(1)}\right]\\ & +p_{11}II_2\left[a_p^{(1)}A^{-1}a_{rs}^{(2)}+a_r^{(1)}A^{-1}a_{sp}^{(2)}+a_s^{(1)}A^{-1}a_{pr}^{(2)}\right]\\ & +p_{22}II_1\left[b_p^{(1)}A^{-1}b_{rs}^{(2)}+b_r^{(1)}A^{-1}b_{sp}^{(2)}+b_s^{(1)}A^{-1}b_{pr}^{(2)}\right]\\ & +p_{33}II_1\left[c_p^{(1)}A^{-1}c_{rs}^{(1)}+c_r^{(1)}A^{-1}c_{sp}^{(1)}+c_s^{(1)}A^{-1}c_{pr}^{(1)}\right]\\ & +p_{12}II_1+\left[a_r^{(1)}A^{-1}b_{sp}^{(1)}+a_s^{(1)}A^{-1}a_{pr}^{(1)}+b_p^{(1)}A^{-1}a_{rs}^{(1)}\right]\\ & +p_{12}II_2\left[b_p^{(1)}A^{-1}a_{rs}^{(2)}\right]\\ & +p_{12}II_1\left[b_r^{(1)}A^{-1}a_{sp}^{(1)}+b_s^{(1)}A^{-1}a_{pr}^{(1)}+a_p^{(1)}A^{-1}b_{rs}^{(1)}\right]\\ & +p_{12}II_2\left[b_r^{(1)}A^{-1}a_{sp}^{(2)}+b_s^{(1)}A^{-1}a_{pr}^{(2)}\right]\end{aligned} \tag{31}$$

where,

$$II_1=\frac{\sin^3(2\pi n)}{3} \tag{32}$$

$$II_2=\frac{\sin(2\pi n)(2+\cos^2(2\pi n))}{3n} \tag{33}$$

and

$$
\begin{aligned}
G2(p,q) = \frac{3}{16}(p_{11}+p_{22}+2p_{12})a_{pl}^{(1)}a_{kq}^{(1)} + 3\left(p_{11}a_{pl}^{(2)}a_{kq}^{(2)} + p_{22}b_{pl}^{(1)}b_{kq}^{(1)}\right) \\
+ p_{12}\left(a_{pl}^{(2)}b_{kq}^{(1)} + b_{pl}^{(1)}a_{kq}^{(2)}\right) + \frac{1}{4}(p_{11}+p_{12})\left(a_{pl}^{(2)}a_{kq}^{(1)} + a_{pl}^{(1)}a_{kq}^{(2)}\right) \\
+ \frac{3}{4}(p_{12}+p_{22})\left(a_{pl}^{(1)}b_{kq}^{(1)} + b_{pl}^{(1)}a_{kq}^{(1)}\right) \\
+ \frac{1}{4}p_{33}\left(c_{pl}^{(1)}c_{kq}^{(1)} + c_{pl}^{(2)}c_{kq}^{(2)} + c_{pl}^{(2)}c_{kq}^{(1)} + c_{pl}^{(1)}c_{kq}^{(2)}\right)
\end{aligned}
\tag{34}
$$

where the terms $a^{(1)}$ and $a^{(2)}$ are given by Equations (25-26). Terms $b^{(1)\cdots}$, $c^{(1)}$…and $c^{(2)}$ are coefficients appearing in expressions for the elements of matrices $[B_{pq}]$ and $[C_{pq}]$ defined in Equations (20). These coefficients are given in Appendix.

3.5 Stress Matrix

The potential energy is given as:

$$
U_i = 1/2\int_0^l\int_0^{2\pi}\left[\overline{N}_x\phi_{\theta\theta}^2 + \overline{N}_\theta\phi_{xx}^2 + (\overline{N}_x+\overline{N}_\theta)\phi_n^2\right]Rd\theta dx \tag{35}
$$

where;

$$
\begin{aligned}
\overline{N}_x &= -\frac{p_x}{2\pi R} \\
\overline{N}_\theta &= p_m R
\end{aligned}
\tag{36}
$$

$\overline{N}_x$, $\overline{N}_\theta$ are stress resultants due to shell internal pressure p_m and axial compression p_x respectively, l is the element length, $\phi_{\theta\theta}$ is about the normal to the $x\theta$ plane, ϕ_{xx} is the strain rotation about x, and ϕ_n is the rotation about the normal to a shell element.

This rotation vector is expressed as [14],

$$
\begin{aligned}
\phi_{\theta\theta} &= -\frac{\partial W}{\partial x} \\
\phi_{xx} &= \frac{1}{R}(V - \frac{\partial W}{\partial \theta}) \\
\phi_n &= \frac{1}{2}(-\frac{1}{R}\frac{\partial U}{\partial \theta} + \frac{\partial V}{\partial x})
\end{aligned}
\tag{37}
$$

Upon insertion of displacements (U,W,V) given in Equation (8), the potential energy is rewritten in terms of the nodal degrees of freedom, which leads to the initial stiffness matrix for each element in the following form:

$$[k_I] = \int_0^l \int_0^{2\pi} [N]^T [C_0]^T \begin{bmatrix} \overline{N}_x & 0 & 0 \\ 0 & \overline{N}_\theta & 0 \\ 0 & 0 & \overline{N}_x + \overline{N}_\theta \end{bmatrix} [C_0]^T [N]^T \, R d\theta dx \tag{38}$$

where;

$$[C_0] = \begin{bmatrix} 0 & -\dfrac{\partial}{\partial x} & 0 \\ 0 & -\dfrac{1}{R}\dfrac{\partial}{\partial \theta} & 0 \\ -\dfrac{1}{2R}\dfrac{\partial}{\partial \theta} & 0 & \dfrac{1}{2}\dfrac{\partial}{\partial x} \end{bmatrix} \tag{39}$$

3.6 Aerodynamic Model

The pressure on the body surface is approximated by the pressure exerted by a piston moving in the flow with a velocity equivalent to the superposition of the velocity due to the changing of body shape and the velocity due to the rigid-body motion of the body:

$$\frac{p}{p_\infty} = \left\{ 1 + \left[(\gamma - 1)/2 \right] \left(\omega / a_\infty \right) \right\}^{2\gamma/(\gamma-1)} \tag{40}$$

where;

p is the aerodynamic pressure,

p_∞ is the freestream static pressure,

γ is the adiabatic exponent,

a_∞ is the freestream speed of sound

ω is the velocity of the piston.

The piston velocity ω is given by [18,19]:

$$\omega = \frac{\partial W}{\partial t} + U_\infty \frac{\partial W}{\partial x} \tag{41}$$

U_∞ is the freestream velocity and W is the radial displacement.

Considering the linear terms in the binomial expansion of Equation (40), we obtain:

$$P_a = -\gamma P_\infty \left[M \frac{\partial W}{\partial x} + \frac{1}{a_\infty} \frac{\partial W}{\partial t} \right] \tag{42}$$

The form of the radial displacement assumed is the same as that considered by Lakis and Paidoussis in [15]:

$$W = \sum_{j=1}^{8} e^{i(\lambda_j \frac{x}{R} + \omega t)} cos(n\theta) = \sum_{j=1}^{8} W_j \tag{43}$$

Where λ_j is the j[th] root of the characteristic equation, ω is the natural angular frequency and n is the circumferential wave number.

Substituting Equation (43) into Equation (42), we obtain the equation for the aerodynamic pressure on the cylindrical shell wall:

$$\{p_a\} = \begin{Bmatrix} 0 \\ p_{radial} \\ 0 \end{Bmatrix} = -\left(i \frac{\lambda_j}{R} \right) \gamma p_\infty M [T][R_f][A^{-1}] \begin{Bmatrix} \delta_i \\ \delta_j \end{Bmatrix} - \gamma \frac{p_\infty}{a_\infty} [T][R_f][A^{-1}] \begin{Bmatrix} \dot{\delta}_i \\ \dot{\delta}_j \end{Bmatrix} \tag{44}$$

The damping and stiffness for fluid flow are then obtained by substituting Equations (9) and (44) into the integral (45);

$$\{F_p\} = \iint [N]^T \{p_a\} dA \tag{45}$$

The linear matrix of aerodynamic damping $[C_f]$ and stiffness matrix $[K_f]$ are given as follows:

$$[C_f] = [A^{-1}]^T [D_f] [A^{-1}] \tag{46}$$

$$[K_f] = [A^{-1}]^T [G_f] [A^{-1}] \tag{47}$$

where;

$$[D_f] = -\frac{\gamma}{a_\infty} P_\infty \pi r \int_0^l [R]^T [R_f] dx \tag{48}$$

$$[G_f] = -i \frac{\lambda_j}{r} \gamma P_\infty M \pi r \int_0^l [R]^T [R_f] dx \tag{49}$$

3.7 Nonlinear Analysis

The motion of a cylindrical shell subjected to an external supersonic flow is governed by the equation of motion which may be presented as follows:

$$\left[M_s^{(L)}\right]\begin{Bmatrix}\ddot{\delta}_i\\ \ddot{\delta}_j\end{Bmatrix}-\left[C_f^{(L)}\right]\begin{Bmatrix}\dot{\delta}_i\\ \dot{\delta}_j\end{Bmatrix}+\left[K^{(L)}\right]\begin{Bmatrix}\delta_i\\ \delta_j\end{Bmatrix}+\left[K^{(NL2)}\right]\begin{Bmatrix}\delta_i\\ \delta_j\end{Bmatrix}^2+\left[K^{(NL3)}\right]\begin{Bmatrix}\delta_i\\ \delta_j\end{Bmatrix}^3=0 \qquad (50)$$

where subscripts s and f refer to the shell in vacuo and in fluid flow respectively, and $\{\delta\}$ is the degrees of freedom vector for the total nodes.

Further useful expressions are:

$$\left[K^L\right]=\left[K_s\right]+\left[K_I\right]-\left[K_f^L\right] \qquad (51)$$

$$[K_I]=\int_0^l\int_0^{2\pi}[N]^T[C_0]^T\begin{bmatrix}\overline{N}_x & 0 & 0\\ 0 & \overline{N}_\theta & 0\\ 0 & 0 & \overline{N}_x+\overline{N}_\theta\end{bmatrix}[C_0]^T[N]^T R d\theta dx \qquad \left[K_s\right]=\iint\left[B\right]^T\left[P\right]\left[B\right]dA \qquad (52)$$

$$\left[K_f^L\right]=\left[A^{-1}\right]^T\left[G_f\right]\left[A^{-1}\right] \qquad (53)$$

where; $$\left[G_f\right]=-\gamma p_\infty M\frac{i\lambda_k}{R}\int\left[R\right]^T\left[T\right]^T\left[T\right]\left[R_f\right]dA \qquad (54)$$

Let us set:

$$\left\{\delta\right\}=\left[\Phi\right]\left\{q\right\} \qquad (55)$$

where $\left[\Phi\right]$ represents the square matrix for eigenvectors of the linear system and $\{q\}$ is a time-related vector. Substituting Equation (55) into system (50) and pre-multiplying the whole equation by $\left[\Phi\right]^T$, we obtain;

(56)

$$\left[M_s^{(L)}\right]^D\left\{\ddot{q}\right\}-\left[C_f^{(L)}\right]^D\left\{\dot{q}\right\}+\left[K^{(L)}\right]^D\left\{q\right\}+\left[\Phi\right]^T\left[K^{(NL2)}\right]\left(\left[\Phi\right]\left\{q\right\}\right)^2+\left[\Phi\right]^T\left[K^{(NL3)}\right]\left(\left[\Phi\right]\left\{q\right\}\right)^3=0$$

where;

$$\left[M_s^{(L)}\right]^D=[\Phi]^T\left[M_s^{(L)}\right][\Phi],\ \left[C_f^{(L)}\right]^D=[\Phi]^T\left[C_f^{(L)}\right][\Phi],\ \left[K^{(L)}\right]^D=[\Phi]^T\left[K^{(L)}\right][\Phi] \quad (57)$$

D denotes diagonal, and the matrices quantifying the fluid contribution to the matrix equations of motion are non-symmetric. To facilitate the analysis, therefore, we consider only the symmetric portion of the matrices. This simplifying hypothesis is valid since the original and simplified systems have comparable dynamic behavior [20].

By neglecting the cross-product in $\left([\Phi]\{q\}\right)^2$ of Equation (56), we obtain;

$$m_{ii}\ddot{q}_i-c_{ii}^{(L)}\dot{q}_i+k_{ii}^{(L)}q_i+\sum_{j=1}^{NREDUC}\left(K_{ij}^{(NL2)}q_j^2+K_{ij}^{(NL3)}q_j^3\right)=0 \quad (58)$$

Here we have ‘‘NREDUC’’ simultaneous equations of the form of Equation (58).

At first, we limit ourselves to solving Equation (56) by taking into account only the diagonal terms of the products $[\Phi]^T\left[K^{(NL2)}\right][\Phi]^2$ and $[\Phi]^T\left[K^{(NL3)}\right][\Phi]^3$, therefore Equation (58) is written in this form:

$$m_{ii}\ddot{q}_i-c_{ii}^{(L)}\dot{q}_i+k_{ii}^{(L)}q_i+K_{ii}^{(NL2)}q_i^2+K_{ii}^{(NL3)}q_i^3=0 \quad (59)$$

Setting; $$q_i(\tau)=A_i f_i(\tau) \quad \text{with} \quad f_i(0)=1 \text{ and } \dot{f}_i(0)=0 \quad (60)$$

Equation (59) becomes, after the A_i simplification and dividing by m_{ii}:

$$\ddot{f}_{ii}-\eta_i\dot{f}_i+\omega_i^2 f_i+\lambda_i\left(\frac{A_i}{t}\right)f_i^2+\sigma_i\left(\frac{A_i^2}{t^2}\right)f_i^3=0 \quad (61)$$

where;

$$\eta_i=\frac{c_{ii}^{(L)}}{m_{ii}}\ ;\qquad \omega_i^2=\frac{k_{ii}^{(L)}}{m_{ii}}\ ;\qquad \lambda_i=\frac{K_{ii}^{(NL2)}}{m_{ii}}t\ ;\qquad \sigma_i=\frac{K_{ii}^{(NL3)}}{m_{ii}}t^2 \quad (62)$$

and t represents the shell thickness. The square root of coefficient k_{ii}/m_{ii} represents the ith linear vibration frequency of system. The solution $f_i(\tau)$ of these ordinary nonlinear differential

equations which satisfies the initial conditions (60) is approximated by a fourth-order Runge-Kutta numerical method. The linear and nonlinear natural angular frequencies are evaluated using a systematic search for the $f_i(\tau)$ roots as a function of time. The ω_{NL}/ω_L ratio is expressed as a function of the non-dimensional ratio A_i/t, where A_i is the vibration amplitude.

3.8 Calculation and Discussion

The influence of nonlinearities associated with the wall of the shell on the vibration characteristics of closed cylindrical shells subjected to linear supersonic flow is expressed by Equation (59).

For a shell with given characteristics, we first present the results for convergence of the model, and the ratio W_{nl}/W_l of linear and nonlinear frequencies is graphically represented in Figures 3.5 to 3.10 with respect to the non-dimensional ration A_i/t.

The shell and flow properties are given by:

$$E = 16\times10^6 \ lb/in \quad (11\times10^{10} N/m^2)$$
$$\upsilon = 0.35$$
$$h = 0.0040 \ in \quad (0.0001015 \ m)$$
$$L = 15.4 \ in \quad (0.381 \ m)$$
$$R = 8.00 \ in \quad (0.203 \ m)$$
$$\rho_s = 0.000833 \ lb-s^2/in^4 \quad (8900 \ kg/m^3)$$
$$M = 3.00$$
$$a_\infty = 8400 \ in/s \quad (213 \ m/s)$$

The influence of nonlinearities associated with large amplitude of cylindrical shells subjected to a fluid at supersonic flow is the main focus of this analysis.

3.8.1 Convergence of the Method

A first calculation was made to determine the required number of finite elements for precise determination of the results, which is very important in finite element analysis. Calculations were made for a closed circular cylindrical shell subjected to supersonic flow for the number of finite elements N = 2, 4, 6, 8...25. The shell is simply supported at both ends. The results for n = 23 and for m = 1, 2 and 3, are shown in Figure 3.3. Convergence of natural frequency is reached for 20 elements.

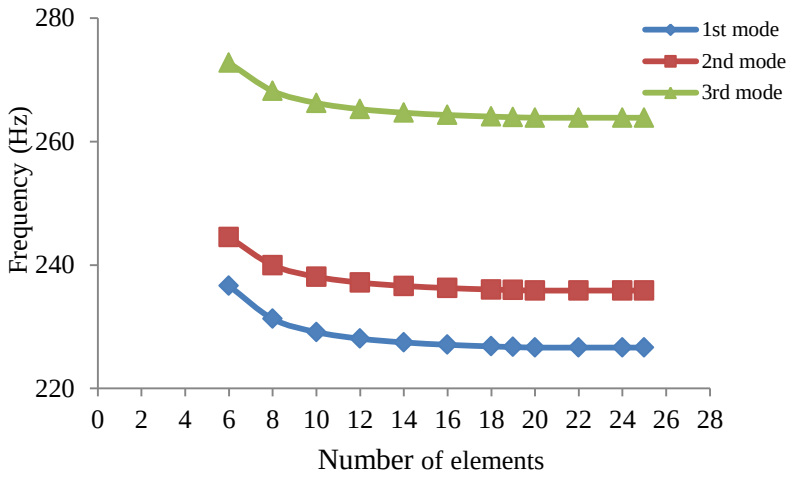

Figure 3.3: Natural frequency vs Number of elements

3.8.2 Onset of Flutter Predictions for Cylindrical Shells in Supersonic Flow

Figure 3.4, shows the eigenvalues associated with the first and second longitudinal modes (m=1, 2) with n = 23 (circumferential wave number) vs freestream static pressure p_∞. The real part of the eigenvalues gives the oscillation frequency, and the imaginary part gives the damping for positive values and instability for negative values. Flutter begins where the imaginary part crosses the zero and becomes negative. It can be seen that the shell loses stability at p_{cr} = 0.75 psi,

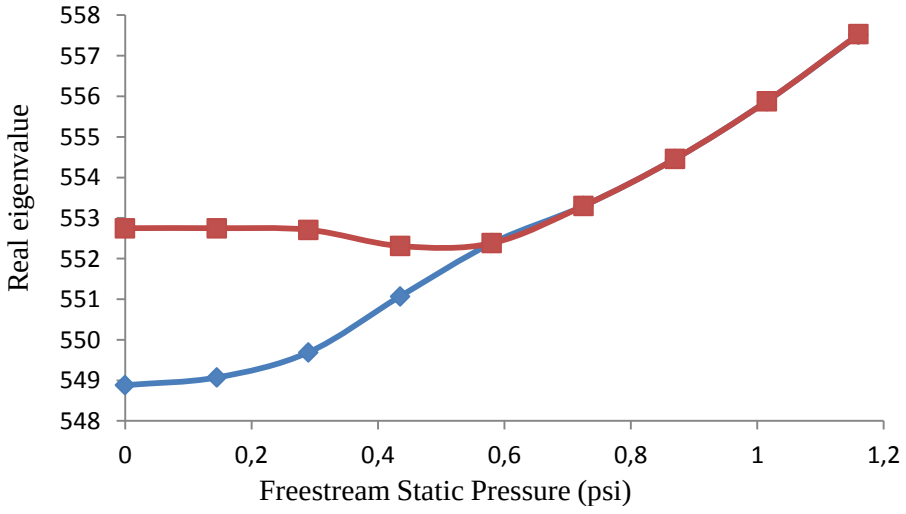

a)

Figure 3.4: a) Real part and b) imaginary part of eigenvalues of the system vs freestream static pressure p_∞, n = 23, p_m = 0.5 psi, p_x = 0.0 psi.

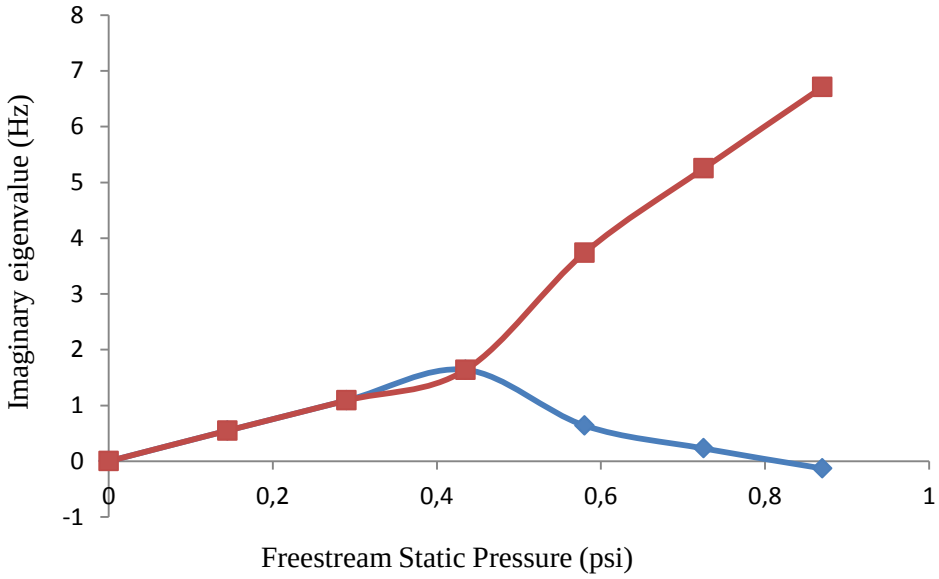

b)

Figure 3.4 (suite): a) Real part and b) imaginary part of eigenvalues of the system vs freestream static pressure p_∞, n = 23, p_m = 0.5 psi, p_x = 0.0 psi.

which is called the critical freestream static pressure. This instability is known as coupled-mode flutter. This results in good agreement to Amabili results [10,21], which is found p_{cr} = 0.77 psi, and coincide with value obtained by Evensen and Olson [4,5].

3.8.3 Behavior of nonlinearity flutter for a pressurized cylindrical shell

Figure 3.5 shows how the flutter frequency varies with amplitude for the first longitudinal mode (m=1). The flutter frequency is seen to decrease slowly with increasing amplitude (softening type of nonlinearity), which is in very good agreement with the study by Olson and Fung [3]. M=3, p_m=0.5 psi, p_∞=0.66 psi; n=23; knowing that the nonlinearity is considered by large amplitude vibrations of cylindrical shell subjected to linear supersonic flowing fluid.

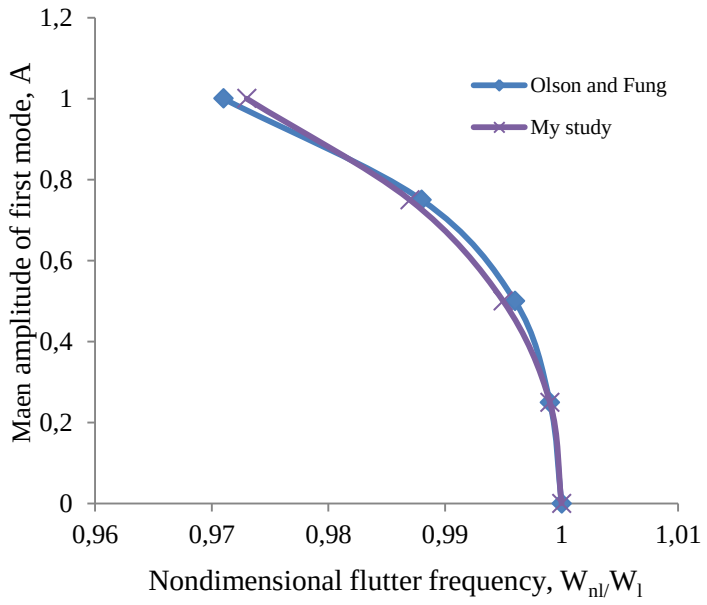

Figure 3.5: Flutter frequency vs mean amplitude of first mode

3.8.4 Effect of freestream static pressure during the flutter

The shell tested is simply supported at both ends, and pressurized; the pressure exerted by the supersonic flow is considered a multiple of critical freestream static pressure to study the nonlinear behavior of flutter of a cylindrical shell during the period following the onset of the flutter. Figure 3.6 shows how the flutter frequencies vary with flutter amplitude. The flutter frequency is seen to decrease slowly with increasing amplitude. This is typical of the so-called ‘‘softening’’ type of nonlinearity, and the tendency is more pronounced at high supersonic flow pressure as seen in $p_{\infty} = 1.5\ p_{cr}$.

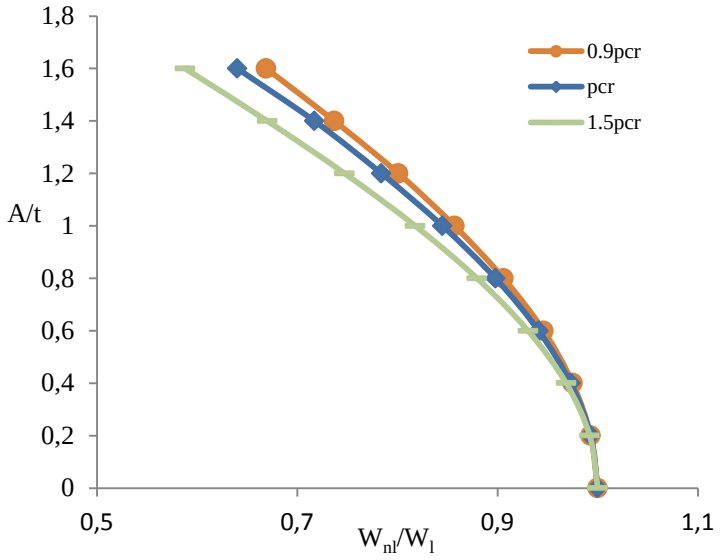

Figure 3.6: Amplitude of flutter vs frequency flutter for different regions of flutter

3.8.5 Effect of internal stresses in the flutter stage of cylindrical shells subjected to supersonic flow

The effect of internal pressure on the nonlinear flutter stage is shown in Figure 7. Two values of supersonic flow pressure $p_\infty = 1.5\ p_{cr}$ and $p_\infty = 3.0\ p_{cr}$, that exceed the critical freestream static pressure (given the flutter $p_{cr} = 0.75$ psi) are investigated here. It can be observed that the effect of internal pressure becomes stronger at supersonic flow pressures ($p_\infty = 2.25$ psi) that are larger than the critical freestream static pressure. Otherwise, when the $p_m = 0.5$ psi (pressurized case), the flutter frequency gradually decreases with increasing vibration amplitude, which explains the stabilizing effect of internal pressure applied to cylindrical shells in supersonic flow. This confirms the conclusion of Amabili and Olson and Fung in their researches. It is also noted that in the region near the onset of flutter ($p_\infty = 1.5\ p_{cr}$), no difference was observed according to the Figure 3.7. Also the softening type nonlinearity of the shell is still observed.

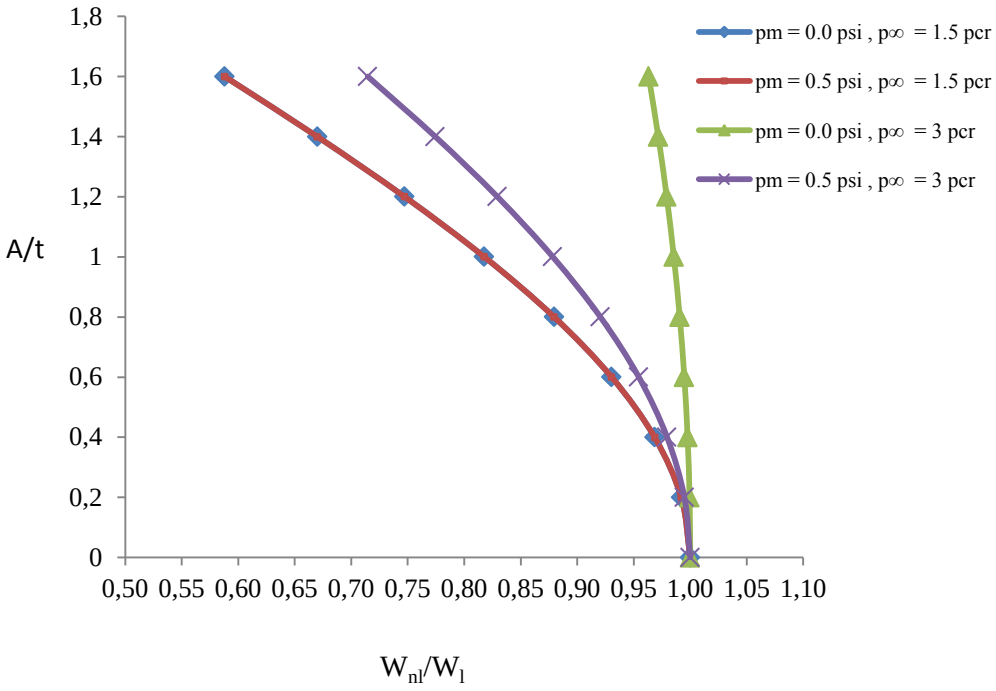

Figure 3.7: Effect of internal pressure during flutter

3.8.6 Effect of length-radius ratios of cylindrical shells on the supersonic flutter

Figure 3.8 shows the variation of flutter amplitude versus flutter frequency of cylindrical shells under supersonic flow in the region corresponding to onset of flutter and during flutter stages, depending on each length-radius case. On one side, the trend of the nonlinearity is a softening type for L/R = 4 and 2, and a hardening type for the L/R = 1. The same behavior is observed for supersonic flow pressure (p_∞ = 2 psi). On the other side, the critical freestream static pressures increase when L/R ratios decrease, and the trend of flutter frequency variation vs flutter amplitude is more pronounced for L/R = 2. For case L/R = 1, the nonlinearity is a hardening type and may indicate that the nonlinear geometry of the cylindrical shell modeled creates a critical area, in which the flutter frequency is superior to natural frequency.

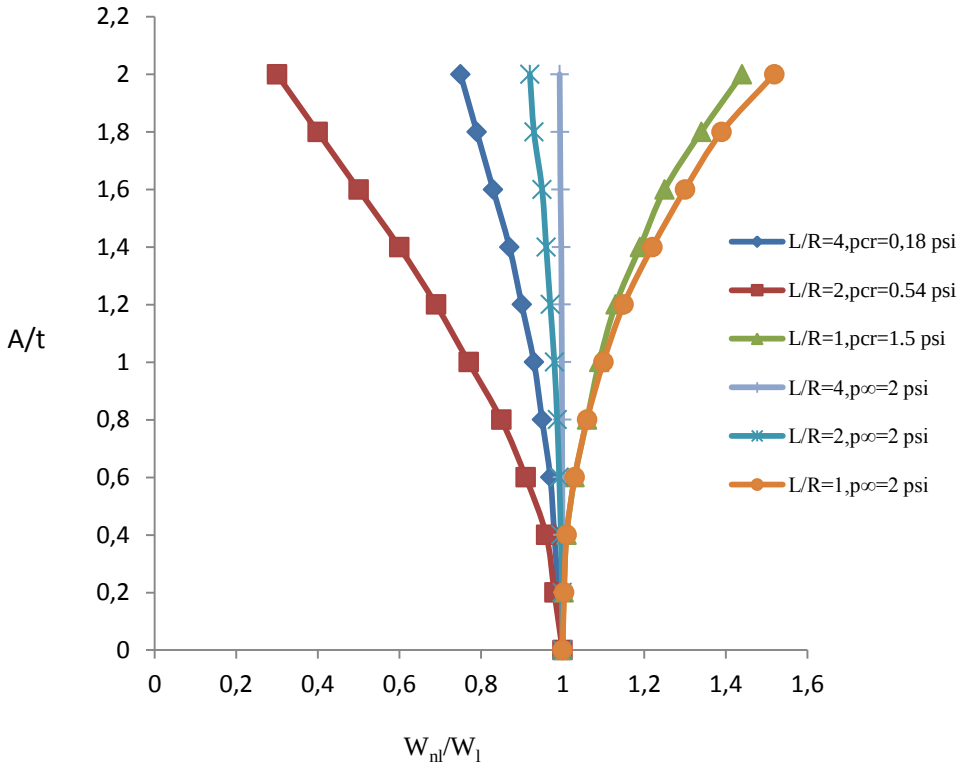

Figure 3.8: Flutter amplitude vs frequency flutter for different L/R

3.8.7 Effect of Shell Boundary Conditions

According to Table 3.1, simply-supported - free shells experience early onset of flutter at low values of supersonic flow pressure (p_{cr} = 0.37 psi). This can be compared to the case of shells clamped at both ends; flutter instability occurs at higher values of supersonic flow pressure (p_{cr} = 1.07 psi).This clarifies the effect of boundary conditions, which can delay the onset of flutter.

In order to illustrate the effect of boundary conditions on cylindrical shell flutter, the mode (n = 23, m = 1) for the same pressurized closed shell with different boundary conditions is shown in Figure 3.9. The shell with simply-supported – free boundary conditions is the one with the more pronounced nonlinearity effect. This effect is small for a panel that is simply supported at both ends.

Table 3.1: Critical freestream static pressure for different shells boundary conditions, p_x=0.0 psi

	p_{cr} (psi)	$n_{critical}$	p_m (psi)
Clamped at both ends	0.84	23	0
Clamped at both ends	1.07	23	0.5
Free simply supported at both ends	0.75	23	0.5
Free simply supported at one end, free at the other end	0.37	23	0.5

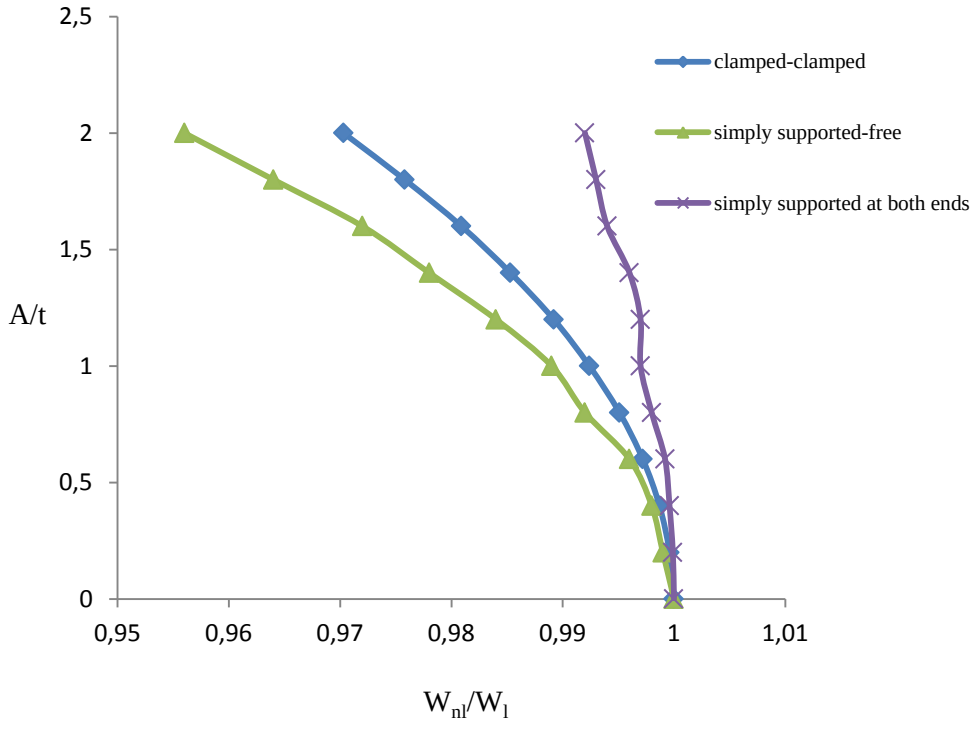

Figure 3.9: Flutter amplitude vs flutter frequency for different shell boundary conditions

3.8.8 Effect of supersonic flow on the nonlinear behavior of cylindrical shells

The effect of supersonic flow on the nonlinear behavior of unpressurized cylindrical shells is presented in Figure 3.10. The flutter frequency decreases rapidly at higher values of flutter amplitude for the shells subjected to supersonic flow than empty shells indicating the softening type of nonlinearity becomes more severe. The results were found for the same data of the cylindrical shells, therefore the existence of the airflow equation in linear form is capable to influence the geometrically nonlinear cylindrical shell, which is refer to flow velocity (supersonic), not to density.

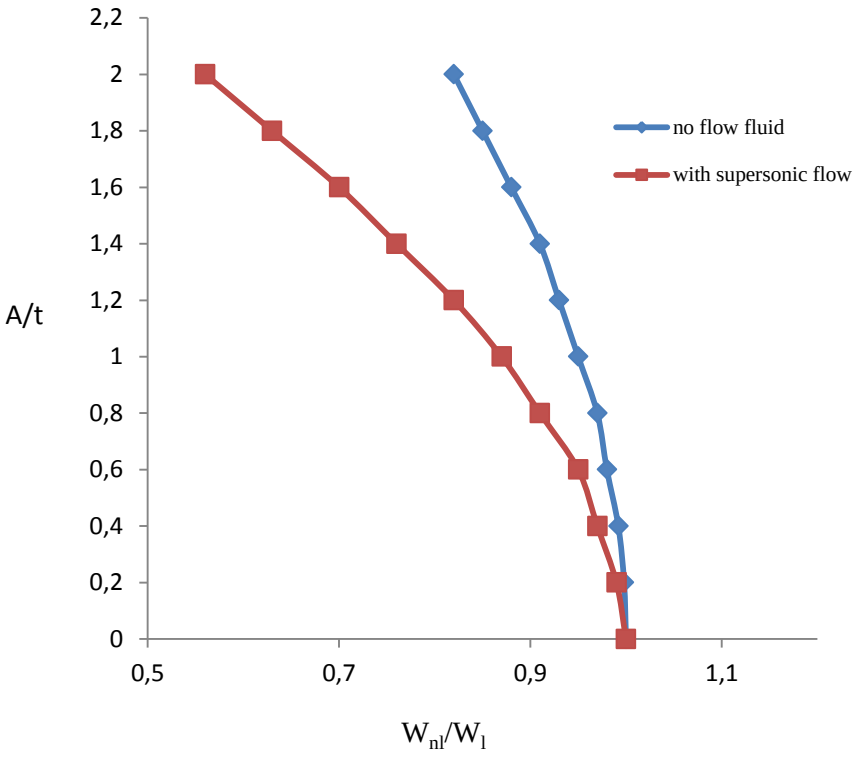

Figure 3.10: Effect of supersonic flow in nonlinear behavior of cylindrical shells

M=3, p_{∞}=0.5 psi, p_m=0.0 psi, n=23.

3.8.9 Effect of circumferential wave number

In Figure 3.11, the effect of large amplitude on the flutter frequency for axial mode m = 1 and various circumferential modes n (20 to 25) is presented. The closed cylindrical shell is simply

supported and has the same data as other cases studied. The Figure shows that the nonlinearity is of the softening type for all circumferential modes. It is also seen that the flutter amplitude vs flutter frequency becomes more pronounced as the circumferential wave number increases.

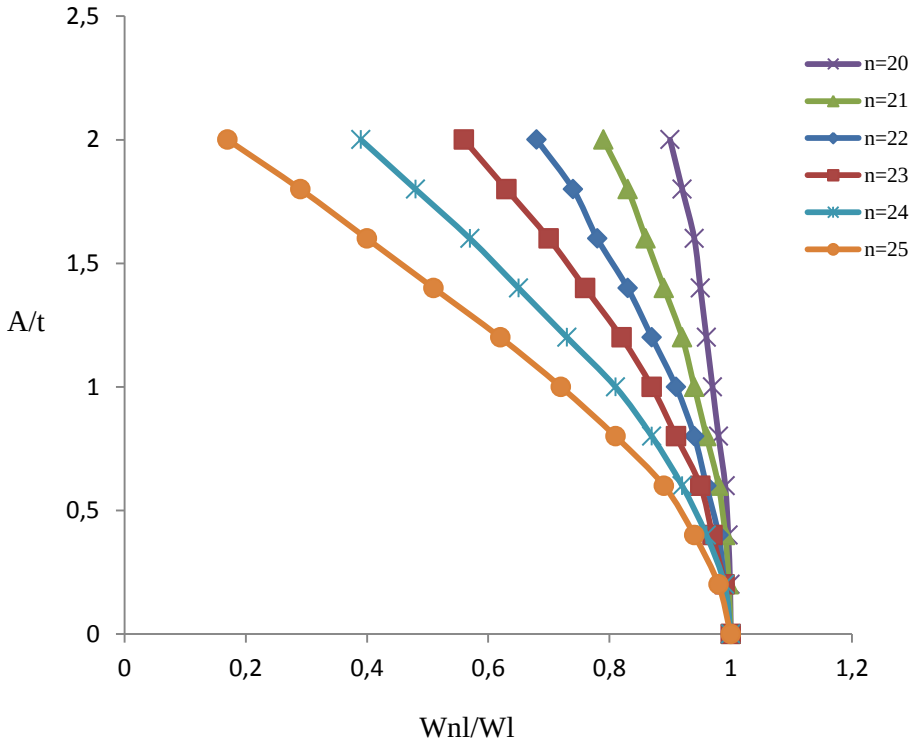

Figure 3.11: Flutter amplitude versus frequency flutter of cylindrical shells at different circumferential wave numbers

3.9 Conclusion

The method developed in this paper demonstrates the combined effect of the nonlinearity associated with the wall of a shell and linear supersonic fluid flow on the resulting flutter frequency and flutter amplitude for the specific case of closed cylindrical shells subjected to external supersonic flow. It is a hybrid method, based on Sanders-Koiter nonlinear thin shell theory, the linear aerodynamic piston theory and the finite element method.

The method combines the advantages of finite element analysis which deals with complex shells, and the precision of a formulation employing displacement functions derived from shell and fluid theories. This approach results in fast and efficient convergence of the calculations. The calculated values show good agreement with experimental and theoretical results published in the

literature. These numerical results provide the nonlinear behaviors of cylindrical shells for different boundary conditions when the shells are subjected to supersonic flow beyond the onset of flutter. These results cannot be found using linear analysis. Several parameters which are dependent on shell geometry and fluid flow are studied. In all study cases, the nonlinear softening type is dominant, and mild flutter instability has been detected. The effect of geometric nonlinearities associated with the walls is non-negligible and should be taken into account when calculating the nonlinear flutter of a shell-flowing fluid system when the amplitude of vibration is larger than the thickness of the shell.

3.10 Appendix

Sander's linear equations for thin cylindrical shells in terms of axial, tangential and circumferential displacements are:

$$L_1(U,V,W,P_{ij}) = P_{11}\frac{\partial^2 U}{\partial x^2} + \frac{P_{12}}{R}\frac{\partial^2 U}{\partial x^2}\left(\frac{\partial^2 V}{\partial x \partial \theta} + \frac{\partial W}{\partial x}\right) - P_{14}\frac{\partial^3 W}{\partial x^3} + \frac{P_{15}}{R^2}\left(\frac{\partial^3 W}{\partial x \partial \theta^2} + \frac{\partial^2 V}{\partial x \partial \theta}\right) + \left(\frac{P_{33}}{R} - \frac{P_{63}}{2R^2}\right)\left(\frac{\partial^2 V}{\partial x \partial \theta} + \frac{1}{R}\frac{\partial^2 U}{\partial \theta^2}\right)$$
$$+ \left(\frac{P_{36}}{R^2} - \frac{P_{66}}{2R^3}\right)\left(-2\frac{\partial^3 W}{\partial x \partial \theta^2} + \frac{3}{2}\frac{\partial^2 V}{\partial x \partial \theta} - \frac{1}{2R}\frac{\partial^2 U}{\partial \theta^2}\right)$$

$$L_2(U,V,W,P_{ij}) = \left(\frac{P_{21}}{R} - \frac{P_{51}}{R^2}\right)\frac{\partial^2 U}{\partial x \partial \theta} + \frac{1}{R}\left(\frac{P_{22}}{R} + \frac{P_{52}}{R^2}\right)\left(\frac{\partial^2 V}{\partial \theta^2} + \frac{\partial W}{\partial \theta}\right) - \left(\frac{P_{24}}{R} + \frac{P_{54}}{R^2}\right)\frac{\partial^3 W}{\partial x^2 \partial \theta} + \frac{1}{R^2}\left(\frac{P_{25}}{R} + \frac{P_{55}}{R^2}\right)\left(-\frac{\partial^3 W}{\partial \theta^3} + \frac{\partial^2 V}{\partial \theta^2}\right)$$
$$+ \left(P_{33} + \frac{3P_{63}}{2R}\right)\left(\frac{\partial^2 V}{\partial x^2} + \frac{\partial^2 U}{R \partial x \partial \theta}\right) + \frac{1}{R}\left(P_{36} + \frac{3P_{66}}{2R}\right)\left(-2\frac{\partial^3 W}{\partial x^2 \partial \theta} + \frac{3}{2}\frac{\partial^2 V}{\partial x^2} - \frac{1}{2R}\frac{\partial^2 U}{\partial x \partial \theta}\right)$$

$$L_3(U,V,W,P_{ij}) = P_{41}\frac{\partial^3 U}{\partial x^3} + \frac{P_{42}}{R}\left(\frac{\partial^3 V}{\partial x^2 \partial \theta} + \frac{\partial^2 W}{\partial x^2}\right) - P_{44}\frac{\partial^4 W}{\partial x^4} + \frac{P_{45}}{R^2}\left(-\frac{\partial^4 W}{\partial x^2 \partial \theta^2} + \frac{\partial^3 V}{\partial x^2 \partial \theta}\right) + \frac{2P_{63}}{R}\left(\frac{1}{R}\frac{\partial^3 U}{\partial x \partial \theta^2} + \frac{\partial^3 V}{\partial x^2 \partial \theta}\right)$$
$$+ \frac{2P_{66}}{R^2}\left(-2\frac{\partial^4 W}{\partial x^2 \partial \theta^2} + \frac{3}{2}\frac{\partial^3 V}{\partial x^2 \partial \theta} - \frac{1}{2R}\frac{\partial^3 U}{\partial x \partial \theta^2}\right) + \frac{P_{51}}{R^2}\frac{\partial^3 U}{\partial x \partial \theta^2} + \frac{P_{52}}{R^3}\left(\frac{\partial^3 V}{\partial \theta^3} + \frac{\partial^2 W}{\partial \theta^2}\right) + \frac{P_{55}}{R^4}\left(-\frac{\partial^4 W}{\partial \theta^4} + \frac{\partial^3 V}{\partial \theta^3}\right)$$
$$- \frac{P_{21}}{R}\frac{\partial U}{\partial x} - \frac{P_{54}}{R^2}\frac{\partial^4 W}{\partial x^2 \partial \theta^2} + \frac{P_{22}}{R^2}\left(\frac{\partial V}{\partial \theta} + W\right) + \frac{P_{24}}{R^2}\frac{\partial^2 W}{\partial \theta^2} - \frac{P_{25}}{R^3}\left(-\frac{\partial^2 W}{\partial \theta^2} + \frac{\partial V}{\partial \theta}\right)$$

The coefficients of characteristic Equation (5) are given by:

$$f_8 = \left(f_9 \big/ r^2\right)\left(p_{11}p_{44} - p_{14}^2\right)$$

$$f_6 = \left(n^2 \big/ r^2\right)\left[f_9\left(f_1 p_{44} + 2p_{11}p_{45} + 4p_{11}p_{66} - 2f_5 r p_{14}\right) + f_7\left(p_{11}p_{44} - p_{14}^2\right) - r^2 f_{11}^2 p_{11} - f_3^2 p_{44} + 2r f_3 f_{11} p_{14}\right] +$$
$$\left(2 \big/ r\right) f_9\left(p_{11}p_{24} - p_{14}p_{12}\right)$$

$$f_4 = \left(n^4 \big/ r^2\right)\left[f_1 f_7\, p_{44} + f_9 p_{11} p_{55} + \left(2p_{45} + 4p_{66}\right)\left(f_1 f_9 + f_7 p_{11} - f_3^2\right) + \left(p_{25} + \left(1 \big/ r\right) p_{55}\right).\left(2f_3 p_{14} - 2f_{11} p_{11} r\right) +\right.$$
$$f_{11} r^2 (2f_3 f_5 - f_1 f_{11}) - r f_5 (2f_7 p_{14} + r f_5 f_9)\left.\right] + (n^2/r).\left[2\left(p_{25} + r p_{22}\right)\left(\left(f_3/r\right)p_{14} - f_{11}p_{11}\right) -\right.$$
$$\left.2p_{12}\left(f_5 f_9 r + f_7 p_{14} - f_3 f_{11} r\right) - 2p_{24}\left(f_3^2 - f_1 f_9 - f_7 p_{11}\right) + 2 f_9 p_{11} p_{25}\right] + f_9\left(p_{11}p_{22} - p_{12}^2\right)$$

$$f_2 = \left(n^6/r^2\right) f_7\left(2p_{45} + 4p_{66}\right) + p_{55}\left(f_1 f_9 + f_7 p_{11} - f_3^2\right) - r^2 f_5^2 f_7 +$$
$$\left(p_{25} + \left(1/r\right) p_{55}\right).\left(-2r f_1 f_{11} + 2r f_3 f_5 - p_{11}p_{25} - \left(1/r\right) p_{11}p_{55}\right)\Big] +$$
$$\left(n^4/r\right)\left[2 f_1 f_7 p_{24} + 2p_{25}\left(f_1 f_9 + f_7\, p_{11} - f_3^2\right) - 2p_{12}\left(r f_5 f_7 - f_3 p_{25} - \left(f_3/r\right) p_{55}\right)\right] -$$
$$2\left(p_{25} + r p_{22}\right)\left(f_1 f_{11} + \left(1/r\right) p_{11}p_{25} + \left(1/r^2\right) p_{11}p_{55} - f_3 f_5\right)\Big] +$$
$$n^2\left[p_{22}\left(f_1 f_9 + f_7 p_{11} - f_3^2\right) - \left(1/r\right)\left(p_{25} + r p_{22}\right)\left(\left(1/r\right) p_{11}p_{25} + p_{11}p_{22} - 2f_3 p_{12}\right) - f_7 p_{12}^2\right]$$

$$f_0 = n^4 f_1 f_7\left[p_{22} + \left(2/r\right) n^2 p_{25} + \left(n^4/r^2\right) p_{55}\right] - n^2 f_1\left[\left(n^3/r\right)\left(p_{25} + \left(1/r\right) p_{55}\right) + \left(n/r\right)\left(p_{25} + r p_{22}\right)\right]^2$$

Where

$$f_1 = p_{33} - p_{36}/R + p_{66}/4R^2$$
$$f_3 = p_{12} + p_{33} + (p_{15} + p_{36})/R - 3p_{66}/4R^2$$
$$f_5 = (p_{15} + 2p_{36} - p_{66}/R)/R$$
$$f_7 = p_{22} + p_{55}/R^2 + 2p_{25}/R$$
$$f_9 = p_{33} + 3p_{36}/R + 9p_{66}/4R^2$$
$$f_{11} = (2p_{36} + p_{24} + 3p_{66}/R + p_{54}/R)/R$$

Matrices $[T]_{3\times3}$, $[R]_{3\times8}$, and $[A]_{8\times8}$ are defined as:

$$[T] = \begin{bmatrix} \cos(n\theta) & 0 & 0 \\ 0 & \cos(n\theta) & 0 \\ 0 & 0 & \sin(n\theta) \end{bmatrix}$$

$$R(1,i) = \alpha_i e^{\lambda_i x/R} \quad , \quad R(2,i) = e^{\lambda_i x/R} \quad , \quad R(3,i) = \beta_i e^{\lambda_i x/R} \qquad i = 1,2,...,8$$

$$A(1,i) = \alpha_i, \quad A(2,i) = 1, \quad A(3,i) = \frac{\lambda_i}{R}, \quad A(4,i) = \beta_i, \quad A(5,i) = \alpha_i e^{\lambda_i l/R}$$

$$A(6,i) = e^{\lambda_i l/R}, \quad A(7,i) = \frac{\lambda_i}{R} e^{\lambda_i l/R}, \quad A(8,i) = \beta_i e^{\lambda_i l/R} \qquad i = 1,2,...8$$

Expressions $\{\varepsilon_L\}$ and $\{\varepsilon_{NL}\}$ for cylindrical shells are given by:

$$\{\varepsilon_L\} = \begin{Bmatrix} \dfrac{\partial U}{\partial x} \\ \dfrac{1}{R}\left(\dfrac{\partial V}{\partial \theta} + W\right) \\ \dfrac{\partial V}{\partial x} + \dfrac{1}{R}\dfrac{\partial U}{\partial \theta} \\ -\dfrac{\partial^2 W}{\partial x^2} \\ -\dfrac{1}{R^2}\left(\dfrac{\partial^2 W}{\partial \theta^2} - \dfrac{\partial V}{\partial \theta}\right) \\ -\dfrac{2}{R}\dfrac{\partial^2 W}{\partial x \partial \theta} + \dfrac{3}{2R}\dfrac{\partial V}{\partial x} - \dfrac{1}{2R^2}\dfrac{\partial U}{\partial \theta} \end{Bmatrix}$$

and;

$$\{\varepsilon_{NL}\} = \begin{Bmatrix} \frac{1}{2}\left(\frac{\partial W}{\partial x}\right)^2 + \frac{1}{8}\left(\frac{\partial V}{\partial x} - \frac{1}{R}\frac{\partial U}{\partial \theta}\right)^2 \\ \frac{1}{2R^2}\left(V - \frac{\partial W}{\partial \theta}\right)^2 + \frac{1}{8}\left(\frac{\partial V}{\partial x} - \frac{1}{R}\frac{\partial U}{\partial \theta}\right)^2 \\ \frac{1}{2R}\left(\frac{\partial W}{\partial x}\frac{\partial W}{\partial \theta} - V\frac{\partial W}{\partial x}\right) \\ 0 \\ 0 \\ 0 \end{Bmatrix}$$

Matrices $\left[B_{pq}\right]$ and $\left[C_{pq}\right]$

$$B_{pq} = b_{pq} e^{\left(\lambda_p + \lambda_q\right)x/R}$$

$$C_{pq} = c_{pq} e^{\left(\lambda_p + \lambda_q\right)x/R}$$

where

$$b_{pq} = \frac{1}{2R^2}\left[\frac{1}{4}a_{pq}^{(1)} + b_{pq}^{(1)}\right]\sin^2\left(n\theta\right)$$

$$c_{pq} = -\frac{1}{4R^2}\left[c_{pq}^{(1)} + c_{pq}^{(2)}\right]\sin\left(n\theta\right)\cos\left(n\theta\right)$$

with

$$a_{pq}^{(1)} = \left(\beta_p\lambda_p + n\alpha_p\right)\left(\beta_q\lambda_q + n\alpha_q\right)$$

$$b_{pq}^{(1)} = \left(n + \beta_p\right)\left(n + \beta_q\right) \qquad p,q = 1,...,8$$

$$c_{pq}^{(1)} = n\left(\lambda_p + \lambda_q\right)$$

Matrix $\left[R_f\right]_{3\times 8}$ is defined by

$$[R_f] = \begin{bmatrix} 0 & ... & 0 \\ e^{i(\lambda_1 x/R)} & ... & e^{i(\lambda_8 x/R)} \\ 0 & ... & 0 \end{bmatrix}$$

3.11 References

[1] Librescu L. Aeroelastic stability of orthotropic heterogeneous thin panels in the vicinity of the flutter critical boundary, Part I: Simply supported panels. J. Mec 1965; 4: 51-76.

[2] Librescu L . Aeroelastic stability of orthotropic heterogeneous thin panels in the vicinity of the flutter critical boundary, Part II: J. Mec 1967; 6:133-152.

[3] Olson MD, Fung YC. Comparing theory and experimental for the supersonic flutter of circular cylindrical shells. AIAA 1967; 5:1849-1856.

[4] Evensen DA, Olson MD. Nonlinear flutter of a circular cylindrical shell in supersonic flow. NASA 1967; TN D-4265.

[5] Evensen DA, Olson MD. Circumferentially travelling wave flutter of a circular cylindrical shell. AIAA 1968; 6: 1522-1527.

[6] Carter LL, Stearman RO. Some aspects of cylindrical shell panel flutter. AIAA 1968; 6: 37-43.

[7] Barr GW, Stearman RO, Aeroelastic stability characteristics of cylindrical shells considering imperfections and edge constraint. AIAA 1969; 7:912-919.

[8] Barr GW, Stearman RO. Influence of a supersonic flow-field on the elastic stability of cylindrical shells, AIAA 1970; 8: 993-1000.

[9] Vol'mir AS, Medvedeva, Investigation of the flutter of cylindrical panels in a supersonic gas flow. Sov Phys Dokl 1973; 17: 1213-1214.

[10] Amabili, M. Pellicano, (2001), Nonlinear supersonic flutter of circular cylindrical shells, AIAA J.39, 564-573.

[11] Horn, W, et al. Recent Contributions to Experiments on Cylindrical Shell Panel Flutter. AIAA Journal 1974; 12(11):1481-1490.

[12] Olson MD, Fung YC. Supersonic flutter of circular cylindrical shells subjected to internal pressure and axial compression. AIAA 1966; 4: 858-864.

[13] Radwan H, Genin J. Non-linear modal equations for thin elastic shells. International Journal of Non-linear Mechanics 1975; 10:15-29.

[14] Sanders, J.L. An Improved First-Approximation Theory for Thin Shell. NASA 1959; R-24.

[15] Lakis, A.A, M.P. Paidoussis. Dynamic Analysis of Axially Non-Uniform Thin Cylindrical Shells. Journal of Mechanical Engineering Science 1972; 14(1):49-71.

[16] H. Ashley and G. Zartarian, Piston Theory-New Aerodynamic Tool for Aeroelastician, Journal of the Aeronautical Sciences, 23 (1956),1109-1118.

[17] W. Horn et al, Recent Contributions to Experiments on Cylindrical Shell Panel Flutter, AIAA Journal, 12 (1974), 1481-1490.

[18] E.H. Dowell, Flutter of Infinitely Long Plates and Shells, Part I, AIAA Journal, 4(1966), 1510-1518.

[19] E.H. Dowell, Aeroelasticity of Plates and Shells, Noordhoff International Publishing, Leyden, 1975.

[20] A. Selmane, and A.A. lakis, Non-Linear Dynamic Analysis of orthotropic Open Cylindrical Shells Subjected to a Flowing Fluid, Journal of Sound and Vibration, 202(1997), 67-93.

[21] M. Amabili, F. Pellicano, M.P. Paidoussis, Non-linear vibrations of simply supported circular cylindrical shells coupled to quiescent fluid, J. Fluids Struct. 12(1998), 883-918

CHAPITRE 4: ARTICLE 3 - EFFECT OF GEOMETRIC AND FLUID FLOW NONLINEARITIES ON CYLINDRICAL SHELLS SUBJECTED TO A SUPERSONIQUE FLOW

Submitted, 07 June 2012 to International Journal of Numerical Methods and Applications

Redouane Ramzi and Aouni Lakis

4.1 Abstract

An analytical model incorporating a combination of the finite element method, Sanders-Koiter nonlinear shell theory and third-order piston theory is presented in this paper to study the influence of nonlinearities associated with structure geometry and supersonic fluid flow on the dynamic and flutter instability behavior of thin anisotropic cylindrical shells. The shell is subdivided into cylindrical finite elements and the displacement functions are derived from exact solutions of Sander's equations for thin cylindrical shells. These functions are treated using the finite element method, which is developed to determine the linear and nonlinear mass and stiffness matrices of the structure. The internal and external pressure and axial compression are taken into account. All expressions of founding matrices are determined by exact analytical integration. By applying the nonlinear dynamic pressure, which represents the effect of nonlinearities of supersonic fluid flow on cylindrical shells, the linear and nonlinear matrices for stiffness, damping and coupling are found. The nonlinear equation of motion is then solved using a fourth-order Runge-Kutta numerical method. Nonlinear vibrations are determined with respect to the amplitude of vibrations and thickness ratio for different cases. This approach leads to the development of a powerful model capable of predicting linear, nonlinear vibrations and flutter instability of cylindrical shells subjected to external supersonic flow. One specific application of this model is the aeroelastic design of aerospace vehicles. This research is part of a series of current studies in the literature that tackle the effects of the nonlinearity of external supersonic fluid flow on cylindrical shells; an area of study that has been neglected by most research to-date.

4.2 Nomenclature

a_∞	Freestream speed of sound
A_i	Motion amplitude

$[A]$	Matrix defined in Appendix
$[B]$	Defined by Equation 11
$[C_f]$	Aerodynamic damping matrix of fluid
$[C_F^{NL2}]$	Second order aerodynamic damping matrix of fluid
$[C_f^{NL3}]$	Third order aerodynamic damping matrix of fluid
a_p, b_p, c_p	Modal coefficients determined by equation 20
a_{pq}, b_{pq}, c_{pq}	Coefficients determined by equations in Appendix
$a^{(i)}_{pq}, b^{(i)}_{pq}, c^{(i)}_{pq}$	Coefficients determined by equations in Appendix
A_{pq}, B_{pq}, C_{pq}	Modal coefficients determined by equations in Appendix
$A_{prs}, B_{prs}, C_{prs}$	Modal coefficients determined by equation 19
D_{prs}, E_{prs}	
$A_{prsq}, B_{prsq}, C_{prsq}$	Modal coefficients determined by equation (19, 22)
D_{prsq}, E_{prsq}	
D	Membrane stiffness, defined by Equation 3
$\{\varepsilon\}$	Deformation vector giving in Appendix
E	Young's modulus
$[E]$	Matrix defined by Equation 23
$\{F_p\}$	Force vector due to the aerodynamic pressure field
h	Shell thickness
K	Bending stiffness of shell, defined by Equation 3
$[K_s]$	Global stiffness matrix for a shell
$[k]$	Stiffness matrix for a shell element
$[k_f]$	Local aerodynamic stiffness matrix
$[k_I]$	Initial stiffness matrix for a shell element
$[K_f]$	Global aerodynamic damping matrix
$[K_I]$	Global initial stiffness matrix for a shell
$[K^{NL2}]$	Nonlinear stiffness matrix of second order
$[K^{NL3}]$	Nonlinear stiffness matrix of third order
L	Shell length
M	Mach number
$[M_s]$	Global mass matrix for a shell

n	Circumferential number
[m]	Mass matrix for a shell element
N	Cylindrical shell number
N_x,N_θ,$N_{x\theta}$	Stress resultant for a circular cylindrical shell
$\overline{N}_x$, $\overline{N}_\theta$	Stress resultant due to shell internal pressure and axial compression
[N]	Defined by Equation 10
p_a	Aerodynamic pressure
p_∞	Freestream static pressure
p_m, p_x	Shell internal pressure and axial compression
[P]	Elasticity matrix
Q_x, Q_θ	Transverse stress resultant for a circular cylindrical shell
R	Shell radius
$[R_f]$	Matrix defined in Appendix
U	Axial displacement
U_i	Potential energy due to initial strain
V	Circumferential displacement
W	Radial displacement
x	Longitudinal coordinate
δ_i, δ_j	Displacement at node i and j
λ_j	Complex roots of the characteristic equation
υ	Poisson's ratio
γ	Adiabatic exponent
θ	Circumferential coordinate
ρ	Shell density
ρ_f	Fluid density
ω	Oscillation frequency
ϕ_{xx}, $\phi_{x\theta}$, ϕ_n	Elastic rotations for a circular cylindrical shell
$\{\sigma\}$	Stress vector

4.3 Introduction

The design of modern missiles, military fighter planes, space shuttles and aerospace structures requires a very advanced, precise and high-performance analytical method capable of investigating the effects of various parameters that influence the reliability and control of sensitive functional and safety systems.

These structures are composed of elements of shells and plates subjected to the effects of external supersonic and hypersonic airflow, which create a phenomenon of dynamic instability. Cylindrical shells also exhibit this type of aeroelastic instability, and prevention of this behavior has become a priority in the aerospace and military industry.

The V-2 rocket was the first cylindrical shell known to have experienced the phenomenon of flutter instability. From the moment the phenomenon was discovered, the study of dynamic instability and flutter became crucial, especially after the introduction of Piston theory published by Ashley and Zartarian [1]. Many authors have investigated the stability of shells in supersonic flow using a linear model of shell and fluid flow through both theoretical and experimental studies. Most researchers have tried to find an analytical formulation assembling various parameters of the shell and the fluid flow to develop a predictive model of aeroelastic flutter characteristics that may describe the reaction of cylindrical shells. Their models were based on shell theory (linear and nonlinear Donnell thin shell theory) combined with linear and nonlinear modeling using the piston theory for fluid-structure interaction. The equation of motion is solved using the Galerkin method. However, the results obtained are not in agreement with those observed experimentally [2]. After Olson and Fung [3] studied the boundary conditions and the effects of internal pressure and axial compression, they concluded that cylindrical shells flutter due to a low-level freestream static pressure as cited by the theory [4]. A nonlinear study to calculate the limit cycle amplitude of cylindrical shells using four modes for the deflection of the shell is given by Evensen and Olson [5]. They reached the same result as given in Ref [3], indicating that flutter is a type of circumferential travelling wave. Also Dowell [6,7] analyzed the behaviour of cylindrical shells in supersonic flow by studying various parameters of the shell and flow. Barr and Stearman [8,9] considered the initial geometric imperfections in cylindrical shells. They noticed that supersonic flow has no effect on the critical buckling load when a small amount of axial load decreases the speed of the flutter. Amabili and Pellicano [10] studied the

geometric nonlinearities of cylindrical shells in a supersonic regime based on the selection of expansion modes. In their study [11] they apply pressure derived from nonlinear piston theory on shells with imperfections in order to study fluid-structure interaction. They conclude that the nonlinearity has no influence on the onset of flutter. In the literature there are several studies on the dynamic behavior and instability of cylindrical shell flutter but these are generally either based on linear analysis of shell and fluid flow, or nonlinearity of the shell and linearity of the fluid flow, or a condition where both are nonlinear. The case which deals with linear analysis of a structure subjected to nonlinear fluid flow has not yet been investigated. This current study consists of an in-depth investigation of the nonlinear dynamic behaviour of structures and their stability versus the nonlinearity of the fluid flow. It has helped fill the void in this specific area and advanced the field of design and preventive control of cylindrical shell structures used under supersonic conditions, which are often found in the aerospace industry. The structural modeling approach using the finite element method for cylindrical shells is inspired from a Lakis and Paidoussis study [12]. This methodology is characterized by its accuracy and rapidity with less numerical difficulties because the displacement functions are derived directly from equations governing the shell instead of polynomial functions. This study presents the effects of the nonlinearities of geometry and fluid flow on the dynamic behavior of cylindrical shells under supersonic airflow. The method is based on a combination of the finite element method, Sanders-Koiter nonlinear theory [11, 12, 13, 16, 17, 18, 19 and 20] and nonlinear aerodynamics theory. This method satisfies the finite element method convergence criteria [12] and provides greater accuracy than polynomial functions, which are typically chosen for this type of analysis.

The treatment of this problem involves two steps:

1. Using linear strain-displacement, stress-strain relationships which were introduced into Sander's equation of equilibrium, the modal displacements describing large amplitude vibration are derived using the developed method seen in the Radwan and Genin study [21]. Then all the displacement functions are determined by solving the system of equations. Following this, the linear and nonlinear mass and stiffness matrices for the finite element are found and assembled for the complete shell.
2. From third-order piston theory [1, 22] we derive an expression for nonlinear pressure as a function of:

- the nodal displacement of the shell element
- a combination of nonlinear effects.

Using this nonlinear dynamic pressure, we obtain two linear matrices and four nonlinear matrices from third-order piston theory.

4.4 Structural model development

4.4.1 Masse and stiffness matrices for linear structural model

The equations of motion of an anisotropic cylindrical shell in terms of U, V, and W (axial, tangential and radial displacements) (Figure 4.1) are written as follows:

$$L_J(U,W,V,P_{ij}) = 0 \tag{1}$$

Where $L_{J(J=1,2,3)}$ are three linear partial differential equations (given in Appendix) and p_{ij} are elements of the elasticity matrix for anisotropic shells which is given by:

$$[P] = \begin{bmatrix} p_{11} & p_{12} & 0 & p_{14} & p_{15} & 0 \\ p_{21} & p_{22} & 0 & p_{24} & p_{25} & 0 \\ 0 & 0 & p_{33} & 0 & 0 & p_{36} \\ p_{41} & p_{42} & 0 & p_{44} & p_{45} & 0 \\ p_{51} & p_{52} & 0 & p_{54} & p_{55} & 0 \\ 0 & 0 & p_{63} & 0 & 0 & p_{66} \end{bmatrix} \tag{2}$$

For the isotropic case,

$$[P] = \begin{bmatrix} D & \upsilon D & 0 & 0 & 0 & 0 \\ \upsilon D & D & 0 & 0 & 0 & 0 \\ 0 & 0 & \frac{D(1-\upsilon)}{2} & 0 & 0 & 0 \\ 0 & 0 & 0 & K & \upsilon K & 0 \\ 0 & 0 & 0 & \upsilon K & K & 0 \\ 0 & 0 & 0 & 0 & 0 & \frac{K(1-\upsilon)}{2} \end{bmatrix}$$

where,

$$K = \frac{Eh^3}{12(1-\upsilon^2)} \quad \text{Bending stiffness,} \qquad D = \frac{Eh}{1-\upsilon^2} \quad \text{Membrane stiffness} \tag{3}$$

The displacement functions associated with the circumferential wave number are assumed in the normal manner, as:

$$U(x,\theta) = Ae^{\frac{\lambda x}{R}}\cos(n\theta)$$
$$W(x,\theta) = Be^{\frac{\lambda x}{R}}\cos(n\theta) \qquad (4)$$
$$V(x,\theta) = Ce^{\frac{\lambda x}{R}}\sin(n\theta)$$

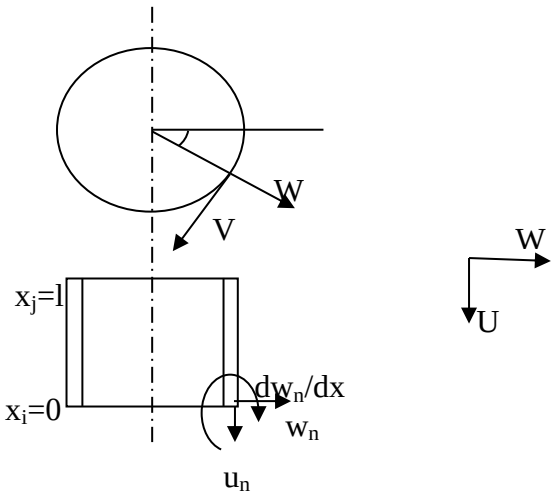

Figure 4.1: Finite element discretization and nodal displacement

where n is the circumferential mode,

Note that this approach treats closed cylindrical shells based on the circumferential wave number, not on the longitudinal wave number.

Substituting (4) into the equations of motion (1), a system of three homogeneous equations, linear functions of constants A, B, C, are obtained. For the solution to be non-trivial, the determinant of this system must be equal to zero. This brings us to the following characteristic equation:

$$Det([H]) = f_8\lambda^8 + f_6\lambda^6 + f_4\lambda^4 + f_2\lambda^2 + f_0 \qquad (5)$$

The values of coefficients f_i in this eighth-degree polynomial are given in Appendix.

Each root of this equation yields a solution to the linear equations of motion (1). The complete solution is obtained by adding the eight solutions independently with constants A_i, B_i and C_i

(i = 1,2,….,8). These constants are not independent. We can therefore express A_i and B_i as a function of C_i, as follows:

$$A_i = \alpha_i C_i$$
$$B_i = \beta_i C_i \qquad (6)$$

The values of α_i and β_i can be obtained from system (1) by introducing relation (6). To determine eight C_i constants, it is necessary to formulate eight boundary conditions for the finite elements. The axial, tangential and radial displacements will be specified for each node. The following relation defines the element displacement vector at the boundaries:

$$\begin{Bmatrix}\delta_i \\ \delta_j\end{Bmatrix} = \{u_i \;\; v_i \;\; w_i \;\; u_j \;\; v_j \;\; w_j\}^T \tag{7}$$

$$\begin{Bmatrix}\delta_i \\ \delta_j\end{Bmatrix} = [A]\{C\} \tag{8}$$

where the elements of matrix [A] are given in Appendix.

Multiplying Eq.(8) by $[A]^{-1}$ and substituting the result into Eq.(4), we obtain:

$$\begin{Bmatrix}U(x,\theta) \\ V(x,\theta) \\ W(x,\theta)\end{Bmatrix} = [N]\begin{Bmatrix}\delta_i \\ \delta_j\end{Bmatrix} \tag{9}$$

where [N] represents the shape function matrix given in this form:

$$[N] = [T][R]\left[A^{-1}\right] \tag{10}$$

and [T], [R], [A] are described in Appendix.

The constitutive relation between the stress and deformation vector of a cylindrical shell is given as:

$$\{\sigma\} = [P][B]\begin{Bmatrix}\delta_i \\ \delta_j\end{Bmatrix} \tag{11}$$

The mass and stiffness matrices for each element are derived using the classic finite element procedure and can then be expressed as:

$$[m] = \rho h \iint [N]^T [N] dA$$
$$[k_L] = \iint [B]^T [P][B] dA \qquad (12)$$

Where ρ is the density of the shell, h its thickness and $dA = Rdxd\theta$. The matrices [m] and [k] are obtained analytically by carrying out the necessary matrix operations over x and θ in the equation. The global matrices $\left[M_s\right]$ and $\left[K_s\right]$ may be obtained, respectively, by assembling the mass and stiffness matrices for each individual finite element.

4.4.2 Stiffness matrices for nonlinear structural model

The coefficients of the modal equations are obtained using the Lagrange method in the same way developed by Radwan and Genin [21], paying attention to geometric non-linearities. Following this, the second and third non-linear stiffness matrices corresponding to geometric non-linearities are computed and superimposed on the linear system.

Shell displacements (u, v, w) are expressed as sums of generalized product coordinates $q_i(t)$ and spatial functions U, V, W (see Eq. (4)).

$$u = \sum_i q_i(t) U_i(x,\theta)$$
$$v = \sum_i q_i(t) V_i(x,\theta) \qquad (13)$$
$$w = \sum_i q_i(t) W_i(x,\theta)$$

The deformation vector is written as a function of the generalized coordinates by separating the linear part from the non-linear part.

$$\{\varepsilon\} = \{\varepsilon_L\} + \{\varepsilon_{NL}\} = \{\varepsilon_{xx}, \varepsilon_{\theta\theta}, 2\varepsilon_{x\theta}, \kappa_{xx}, \kappa_{\theta\theta}, 2\kappa_{x\theta}\}^T \qquad (14)$$

Where subscripts ``L`` and ``NL`` mean ``linear`` and ``non-linear``, respectively, and ε_L and ε_{NL} are defined in Appendix.

The Lagrange's equations of motion in generalized coordinates $q_i(t)$ are found using Hamilton's principle and Eq. (13):

$$\frac{d}{dt}\left(\frac{\partial T}{\partial \dot{q}_i}\right) - \frac{\partial T}{\partial q_i} + \frac{\partial V}{\partial q_i} = Q_i \qquad (15)$$

where T is the total kinetic energy, V is the total elastic strain energy of deformation and the Q_i's are the generalized forces.

Using the vector deformation given by (14), the developed formulation for total kinetic and strain energy and inserting these into the Lagrange equation (15), the following non-linear modal equations are obtained after a long development of equations:

$$\sum_r m_{pr}\ddot{\delta}_r + \sum_r k_{pr}^{(L)}\delta_r + \sum_r \sum_s k_{prs}^{(NL2)}\delta_r\delta_s + \sum_r \sum_s \sum_q k_{prsq}^{(NL3)}\delta_r\delta_s\delta_q = 0 \qquad (16)$$

$$p = 1, 2, \ldots.$$

where m_{pr}, $k_{pr}^{(L)}$ are terms of the mass and linear stiffness matrices given by Equation (12). The terms $k_{prs}^{(NL2)}$ and $k_{prsq}^{(NL3)}$ represent the second and third-order non-linear stiffness and are given by the following integrals for the case of an isotropic closed cylindrical shell:

$$K_{prs}^{(NL2)} = \iint \{p_{11}A_{prs} + p_{22}B_{prs} + p_{12}(D_{prs} + E_{prs}) + p_{33}C_{prs}\}dA \qquad (17)$$

and

$$K_{prsq}^{(NL3)} = \iint \{p_{11}A_{prsq} + p_{22}B_{prsq} + p_{12}(D_{prsq} + E_{prsq}) + p_{33}C_{prsq}\}dA \qquad (18)$$

Where $dA = Rdxd\theta$, p_{ij} are the terms of the elasticity matrix [P], and the terms A_{prs},B_{prs},C_{prs},D_{prs},E_{prs} and A_{prsq},B_{prsq},C_{prsq},D_{prsq},E_{prsq} represent the coefficients of the modal equations. These coefficients are given by the following equations:

$$
\begin{aligned}
A_{prs} &= a_p A_{rs} + a_r A_{sp} + a_s A_{pr} & \qquad A_{prsq} &= 2A_{pq} A_{rs} \\
B_{prs} &= b_p B_{rs} + b_r A_{sp} + b_s B_{pr} & \qquad B_{prsq} &= 2B_{pq} B_{rs} \\
C_{prs} &= c_p C_{rs} + c_r C_{sp} + c_s C_{pr} & \qquad C_{prsq} &= 2C_{pq} C_{rs} \\
D_{prs} &= a_r B_{sp} + a_s B_{pr} + b_p A_{rs} & \qquad D_{prsq} &= 2A_{pq} B_{rs} \\
E_{prs} &= b_r A_{sp} + b_s A_{pr} + a_s B_{rs} & \qquad E_{prsq} &= 2B_{pq} A_{rs}
\end{aligned}
\tag{19}
$$

with;

$$
\begin{aligned}
a_p &= U_{p,x}\,, \qquad b_p = 1/R\,(\,V_{p,\theta} + W_p\,), \qquad c_p = 1/2\,(\,U_{p,\theta}/R + V_{p,x}\,) \\
A_{pq} &= 1/8\,R^2\,(\,R\,V_{p,x} - U_{p,\theta}\,)\,.\,(\,R\,V_{q,x} - U_{q,\theta}\,) + 1/2\,W_{p,x}W_{q,x} \\
B_{pq} &= 1/8\,R^2\,(\,R\,V_{p,x} - U_{p,\theta}\,)\,.\,(\,R\,V_{q,x} - U_{q,\theta}\,) + 1/2\,R^2\,(\,W_{p,\theta} - V_p\,)\,.\,(\,W_{q,\theta} - V_q\,) \\
C_{pq} &= 1/4\,R\,(\,W_{p,x}\,W_{q,\theta} - W_{q,x}\,W_{p,\theta}\,) - 1/4\,R\,(\,V_p\,W_{q,x} + V_q\,W_{p,x}\,)
\end{aligned}
\tag{20}
$$

Where U, V and W are spatial functions determined by Equation (4).

In Equations (16) - (20), the subscripts ‘p,q’, ’p,r,s’ and ‘p,r,s,q’ represent the coupling between two, three and four modes, respectively.

Let us illustrate the development of the expression for the (p,q) term of matrices A_{pq} and A_{pqrs}.

The expression A_{pq} is given by:

$$A_{pq} = a_{pq} e^{\left(\lambda_p + \lambda_q\right) x/R} \tag{21}$$

and A_{pqrs} is:

$$A_{prsq} = \sum_{r=1}^{8} \sum_{s=1}^{8} a_{rs} a_{pq} \varepsilon_{rs} e^{(\lambda_p + \lambda_r + \lambda_s + \lambda_q) x/R} \tag{22}$$

ε_{rs} is the term (r,s) of matrix [E],where [E] represents a matrix of constants defined by $[E] = \left[A^{-1}\right]^T [A]$ (23), and

$$a_{pq} = \frac{1}{2R^2}\left[\frac{1}{4}a_{pq}^{(1)}\sin^2(n\theta) + a_{pq}^{(2)}\cos^2(n\theta)\right] \tag{24}$$

with

$$a_{pq}^{(1)} = \left(\beta_p\lambda_p + n\alpha_p\right)\left(\beta_q\lambda_q + n\alpha_q\right) \tag{25}$$

$$a_{pq}^{(2)} = \lambda_p\lambda_q \tag{26}$$

Similarly, the matrices $[B_{pq}]$… $[E_{prsq}]$ can be written as a function of α, β, λ, x and θ. The (p, q) terms of these matrices are described in Appendix. For details of the basis of the presented method, consult reference [21].

After integration, we obtain:

$$\left[k_{prs}^{(NL2)}\right] = \left[A^{-1}\right]^T\left[J^{(NL2)}\right]\left[A^{-1}\right] \tag{27}$$

$$\left[k_{prsq}^{(NL3)}\right] = \frac{\pi}{8R^2}\left[A^{-1}\right]^T\left[J^{(NL3)}\right]\left[A^{-1}\right] \tag{28}$$

The (p,q) term in matrix $\left[J_{p,q}^{(NL2)}\right]$ and $\left[J_{p,q}^{(NL3)}\right]$ are written as:

$$J^{(NL2)}(p,q) = \begin{cases} \displaystyle\sum_{l=1}^{8}\sum_{s=1}^{8}\frac{\varepsilon_{sr}}{\left(\lambda_p+\lambda_q+\lambda_r\right)}G1(p,q)\left[e^{\left(\lambda_p+\lambda_q+\lambda_r\right)\frac{\ell}{R}}-1\right] \\ if\ \lambda_p+\lambda_q+\lambda_r \neq 0 \\ \displaystyle\sum_{k=1}^{8}\sum_{l=1}^{8}\varepsilon_{sr}G1(p,q)\frac{\ell}{R} \\ if\ \lambda_p+\lambda_q+\lambda_r = 0 \end{cases} \tag{29}$$

and

$$J^{(NL3)}(p,q)=\begin{cases}\displaystyle\sum_{k=1}^{8}\sum_{l=1}^{8}\frac{\varepsilon_{sr}}{\left(\lambda_p+\lambda_q+\lambda_r+\lambda_s\right)}G2(p,q)\left[e^{\left(\lambda_p+\lambda_q+\lambda_r+\lambda_s\right)\frac{\ell}{R}}-1\right]\\ if\ \lambda_p+\lambda_q+\lambda_r+\lambda_s\neq 0\\ \displaystyle\sum_{k=1}^{8}\sum_{l=1}^{8}\varepsilon_{sr}G2(p,q)\frac{\ell}{R}\\ if\ \lambda_p+\lambda_q+\lambda_r+\lambda_s=0\end{cases} \tag{30}$$

where G1(p,q) and G2(p,q) are coefficients in conjunction with α, β, λ and elements p_{ij} in matrix [P]. The general expressions of G1(p,q) and G2(p,q) are given by :

$$\begin{aligned}\mathrm{G1(p,q)} = {} & p_{11}II_1\left[a_p^{(1)}A^{-1}a_{rs}^{(1)}+a_r^{(1)}A^{-1}a_{sp}^{(1)}+a_s^{(1)}A^{-1}a_{pr}^{(1)}\right]\\ & +p_{11}II_2\left[a_p^{(1)}A^{-1}a_{rs}^{(2)}+a_r^{(1)}A^{-1}a_{sp}^{(2)}+a_s^{(1)}A^{-1}a_{pr}^{(2)}\right]\\ & +p_{22}II_1\left[b_p^{(1)}A^{-1}b_{rs}^{(2)}+b_r^{(1)}A^{-1}b_{sp}^{(2)}+b_s^{(1)}A^{-1}b_{pr}^{(2)}\right]\\ & +p_{33}II_1\left[c_p^{(1)}A^{-1}c_{rs}^{(1)}+c_r^{(1)}A^{-1}c_{sp}^{(1)}+c_s^{(1)}A^{-1}c_{pr}^{(1)}\right]\\ & +p_{12}II_1+\left[a_r^{(1)}A^{-1}b_{sp}^{(1)}+a_s^{(1)}A^{-1}a_{pr}^{(1)}+b_p^{(1)}A^{-1}a_{rs}^{(1)}\right]\\ & +p_{12}II_2\left[b_p^{(1)}A^{-1}a_{rs}^{(2)}\right]\\ & +p_{12}II_1\left[b_r^{(1)}A^{-1}a_{sp}^{(1)}+b_s^{(1)}A^{-1}a_{pr}^{(1)}+a_p^{(1)}A^{-1}b_{rs}^{(1)}\right]\\ & +p_{12}II_2\left[b_r^{(1)}A^{-1}a_{sp}^{(2)}+b_s^{(1)}A^{-1}a_{pr}^{(2)}\right]\end{aligned} \tag{31}$$

where,

$$II_1=\frac{\sin^3(2\pi n)}{3} \tag{32}$$

$$II_2=\frac{\sin(2\pi n)(2+\cos^2(2\pi n))}{3n} \tag{33}$$

and

$$
\begin{aligned}
G2(p,q) = \frac{3}{16}\left(p_{11}+p_{22}+2p_{12}\right)a_{pl}^{(1)}a_{kq}^{(1)} + 3\left(p_{11}a_{pl}^{(2)}a_{kq}^{(2)} + p_{22}b_{pl}^{(1)}b_{kq}^{(1)}\right) \\
+ p_{12}\left(a_{pl}^{(2)}b_{kq}^{(1)} + b_{pl}^{(1)}a_{kq}^{(2)}\right) + \frac{1}{4}\left(p_{11}+p_{12}\right)\left(a_{pl}^{(2)}a_{kq}^{(1)} + a_{pl}^{(1)}a_{kq}^{(2)}\right) \\
+ \frac{3}{4}\left(p_{12}+p_{22}\right)\left(a_{pl}^{(1)}b_{kq}^{(1)} + b_{pl}^{(1)}a_{kq}^{(1)}\right) \\
+ \frac{1}{4}p_{33}\left(c_{pl}^{(1)}c_{kq}^{(1)} + c_{pl}^{(2)}c_{kq}^{(2)} + c_{pl}^{(2)}c_{kq}^{(1)} + c_{pl}^{(1)}c_{kq}^{(2)}\right)
\end{aligned}
\tag{34}
$$

where the terms $a^{(1)}$ and $a^{(2)}$ are given by Equations (25-26). Terms $b^{(1)\cdots}$, $c^{(1)}$…and $c^{(2)}$ are coefficients appearing in expressions for the elements of matrices $[B_{pq}]$ and $[C_{pq}]$ defined in Equations (20). These coefficients are given in Appendix.

4.5 Initial stress matrix

The potential energy is given as

$$
U_i = 1/2\int_0^l\int_0^{2\pi}\left[\overline{N}_x\phi_{\theta\theta}^2 + \overline{N}_\theta\phi_{xx}^2 + (\overline{N}_x+\overline{N}_\theta)\phi_n^2\right]Rd\theta dx \tag{35}
$$

where;

$$
\begin{aligned}
\overline{N}_x &= -\frac{p_x}{2\pi R} \\
\overline{N}_\theta &= p_m R
\end{aligned}
\tag{36}
$$

$\overline{N}_x$, $\overline{N}_\theta$ are stress resultants due to shell internal pressure p_m and axial compression p_x respectively, l is the element length, $\phi_{\theta\theta}$ is about the normal to the $x\theta$ plane, ϕ_{xx} is the strain rotation about x, and ϕ_n is the rotation about the normal to a shell element.

This rotation vector is expressed as [14],

$$
\begin{aligned}
\phi_{\theta\theta} &= -\frac{\partial W}{\partial x} \\
\phi_{xx} &= \frac{1}{R}\left(V - \frac{\partial W}{\partial \theta}\right) \\
\phi_n &= \frac{1}{2}\left(-\frac{1}{R}\frac{\partial U}{\partial \theta} + \frac{\partial V}{\partial x}\right)
\end{aligned}
\tag{37}
$$

Upon insertion of displacements (U,W,V) given in Equation (8), the potential energy is rewritten in terms of the nodal degrees of freedom, which leads to the initial stiffness matrix for each element in the following form:

$$[k_I] = \int_0^l \int_0^{2\pi} [N]^T [C_0]^T \begin{bmatrix} \overline{N}_x & 0 & 0 \\ 0 & \overline{N}_\theta & 0 \\ 0 & 0 & \overline{N}_x + \overline{N}_\theta \end{bmatrix} [C_0]^T [N]^T \, R d\theta dx \tag{38}$$

where;
$$[C_0] = \begin{bmatrix} 0 & -\dfrac{\partial}{\partial x} & 0 \\ 0 & -\dfrac{1}{R}\dfrac{\partial}{\partial \theta} & 0 \\ -\dfrac{1}{2R}\dfrac{\partial}{\partial \theta} & 0 & \dfrac{1}{2}\dfrac{\partial}{\partial x} \end{bmatrix} \tag{39}$$

4.6 Aerodynamic model development

The pressure on the body surface is approximated by the pressure experienced by a piston moving in the flow with a velocity equivalent to the superposition of the velocity due to the changing of body shape and the velocity due to the rigid-body motion of the body [1, 22].

$$\frac{p}{p_\infty} = \left\{ 1 + \left[(\gamma - 1)/2 \right] \left(\omega / a_\infty \right) \right\}^{2\gamma/(\gamma - 1)} \tag{40}$$

where;

p is the aerodynamic pressure,

p_∞ is the freestream static pressure,

γ is the adiabatic exponent,

a_∞ is the freestream speed of sound

ω is the velocity of the piston.

The piston velocity ω is given by:

$$\omega = \frac{\partial W}{\partial t} + U_\infty \frac{\partial W}{\partial x} \tag{41}$$

U_∞ is the freestream velocity and W is the radial displacement.

Considering the linear terms in the binomial expansion of Equation (40), we obtain:

$$p_a = -\gamma p_\infty \left[\begin{array}{l} \left(M \frac{\partial W}{\partial x} + \frac{1}{a_\infty} \frac{\partial W}{\partial t} \right) + \frac{\gamma+1}{4} \left(M \frac{\partial W}{\partial x} + \frac{1}{a_\infty} \frac{\partial W}{\partial t} \right)^2 \\ + \frac{\gamma+1}{12} \left(M \frac{\partial W}{\partial x} + \frac{1}{a_\infty} \frac{\partial W}{\partial t} \right)^3 \end{array} \right] \tag{42}$$

The form of the radial displacement assumed is the same as that considered by Lakis and Paidoussis in [12]:

$$W = \sum_{j=1}^{8} e^{i(\lambda_j \frac{x}{R} + \omega t)} \cos(n\theta) = \sum_{j=1}^{8} W_j \tag{43}$$

where; λ_j is the j[th] root of the characteristic equation, ω is the natural angular frequency and n is the circumferential wave number.

Substituting Eq. (43) into Eq. (42), we obtain the equation for the aerodynamic pressure on the cylindrical shell wall:

$$\begin{array}{l} p_a = -\gamma p_\infty \left\{ M \left(\frac{i\lambda_j}{R} \right) [T][R_f][A^{-1}] \begin{Bmatrix} \delta_i \\ \delta_j \end{Bmatrix} + \frac{1}{a_\infty} [T][R_f][A^{-1}] \begin{Bmatrix} \dot{\delta}_i \\ \dot{\delta}_j \end{Bmatrix} + \frac{\gamma+1}{12} M^3 \left(\frac{i\lambda_j}{R} \right)^3 \left([T][R_f][A^{-1}] \right)^3 \begin{Bmatrix} \delta_i \\ \delta_j \end{Bmatrix}^3 + \right. \\ \left. \frac{\gamma+1}{4} \frac{M^2}{a_\infty} \left(-\frac{\lambda_j^2}{R^2} \right) \left([T][R_f][A^{-1}] \right)^3 \begin{Bmatrix} \delta_i \\ \delta_j \end{Bmatrix}^2 \begin{Bmatrix} \dot{\delta}_i \\ \dot{\delta}_j \end{Bmatrix} + \frac{\gamma+1}{4} \frac{M}{a_\infty^2} \left(\frac{i\lambda_j}{R} \right) \left([T][R_f][A^{-1}] \right)^3 \begin{Bmatrix} \delta_i \\ \delta_j \end{Bmatrix} \begin{Bmatrix} \dot{\delta}_i \\ \dot{\delta}_j \end{Bmatrix}^2 + \frac{\gamma+1}{12 a_\infty^3} \left([T][R_f][A^{-1}] \right)^3 \begin{Bmatrix} \dot{\delta}_i \\ \dot{\delta}_j \end{Bmatrix}^3 \right\} \end{array} \tag{44}$$

Then the damping and stiffness for fluid flow are obtained by substituting Equations (9) and (44) into the integral (45),

$$\{F_p\} = \iint [N]^T \{p_a\} dA \tag{45}$$

The linear matrix of aerodynamic damping $[C_f]$ and stiffness matrix $[K_f]$ are given as follows

$$\begin{aligned} \left[C_f\right]&=\left[A^{-1}\right]^T\left[D_f\right]\left[A^{-1}\right] & \left[C_f\right]_{NL3}&=\left[A^{-1}\right]^T\left[D_{fnl3}\right]\left[A^{-1}\right] \\ \left[K_f\right]&=\left[A^{-1}\right]^T\left[G_f\right]\left[A^{-1}\right] & \left[K_f\right]_{NL3}&=\left[A^{-1}\right]^T\left[G_{fnl3}\right]\left[A^{-1}\right] \end{aligned} \tag{46}$$

$$\begin{aligned} \left[K_f^2C_f\right]_{NL3}&=\left[A^{-1}\right]^T\left[H1_{fnl3}\right]\left[A^{-1}\right] \\ \left[K_fC_f^2\right]_{NL3}&=\left[A^{-1}\right]^T\left[H2_{fnl3}\right]\left[A^{-1}\right] \end{aligned} \tag{47}$$

where ,

$$\left[D_f\right]=-\frac{\gamma}{a_\infty}P_\infty\pi r\int_0^l\left[R\right]^T\left[R_f\right]dx \tag{48}$$

$$\left[G_f\right]=-i\frac{\lambda_j}{r}\gamma P_\infty M\pi r\int_0^l\left[R\right]^T\left[R_f\right]dx \tag{49}$$

where $\left[D_f\right]$,$\left[G_f\right]$, $\left[D_{fnl3}\right]$,$\left[G_{fnl3}\right]$,$\left[H1_{fnl3}\right]$,$\left[H2_{fnl3}\right]$ are given in Appendix.

4.7 Nonlinear numerical analysis

The motion of a cylindrical shell subjected to an external supersonic flow is governed by the equation of motion which may be presented as follows:

$$\begin{aligned} &\left[M_s^{(L)}\right]\begin{Bmatrix}\ddot{\delta}_i\\ \ddot{\delta}_j\end{Bmatrix}-\left[C_f^{(L)}\right]\begin{Bmatrix}\dot{\delta}_i\\ \dot{\delta}_j\end{Bmatrix}+\left[K^{(L)}\right]\begin{Bmatrix}\delta_i\\ \delta_j\end{Bmatrix}+\left[K^{(NL2)}\right]\begin{Bmatrix}\delta_i\\ \delta_j\end{Bmatrix}^2+\left[K^{(NL3)}\right]\begin{Bmatrix}\delta_i\\ \delta_j\end{Bmatrix}^3-\left[K_f^{(NL3)}\right]\begin{Bmatrix}\delta_i\\ \delta_j\end{Bmatrix}^3-\left[K_f^{(NL2)}C_f^{(NL)}\right]\begin{Bmatrix}\delta_i\\ \delta_j\end{Bmatrix}^2\begin{Bmatrix}\dot{\delta}_i\\ \dot{\delta}_j\end{Bmatrix}- \\ &\left[K_f^{(NL)}C_f^{(NL2)}\right]\begin{Bmatrix}\delta_i\\ \delta_j\end{Bmatrix}\begin{Bmatrix}\dot{\delta}_i\\ \dot{\delta}_j\end{Bmatrix}^2-\left[C_f^{(NL3)}\right]\begin{Bmatrix}\dot{\delta}_i\\ \dot{\delta}_j\end{Bmatrix}^3=0 \end{aligned} \tag{50}$$

where subscripts s and f refer to the shell in vacuo and in fluid flow respectively, and $\{\delta\}$ is the degrees of freedom vector for the total nodes.

Further useful expressions are:

$$\left[K^L\right]=\left[K_s\right]+\left[K_I\right]-\left[K_f^L\right] \tag{51}$$

$$[K_I]=\int_0^l\int_0^{2\pi}[N]^T[C_0]^T\begin{bmatrix}\overline{N}_x & 0 & 0\\ 0 & \overline{N}_\theta & 0\\ 0 & 0 & \overline{N}_x+\overline{N}_\theta\end{bmatrix}[C_0]^T[N]^T R d\theta dx \qquad [K_s]=\iint[B]^T[P][B]dA \tag{52}$$

$$\left[K_f^L\right]=\left[A^{-1}\right]^T\left[G_f\right]\left[A^{-1}\right] \tag{53}$$

$$\text{where} \quad \left[G_f\right]=-\gamma p_\infty M\frac{i\lambda_k}{R}\int[R]^T[T]^T[T]\left[R_f\right]dA \tag{54}$$

Let us set:

$$\{\delta\}=[\Phi]\{q\} \tag{55}$$

where $[\Phi]$ represents the square matrix for eigenvectors of the linear system and $\{q\}$ is a time-related vector. Substituting Equation (55) into system (50) and pre-multiplying the whole equation by $[\Phi]^T$, we obtain;

$$\begin{aligned}&\left[M_s^{(L)}\right]^D\{\ddot{q}\}-\left[C_f^{(L)}\right]^D\{\dot{q}\}+\left[K^{(L)}\right]^D\{q\}+[\Phi]^T\left[K^{(NL2)}\right]\left([\Phi]\{q\}\right)^2+[\Phi]^T\left[K^{(NL3)}\right]\left([\Phi]\{q\}\right)^3\\ &-[\Phi]^T\left[K_f^{(NL3)}\right]\left([\Phi]\{q\}\right)^3-[\Phi]^T\left[K_f^{(NL2)}C_f\right]\left([\Phi]\{q\}\right)^2[\Phi]\{\dot{q}\}\\ &-[\Phi]^T\left[K_fC_f^{(NL2)}\right][\Phi]\{q\}\left([\Phi]\{\dot{q}\}\right)^2-[\Phi]^T\left[C_f^{(NL3)}\right]\left([\Phi]\{\dot{q}\}\right)^3=0\end{aligned} \tag{56}$$

where;

$$\left[M_s^{(L)}\right]^D=[\Phi]^T\left[M_s^{(L)}\right][\Phi],\left[C_f^{(L)}\right]^D=[\Phi]^T\left[C_f^{(L)}\right][\Phi],\left[K^{(L)}\right]^D=[\Phi]^T\left[K^{(L)}\right][\Phi] \tag{57}$$

D denotes diagonal, and the matrices quantifying the fluid contribution to the matrix equations of motion are non-symmetric. To facilitate the analysis, therefore, we consider only the symmetric portion of the matrices. This simplifying hypothesis is valid since the original and simplified systems have comparable dynamic behavior.

By neglecting the cross-product in $\left(\left[\Phi\right]\{q\}\right)^2$ …of Equation (56), we obtain;

$$m_{ii}\ddot{q}_i - c_{ii}^{(Lf)}\dot{q}_i + k_{ii}^{(L)}q_i + \sum_{j=1}^{NREDUC}\left(K_{ij}^{(NL2)}q_j^2 + K_{ij}^{(NL3)}q_j^3 - K_{ij}^{(NLf3)}q_j^3 - K_{ii}^{(NLf2)}C_{ij}q_j^2\dot{q}_j - K_{ii}C_{ij}^{(NLf2)}q_j\dot{q}_j^2 - C_{ij}^{(NLf3)}\dot{q}_j^3\right) = 0 \qquad (58)$$

Here we have ‘‘NREDUC’’ simultaneous equations of the form of Equation (58).

At first, we limit ourselves to solving Equation (56) by taking into account only the diagonal terms of the products $\left[\Phi\right]^T\left[K^{(NL2)}\right]\left[\Phi\right]^2$ and $\left[\Phi\right]^T\left[K^{(NL3)}\right]\left[\Phi\right]^3$, therefore Equation (58) is written in this form:

$$m_{ii}\ddot{q}_i - c_{ii}^{(L)}\dot{q}_i + k_{ii}^{(L)}q_i + K_{ii}^{(NL2)}q_i^2 + K_{ii}^{(NL3)}q_i^3 - K_{ii}^{(NLf3)}q_i^3 - K_{ii}^{(NLf2)}C_{ii}q_i^2\dot{q}_i - K_{ii}C_{ii}^{(NLf2)}q_i\dot{q}_i^2 - C_{ii}^{(NLf3)}\dot{q}_i^3 = 0 \qquad (59)$$

Setting

$$q_i(\tau) = A_i f_i(\tau) \quad \text{with} \quad f_i(0) = 1 \text{ and } \quad \dot{f}_i(0) = 0 \qquad (60)$$

Equation (59) becomes, after the A_i simplification and dividing by m_{ii},

$$\begin{aligned} &\ddot{f}_{ii} - \eta_i\,\dot{f}_i + \omega_i^2\,f_i + \lambda_i\left(\frac{A_i}{t}\right)f_i^2 + \zeta_i\left(\frac{A_i^2}{t^2}\right)f_i^3 - \sigma_i\left(\frac{A_i^2}{t^2}\right)f_i^3 \qquad (61)\\ &-\chi_i\left(\frac{A_i^2}{t^2}\right)f_i^2\,\dot{f}_i - \psi_i\left(\frac{A_i^2}{t^2}\right)f_i\,\dot{f}_i^2 - \varphi_i\left(\frac{A_i^2}{t^2}\right)\dot{f}_i^3 = 0 \end{aligned}$$

where;

$$\begin{aligned} &\eta_i = \frac{c_{ii}^{(L)}}{m_{ii}}\ ;\omega_i^2 = \frac{k_{ii}^{(L)}}{m_{ii}}\ ;\lambda_i = \frac{K_{ii}^{(NL2)}}{m_{ii}}t\ ;\zeta_i = \frac{K_{ii}^{(NL3)}}{m_{ii}}t^2\ ;\sigma_i = \frac{K_{ii}^{(NLf3)}}{m_{ii}}t^2\ ;\\ &\chi_i = \frac{K_{ii}^{(NLf2)}C_{ii}}{m_{ii}}t^2\ ;\psi_i = \frac{K_{ii}C_{ii}^{(NLf2)}}{m_{ii}}t^2\ ;\ \varphi_i = \frac{C_{ii}^{(NL3)}}{m_{ii}}t^2 \end{aligned} \qquad (62)$$

and t represents the shell thickness. The square root of coefficient k_{ii}/m_{ii} represents the ith linear vibration frequency of system. The solution $f_i(\tau)$ of these ordinary nonlinear differential equations which satisfies the initial conditions (60) is approximated by a fourth-order Runge-Kutta numerical method. The linear and non-linear natural angular frequencies are evaluated

using a systematic search for the $f_i(\tau)$ roots as a function of time. The ω_{NL}/ω_L ratio is expressed as a function of the non-dimensional ratio A_i/t, where A_i is the vibration amplitude.

4.8 Calculation and Discussion

The influence of nonlinearities associated with the wall of the shell and with supersonic fluid flow on closed cylindrical shell vibrations is expressed by Equation (59). For a given set of shell characteristics, we first present results for convergence of the model and the ratio W_{nl}/W_l of linear and nonlinear frequency is graphically represented with respect to the non-dimensional ratio A_i/t. The shell and flow properties are given by:

$$E = 16\times10^6 \ \ lb/in \quad (11\times10^{10}\ N/m^2)$$
$$\upsilon = 0.35$$
$$h = 0.0040 \ \ in \quad (0.0001015 \ \ m)$$
$$L = 15.4 \ in \quad (0.381 \ \ m)$$
$$R = 8.00 \ \ in \quad (0.203 \ \ m)$$
$$\rho_s = 0.000833 \ \ lb-s^2/in^4 \quad (8900 \ \ kg/m^3)$$
$$M = 3.00$$
$$a_\infty = 8400 \ \ in/s \quad (213 \ \ m/s)$$

4.8.1 Convergence of the method for different modes

A first calculation was focused on determining the required number of finite elements for a precise determination of results, which is very important in finite element analysis. Calculations were made for a closed circular cylindrical shell subjected to supersonic flow for the number of finite elements N = 2, 4, 6, 8...25. The shell is simply supported at both ends. The results for n = 23 and for m = 1, 2 and 3, are shown in Figure 4.2. Convergence of natural frequency is reached for 20 elements.

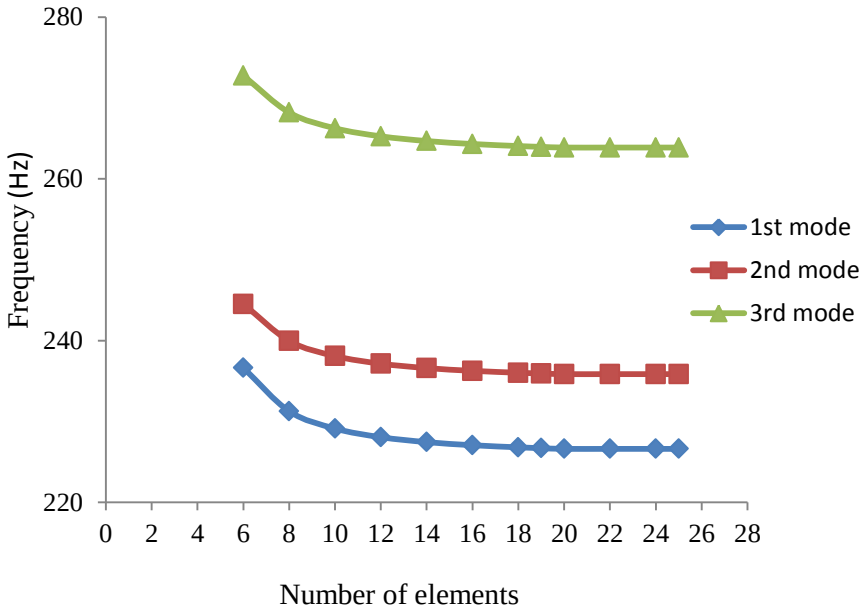

Figure 4.2: Naturel frequency vs Number of elements

4.8.2 Onset of flutter predictions for cylindrical shells subjected to a supersonic flow

Figure 4.3 shows the eigenvalues associated with the longitudinal modes and n = 23 (critical circumferential wave number) versus freestream static pressure p_∞, knowing that the real part of the eigenvalues gives the oscillation frequency and the imaginary part gives the damping for positive values and instability for negative values. Flutter starts where the imaginary parts cross the zero and become negative. It is seen that the shell loses stability at p_{cr} = 0.75 psi, which is called the critical freestream static pressure. This instability is known as coupled-mode flutter.

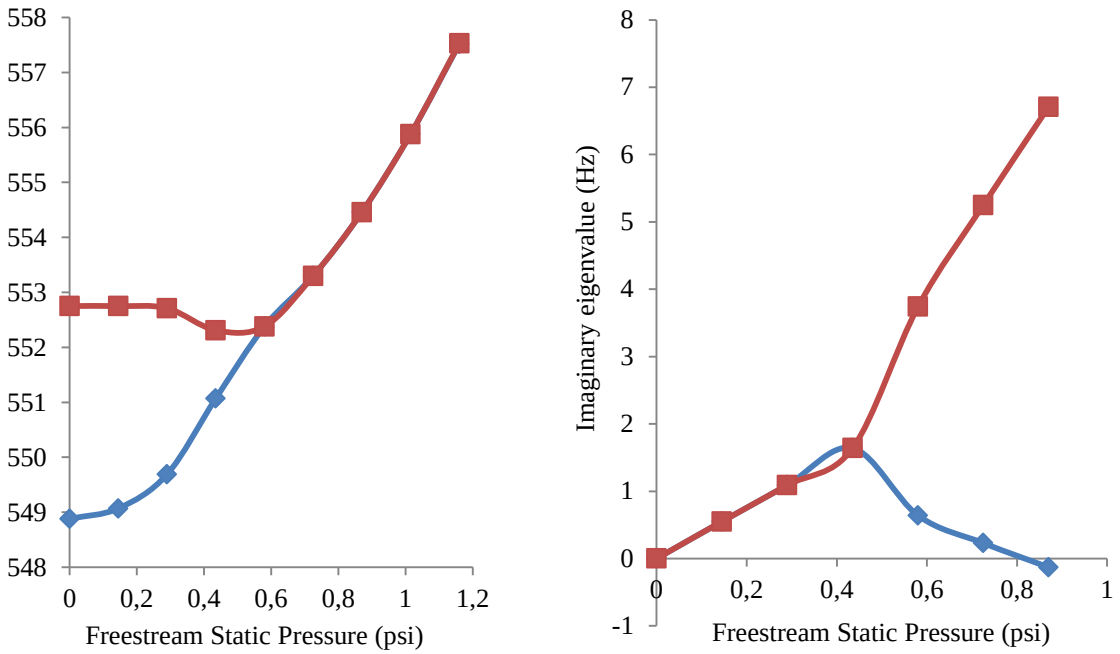

Figure 4.3: a) Real part and b) Imaginary part of eigenvalues of the system vs freestream static pressure p_∞, n = 23, p_m = 0.5 psi, p_x = 0.0 psi.

4.8.3 Validation of model

In Figure 4.4, validation of our model is shown based on the effects of both geometric and supersonic flow nonlinearities which are modeled by a combination of the Koiter-Sanders nonlinear theory for large amplitude vibrations of circular cylindrical shells and third-order of piston theory for describing fluid-structure interaction in supersonic regime. This results show good agreement between the study developed in this paper and Olson research [3]. These results also show that the variation ratio of the nonlinear frequency and linear frequency with respect to increasing of the mean amplitude of the first longitudinal mode (m=1) coincide for first order piston theory (linear) and third order Piston theory (nonlinear). This reveals that the effect of the nonlinearity of supersonic flow is negligible compared to the effect of geometric nonlinearity of circular cylindrical shells subjected to supersonic flow. It is also noted that the nonlinearity is always the softening type, a result which is in quite good agreement with previously published work.

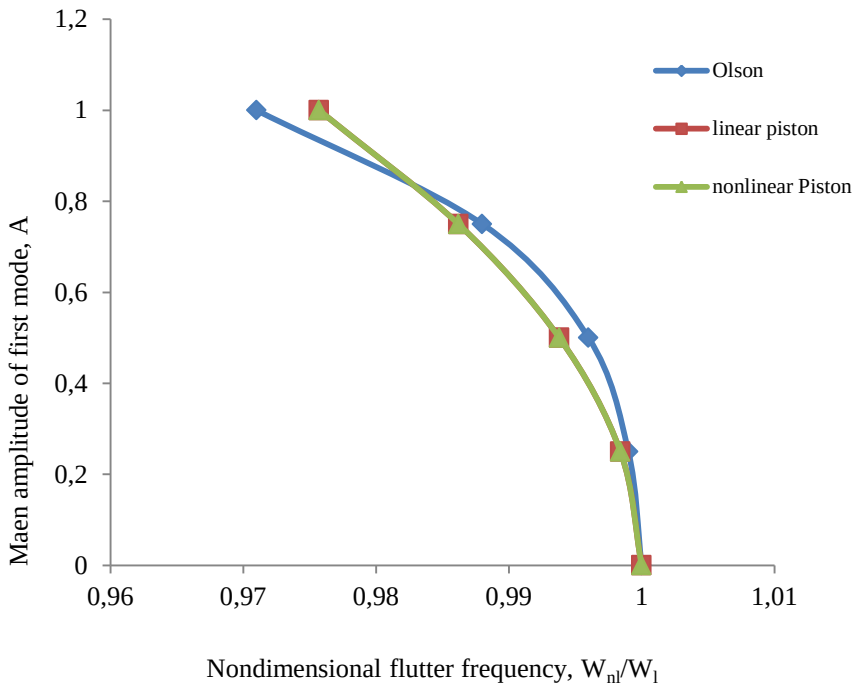

Figure 4.4: Flutter frequency vs amplitude, p_{ec}=0.66 psi.

4.8.4 Effect of circumferential wave mode

Two circumferential wave numbers n = 23 and n = 24 are considered in this section for studying the effect of circumferential mode on the flutter frequency and flutter amplitude for the same physical and mechanical data of the closed circular cylindrical shell described in the previous sections. On one hand, Figure 4.5 shows a more pronounced variation of flutter amplitude versus flutter frequency at n =24. On the other hand, no difference is observed between linear (1^{st}order) and nonlinear (3rd order) modeling for both circumferential modes in this study. The same behavior is observed for other circumferential modes.

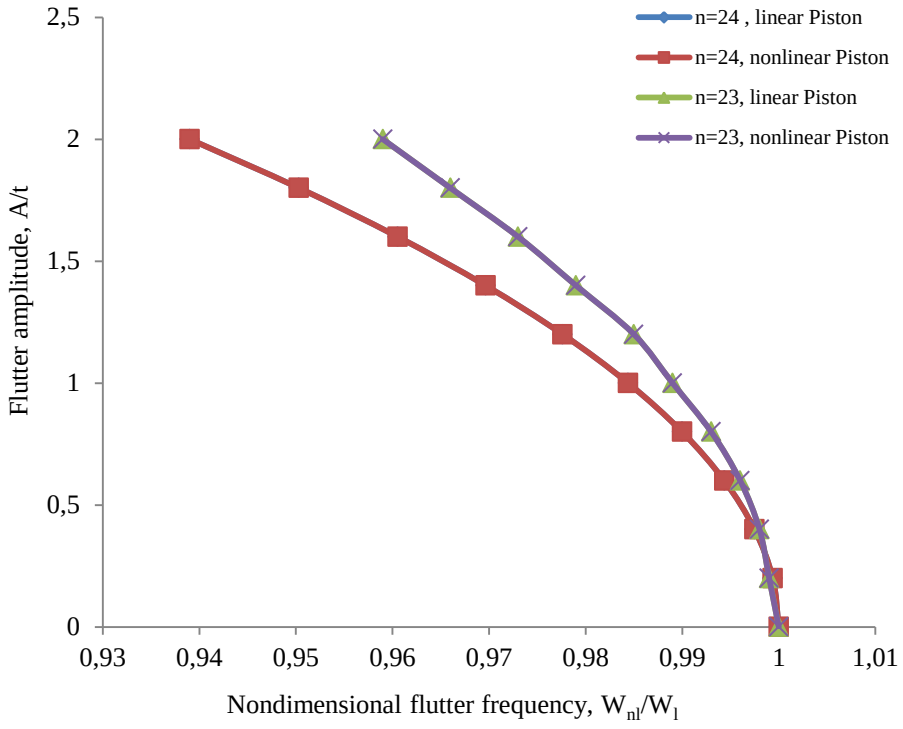

Figure 4.5: Amplitude flutter vs frequency flutter at n=23 and n=24.

4.8.5 Effect of internal pressure

Circular cylindrical shells subjected to internal pressure are analyzed here. The goal is to determine how nonlinear behavior changes the onset of flutter, taking into account the effect of linear or nonlinear supersonic flow. Figure 4.6 shows that curves illustrating the response of two linear and nonlinear approximations of the onset of flutter (characterized by p_{cr} =0.75 psi) coincide. This means that the effect of the nonlinearity of supersonic flow is still negligible at the critical pressure value (at which the flutter begins).

It is also seen that, due to the internal pressure, the frequency ratio does not change as the variation in flutter amplitude increases. However, at a larger value of fluid pressure

p_{ec} = 2.0 psi, variation of flutter amplitude is smaller, and the nonlinear frequency tends toward the value of the linear frequency. This demonstrates the stabilizing effect of internal pressure during the flutter of circular cylindrical shells. The same results were observed in my previous studies on linear flutter in the supersonic regime and also in Amabili [10], and Olson and Fung [3].

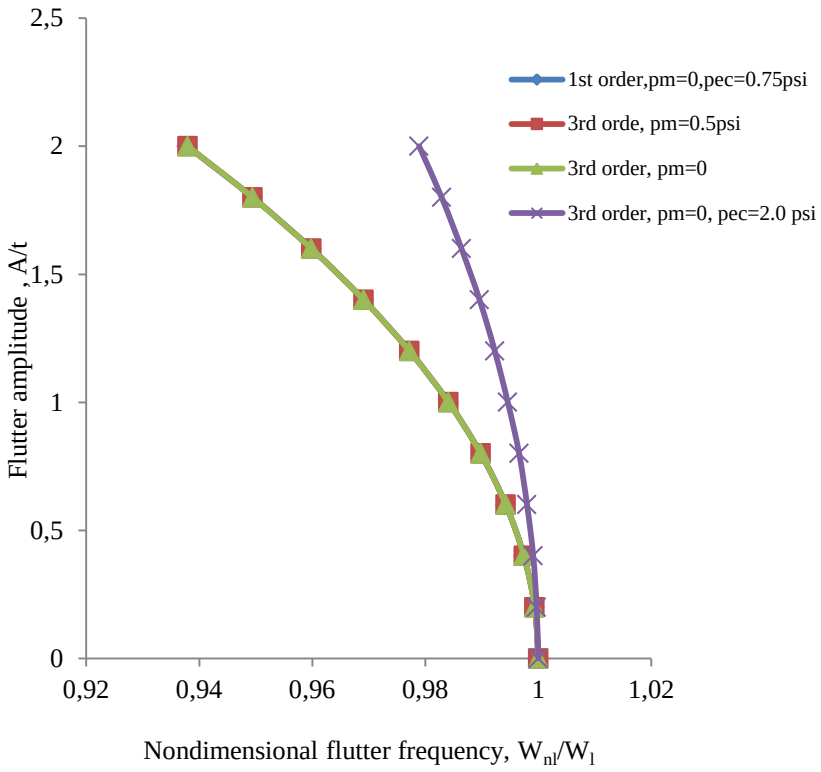

Figure 4.6: Effect of internal stress during the flutter, n=25, p_{ec} =0.75 psi.

4.8.6 Effect of supersonic flow regimes in flutter of circular cylindrical shells

Figure 4.7 shows a comparison between unpressurized circular cylindrical shells under different conditions: empty shells (no fluid flow), linear supersonic flow and nonlinear supersonic flow. A gradual decrease of the flutter frequency as flutter amplitude increases is very evident in the case of nonlinear supersonic flow compared to the other cases. The nonlinear effect of the supersonic flow is almost constant ($W_{nl} / W_l = 1$). This expresses that the fluid plays its usual role of vibration damping for different amplitudes of wall movement for the cylindrical panels.

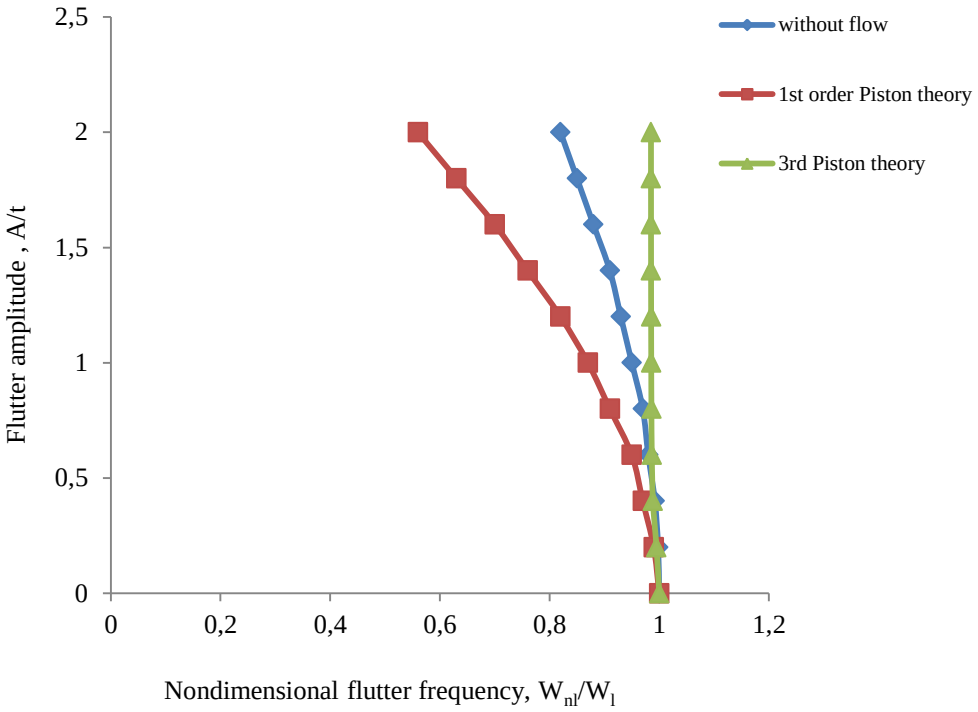

Figure 4.7: Flutter amplitude vs frequency flutter for different L/R.

4.8.7 Nonlinear flutter behavior for different longitudinal modes

Figure 4.8 presents the behavior of nonlinear flutter for circular cylindrical shells subjected to supersonic fluid flow at different longitudinal wave numbers m = 2, ..., 7. It is seen that each curve corresponds to two longitudinal modes because the flutter phenomenon is created by the coalescence of the real parts of successive complex frequencies of two modes. This was seen in Figure 4.3a, and can be predicted by linear analysis of cylindrical shells in the supersonic regime. It can also be predicted by nonlinear analysis using the model presented in this paper. Furthermore the nonlinearities are of the softening type, and the trend of the curves is the same for all three cases of flutter considered in this study, including a slightly pronounced deviation for the case m = 2,3 at high values of vibration amplitude.

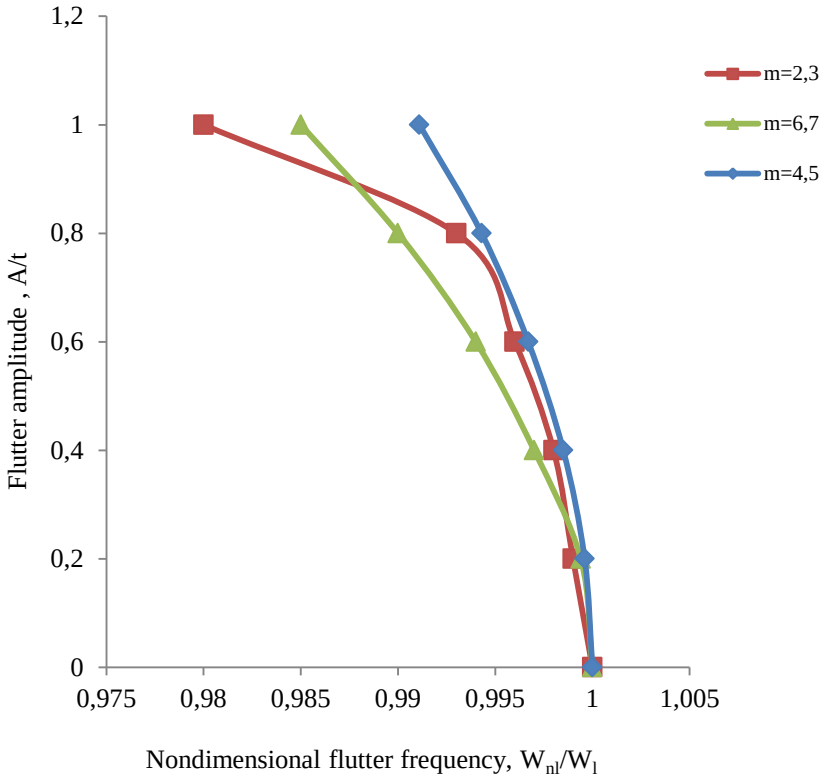

Figure 4.8: Flutter amplitude vs flutter frequency for different longitudinal modes

4.9 Conclusion

The method developed in this paper demonstrates the influence of geometric nonlinearity associated with the wall of the shell and nonlinear supersonic fluid flow (3^{rd} order of Piston theory) on the frequency and amplitude of flutter of closed cylindrical shells subjected to external supersonic flow. It is a hybrid method based on Sanders-Koiter nonlinear thin shell theory, and nonlinear aerodynamic piston theory and the finite element method. The method combines the advantages of finite element analysis which deals with complex shells, and the precision of a formulation in which the use of displacement functions derived from shell and fluid theories allows fast and efficient convergence of the calculations. The results show better agreement with experimental and theoretical results published in the literature. The numerical results provide the nonlinear behaviors for circular cylindrical shells subjected to supersonic flow beyond the onset of flutter. These results cannot be determined by linear analysis. Several parameters that are dependent on geometry and fluid flow are studied, and in all cases nonlinearity of the softening type is dominant. Mild flutter instability and the stabilizing effect of internal pressure has been

demonstrated. The effect of geometric nonlinearities associated with the walls is non-negligible and should be taken into account when calculating the nonlinear flutter of a shell-fluid flow system. In contrast the nonlinearity of supersonic fluid flow can be neglected when the amplitude of vibration is larger than the thickness of the shell.

4.10 Appendix

Sander's linear equations for thin cylindrical shells in terms of axial, tangential and circumferential displacements are

$$L_1(U,V,W,P_{ij}) = P_{11}\frac{\partial^2 U}{\partial x^2} + \frac{P_{12}}{R}\frac{\partial^2 U}{\partial x^2}\left(\frac{\partial^2 V}{\partial x\partial\theta} + \frac{\partial W}{\partial x}\right) - P_{14}\frac{\partial^3 W}{\partial x^3} + \frac{P_{15}}{R^2}\left(\frac{\partial^3 W}{\partial x\partial\theta^2} + \frac{\partial^2 V}{\partial x\partial\theta}\right) + \left(\frac{P_{33}}{R} - \frac{P_{63}}{2R^2}\right)\left(\frac{\partial^2 V}{\partial x\partial\theta} + \frac{1}{R}\frac{\partial^2 U}{\partial\theta^2}\right)$$
$$+\left(\frac{P_{36}}{R^2} - \frac{P_{66}}{2R^3}\right)\left(-2\frac{\partial^3 W}{\partial x\partial\theta^2} + \frac{3}{2}\frac{\partial^2 V}{\partial x\partial\theta} - \frac{1}{2R}\frac{\partial^2 U}{\partial\theta^2}\right)$$

$$L_2(U,V,W,P_{ij}) = \left(\frac{P_{21}}{R} - \frac{P_{51}}{R^2}\right)\frac{\partial^2 U}{\partial x\partial\theta} + \frac{1}{R}\left(\frac{P_{22}}{R} + \frac{P_{52}}{R^2}\right)\left(\frac{\partial^2 V}{\partial\theta^2} + \frac{\partial W}{\partial\theta}\right) - \left(\frac{P_{24}}{R} + \frac{P_{54}}{R^2}\right)\frac{\partial^3 W}{\partial x^2\partial\theta} + \frac{1}{R^2}\left(\frac{P_{25}}{R} + \frac{P_{55}}{R^2}\right)\left(-\frac{\partial^3 W}{\partial\theta^3} + \frac{\partial^2 V}{\partial\theta^2}\right)$$
$$+\left(P_{33} + \frac{3P_{63}}{2R}\right)\left(\frac{\partial^2 V}{\partial x^2} + \frac{\partial^2 U}{R\partial x\partial\theta}\right) + \frac{1}{R}\left(P_{36} + \frac{3P_{66}}{2R}\right)\left(-2\frac{\partial^3 W}{\partial x^2\partial\theta} + \frac{3}{2}\frac{\partial^2 V}{\partial x^2} - \frac{1}{2R}\frac{\partial^2 U}{\partial x\partial\theta}\right)$$

$$L_3(U,V,W,P_{ij}) = P_{41}\frac{\partial^3 U}{\partial x^3} + \frac{P_{42}}{R}\left(\frac{\partial^3 V}{\partial x^2\partial\theta} + \frac{\partial^2 W}{\partial x^2}\right) - P_{44}\frac{\partial^4 W}{\partial x^4} + \frac{P_{45}}{R^2}\left(-\frac{\partial^4 W}{\partial x^2\partial\theta^2} + \frac{\partial^3 V}{\partial x^2\partial\theta}\right) + \frac{2P_{63}}{R}\left(\frac{1}{R}\frac{\partial^3 U}{\partial x\partial\theta^2} + \frac{\partial^3 V}{\partial x^2\partial\theta}\right)$$
$$+\frac{2P_{66}}{R^2}\left(-2\frac{\partial^4 W}{\partial x^2\partial\theta^2} + \frac{3}{2}\frac{\partial^3 V}{\partial x^2\partial\theta} - \frac{1}{2R}\frac{\partial^3 U}{\partial x\partial\theta^2}\right) + \frac{P_{51}}{R^2}\frac{\partial^3 U}{\partial x\partial\theta^2} + \frac{P_{52}}{R^3}\left(\frac{\partial^3 V}{\partial\theta^3} + \frac{\partial^2 W}{\partial\theta^2}\right) + \frac{P_{55}}{R^4}\left(-\frac{\partial^4 W}{\partial\theta^4} + \frac{\partial^3 V}{\partial\theta^3}\right)$$
$$-\frac{P_{21}}{R}\frac{\partial U}{\partial x} - \frac{P_{54}}{R^2}\frac{\partial^4 W}{\partial x^2\partial\theta^2} + \frac{P_{22}}{R^2}\left(\frac{\partial V}{\partial\theta} + W\right) + \frac{P_{24}}{R^2}\frac{\partial^2 W}{\partial\theta^2} - \frac{P_{25}}{R^3}\left(-\frac{\partial^2 W}{\partial\theta^2} + \frac{\partial V}{\partial\theta}\right)$$

- **The coefficients of characteristic Equation (5) are given by**

$$f_8 = \left(f_9/r^2\right)\left(p_{11}p_{44} - p_{14}^2\right)$$

$$f_6 = \left(n^2/r^2\right)\left[f_9\left(f_1p_{44} + 2p_{11}p_{45} + 4p_{11}p_{66} - 2f_5rp_{14}\right) + f_7\left(p_{11}p_{44} - p_{14}^2\right) - r^2f_{11}^2p_{11} - f_3^2p_{44} + 2rf_3f_{11}p_{14}\right] +$$
$$\left(2/r\right)f_9\left(p_{11}p_{24} - p_{14}p_{12}\right)$$

$$f_4 = \left(n^4/r^2\right)\left[f_1f_7\,p_{44} + f_9p_{11}p_{55} + \left(2p_{45} + 4p_{66}\right)\left(f_1f_9 + f_7p_{11} - f_3^2\right) + \left(p_{25} + \left(1/r\right)p_{55}\right).\left(2f_3p_{14} - 2f_{11}p_{11}r\right) +\right.$$
$$f_{11}r^2\left(2f_3f_5 - f_1f_{11}\right) - rf_5\left(2f_7p_{14} + rf_5f_9\right)\left.\right] + \left(n^2/r\right).\left[2\left(p_{25} + rp_{22}\right)\left(\left(f_3/r\right)p_{14} - f_{11}p_{11}\right) -\right.$$
$$\left.2p_{12}\left(f_5f_9r + f_7p_{14} - f_3f_{11}r\right) - 2p_{24}\left(f_3^2 - f_1f_9 - f_7p_{11}\right) + 2f_9p_{11}p_{25}\right] + f_9\left(p_{11}p_{22} - p_{12}^2\right)$$

$$f_2 = \left(n^6/r^2\right)f_7\left(2p_{45} + 4p_{66}\right) + p_{55}\left(f_1f_9 + f_7p_{11} - f_3^2\right) - r^2f_5^2f_7 +$$
$$\left(p_{25} + \left(1/r\right)p_{55}\right).\left(-2rf_1f_{11} + 2rf_3f_5 - p_{11}p_{25} - \left(1/r\right)p_{11}p_{55}\right)\left.\right] +$$
$$\left(n^4/r\right)\left[2f_1f_7p_{24} + 2p_{25}\left(f_1f_9 + f_7\,p_{11} - f_3^2\right) - 2p_{12}\left(rf_5f_7 - f_3p_{25} - \left(f_3/r\right)p_{55}\right)\right] -$$
$$2\left(p_{25} + rp_{22}\right)\left(f_1f_{11} + \left(1/r\right)p_{11}p_{25} + \left(1/r^2\right)p_{11}p_{55} - f_3f_5\right)\left.\right] +$$
$$n^2\left[p_{22}\left(f_1f_9 + f_7p_{11} - f_3^2\right) - \left(1/r\right)\left(p_{25} + rp_{22}\right)\left(\left(1/r\right)p_{11}p_{25} + p_{11}p_{22} - 2f_3p_{12}\right) - f_7p_{12}^2\right]$$

$$f_0 = n^4f_1f_7\left[p_{22} + \left(2/r\right)n^2p_{25} + \left(n^4/r^2\right)p_{55}\right] - n^2f_1\left[\left(n^3/r\right)\left(p_{25} + \left(1/r\right)p_{55}\right) + \left(n/r\right)\left(p_{25} + rp_{22}\right)\right]^2$$

where;

$$f_1 = p_{33} - p_{36}/R + p_{66}/4R^2$$
$$f_3 = p_{12} + p_{33} + (p_{15} + p_{36})/R - 3p_{66}/4R^2$$
$$f_5 = (p_{15} + 2p_{36} - p_{66}/R)/R$$
$$f_7 = p_{22} + p_{55}/R^2 + 2p_{25}/R$$
$$f_9 = p_{33} + 3p_{36}/R + 9p_{66}/4R^2$$
$$f_{11} = (2p_{36} + p_{24} + 3p_{66}/R + p_{54}/R)/R$$

- **Matrices $[T]_{3\times3}$, $[R]_{3\times8}$, and $[A]_{8\times8}$ are defined as**

$$[T] = \begin{bmatrix} \cos(n\theta) & 0 & 0 \\ 0 & \cos(n\theta) & 0 \\ 0 & 0 & \sin(n\theta) \end{bmatrix}$$

$$R(1,i) = \alpha_i e^{\lambda_i x/R} \quad , \quad R(2,i) = e^{\lambda_i x/R} \quad , \quad R(3,i) = \beta_i e^{\lambda_i x/R} \qquad i = 1,2,...,8$$

$$A(1,i) = \alpha_i, \quad A(2,i) = 1, \quad A(3,i) = \frac{\lambda_i}{R}, \quad A(4,i) = \beta_i, \quad A(5,i) = \alpha_i e^{\lambda_i l/R}$$

$$A(6,i) = e^{\lambda_i l/R}, \quad A(7,i) = \frac{\lambda_i}{R} e^{\lambda_i l/R}, \quad A(8,i) = \beta_i e^{\lambda_i l/R} \qquad i = 1,2,...8$$

- **Matrix $\left[R_f\right]_{3\times8}$ is defined by;**

$$[R_f] = \begin{bmatrix} 0 & ... & 0 \\ e^{i(\lambda_1 x/R)} & ... & e^{i(\lambda_8 x/R)} \\ 0 & ... & 0 \end{bmatrix}$$

- **Expressions $\{\varepsilon_L\}$ and $\{\varepsilon_{NL}\}$ for cylindrical shells are given by:**

$$\{\varepsilon_L\} = \begin{Bmatrix} \dfrac{\partial U}{\partial x} \\ \dfrac{1}{R}\left(\dfrac{\partial V}{\partial \theta} + W\right) \\ \dfrac{\partial V}{\partial x} + \dfrac{1}{R}\dfrac{\partial U}{\partial \theta} \\ -\dfrac{\partial^2 W}{\partial x^2} \\ -\dfrac{1}{R^2}\left(\dfrac{\partial^2 W}{\partial \theta^2} - \dfrac{\partial V}{\partial \theta}\right) \\ -\dfrac{2}{R}\dfrac{\partial^2 W}{\partial x \partial \theta} + \dfrac{3}{2R}\dfrac{\partial V}{\partial x} - \dfrac{1}{2R^2}\dfrac{\partial U}{\partial \theta} \end{Bmatrix}$$

and

$$\{\varepsilon_{NL}\} = \begin{Bmatrix} \dfrac{1}{2}\left(\dfrac{\partial W}{\partial x}\right)^2 + \dfrac{1}{8}\left(\dfrac{\partial V}{\partial x} - \dfrac{1}{R}\dfrac{\partial U}{\partial \theta}\right)^2 \\ \dfrac{1}{2R^2}\left(V - \dfrac{\partial W}{\partial \theta}\right)^2 + \dfrac{1}{8}\left(\dfrac{\partial V}{\partial x} - \dfrac{1}{R}\dfrac{\partial U}{\partial \theta}\right)^2 \\ \dfrac{1}{2R}\left(\dfrac{\partial W}{\partial x}\dfrac{\partial W}{\partial \theta} - V\dfrac{\partial W}{\partial x}\right) \\ 0 \\ 0 \\ 0 \end{Bmatrix}$$

- **Matrices $\left[B_{pq}\right]$ and $\left[C_{pq}\right]$**

$$B_{pq} = b_{pq} e^{\left(\lambda_p + \lambda_q\right)x/R}$$

$$C_{pq} = c_{pq} e^{\left(\lambda_p + \lambda_q\right)x/R}$$

where;

$$b_{pq} = \frac{1}{2R^2}\left[\frac{1}{4}a_{pq}^{(1)} + b_{pq}^{(1)}\right]\sin^2(n\theta)$$

$$c_{pq} = -\frac{1}{4R^2}\left[c_{pq}^{(1)} + c_{pq}^{(2)}\right]\sin(n\theta)\cos(n\theta)$$

with;

$$a_{pq}^{(1)} = \left(\beta_p\lambda_p + n\alpha_p\right)\left(\beta_q\lambda_q + n\alpha_q\right)$$

$$b_{pq}^{(1)} = \left(n + \beta_p\right)\left(n + \beta_q\right) \qquad p,q = 1,...,8$$

$$c_{pq}^{(1)} = n\left(\lambda_p + \lambda_q\right)$$

- **Matrices for Equations (46-47)**

$$\left[D_f\right] = -\frac{\gamma p_\infty}{a_\infty}\int [R]^T [T]^T [T]\left[R_f\right] dA$$

$$\left[G_f\right] = -\gamma p_\infty M \frac{i\lambda_k}{R}\int [R]^T [T]^T [T]\left[R_f\right] dA$$

$$\left[G_{fnl3}\right] = -\frac{(\gamma+1)}{12}M^3\frac{i\lambda_k^3}{R^3}\int [R]^T [T]^T \left([T]\left[R_f\right]\right)^3 dA$$

$$\left[H1_{fnl3}\right] = -\frac{(\gamma+1)}{4}\frac{M^3}{a_\infty}\frac{i\lambda_k^3}{R^3}\int [R]^T [T]^T \left([T]\left[R_f\right]\right)^3 dA$$

$$\left[H2_{fnl3}\right] = \frac{(\gamma+1)}{4}\frac{M}{a_\infty^2}\frac{i\lambda_k}{R}\int [R]^T [T]^T \left([T]\left[R_f\right]\right)^3 dA$$

$$\left[D_{fnl3}\right] = \frac{(\gamma+1)}{12}\frac{1}{a_\infty^3}\int [R]^T [T]^T \left([T]\left[R_f\right]\right)^3 dA$$

4.11 References

[1] H. Ashley and G. Zartarian, Piston Theory-New Aerodynamic Tool for Aeroelastician, Journal of the Aeronautical Sciences, 23 (1956),1109-1118.

[2] W. Horn et al, Recent Contributions to Experiments on Cylindrical Shell Panel Flutter, AIAA Journal, 12 (1974), 1481-1490.

[3] M.D. Olson and Y.C. Fung, Supersonic Flutter of Circular Cylindrical Shells Subjected to Internal Pressure and Axial Compression, AIAA Journal, 4(1966), 858-864.

[4] M.D. Olson and Y.C. Fung, Comparing Theory and Experiment for Supersonic Flutter of Circular Cylindrical Shells, AIAA Journal, 5(1967), 1849-1856.

[5] D.A. Evensen and M.D. Olson, Nonlinear Flutter of a Circular Cylindrical Shell in Supersonic Flow, NASA TND - 4265, 1967.

[6] E.H. Dowell, Flutter of Infinitely Long Plates and Shells, Part I, AIAA Journal, 4(1966), 1510-1518.

[7] E.H. Dowell, Aeroelasticity of Plates and Shells, Noordhoff International Publishing, Leyden, 1975.

[8] G.W. Barr and R.O. Stearman, Aeroelastic Stability Characteristics of Cylindrical Shells Considering Imperfections and Edge Constraint, AIAA Journal, 7(1969), 912-919.

[9] G.W, Barr and R.O. Stearman, Influence of a Supersonic Flow-field on the Elastic Stability of Cylindrical Shells, AIAA Journal, 8(1970), 993-1000.

[10] M. Amabili, and F. Pellicano, Nonlinear Supersonic Flutter of Circular Cylindrical Shells, AIAA Journal, 39(2001), 564-573.

[11] M. Amabili and F. Pellicano, Multimode Approach to Nonlinear Supersonic Flutter of Imperfect Circular Cylindrical Shells, Journal of Applied Mechanics, Transactions ASME, 69(1976), 423-435.

[12] A.A. Lakis and M.P. Paidoussis, Dynamic Analysis of Axially Non-Uniform Thin Cylindrical Shells, Journal of Mechanical Engineering Science, 14(1972), 49-71.

[13] M. N. Bismarck-Nasr, Finite Element Method Applied to the Supersonic Flutter of Circular Cylindrical Shells, International Journal for Numerical Methods in Engineering, 10(1976), 423-435.

[14] D.A. Evensen, Nonlinear flexural vibrations of thin-walled circular cylinders, NASA Technical Note, Langley Research Center, NASA- TN D-4090,1967.

[15] D.A. Evensen, Nonlinear vibrations of an infinitely long cylindrical shell. American Institute of Aeronautics and Astronautics Journal. 6(1968), 1401-1403.

[16] F. Sabri and A.A. Lakis, Finite Element Method Applied to Supersonic Flutter of Circular Cylindrical Shells, AIAA Journal, 48 (2010), 73-81.

[17] A. Selmane, and A.A. lakis, Non-Linear Dynamic Analysis of orthotropic Open Cylindrical Shells Subjected to a Flowing Fluid, Journal of Sound and Vibration, 202(1997), 67-93.

[18] A.A. Lakis and A. Laveau, Non-Linear Dynamic Analysis of Anisotropic Cylindrical Shells containing a Flowing Fluid, International Journal of Solids and Structures, 28(1991),1079-1094.

[19] J.L. Sanders, An Improved First-Approximation Theory for Thin Shell, NASA R-24, 1959.

[20] M.H. Toorani, and A.A. Lakis, General equations of Anisotropic Plates and Shells Including Transverse shear Deformations, Rotary Inertia and Initial Curvature Effects, Journal of Sound and Vibration, 237(2000), 561-651.

[21] H.R. Radwan and J. Genin, Non-linear vibrations of thin cylinders. Journal of Applied Mechanics, 43(1976), 370-372.

[22] H. Krumhaar, The Accuracy of Linear Piston Theory When Applied to Cylindrical Shells, AIAA Journal, 1(1963), 1448-1449.

[23] R. Rougui and F. Moussaoui and R. Benamar, Geometrically non- linear free and forced vibrations of simply supported circular cylindrical shells: A semi-analytical approach, International Journal of Non-linear Mechanics. 42(2007), 1102-1115.

[24] M. Amabili, F. Pellicano, M.P. Paidoussis, Non-linear vibrations of simply supported circular cylindrical shells coupled to quiescent fluid, J. Fluids Struct. 12(1998), 883-918

[25] M. Ganapathi and T.K. Varadan, Large amplitude vibrations of circular cylindrical shells, Journal of sound and vibration, 192(1996), 1-14.

CHAPITRE 5 : DISCUSSION GÉNÉRALE

Cette étude représente l'analyse de flottement et la vibration non linéaire des coques cylindriques circulaires vides et soumises à un écoulement supersonique. L'étude des différentes coques analysées dans la littérature, aux nombres d'onde circonférentielle faible ou élevée, nous a permis de savoir exactement le comportement complet de ces structures et de clarifier le désaccord entre les chercheurs dans ce domaine d'aéroélasticité. Plusieurs paramètres ont été analysés à différentes conditions limites et modes axiaux. Dans tous les cas, on a conclu que le degré de la non-linéarité dépend de l'épaisseur, du rayon, de la longueur et des modes circonférentiels et axiaux considérés. Le type de non-linéarité (Softening ou Hardening) est déterminé par un paramètre nommé le rapport d'aspect.

Dans le cas où les coques cylindriques circulaires sont soumises à l'écoulement supersonique, le modèle développé se consacre à la combinaison de la non-linéarité des coques (grandes amplitudes de vibration des parois) analysées largement dans le premier article et l'écoulement supersonique externe sous sa forme linéaire. Les résultats numériques fournissent le comportement linéaire de ce type de panneaux pour différentes conditions limites et prédisent le début du flottement et aussi le comportement non linéaire au-delà du début du flottement caractéristique qui ne peut être prélevé par une analyse linéaire. Plusieurs paramètres dépendant de la géométrie de la coque et de l'écoulement du fluide sont analysés. La non-linéarité la plus dominante est de type softening et une faible instabilité de flottement est détectée, l'instabilité dynamique est produite sous forme de flottement de modes couplés. La pression interne entraine une stabilisation des coques et retarde le flottement en comparaison des cas de coques soumises à aucune pression interne. Dans la dernière partie, on a essayé d'analyser l'effet des non-linéarités de la structure et de l'écoulement supersonique du fluide afin de présenter une étude complète et profonde non linéaire de ce type de structure. Le même type de non-linéarité, effet stabilisant de la pression interne, et l'instabilité de flottement légère ont été remarqués sur tous les résultats trouvés, aucune différence dans la variation des paramètres testés n'a été observée avec la considération de la non-linéarité de l'écoulement supersonique du fluide exprimée par l'équation de la théorie de Piston de troisième ordre. Ceci nous permet de conclure que l'effet d'une telle non-linéarité n'a aucune influence sur les calculs et on peut la négliger devant la non-linéarité géométrique (grande amplitude de vibration), ce qui est en bon accord avec les moindres publications dans ce sujet.

CONCLUSIONS ET RECOMMANDATIONS

Cette recherche nous permet de développer un code efficace basé sur les éléments finis hybrides traitant l'analyse linéaire et non linéaire d'aéroélasticité des coques cylindriques. Ce logiciel peut être utilisé efficacement pour le design avancé de structures aérospatiales et la prédiction du comportement des différents stages de flottement des coques soumises à l'écoulement supersonique pour différentes conditions limites complexes et différents paramètres de la géométrie et de fluide.

Ce logiciel développé permet :

- la modélisation linéaire et non linéaire des coques cylindriques par la méthode des éléments finis hybride;
- la modélisation de l'effet de contraintes créé par la pression interne et la compression axiale;
- la modélisation de la pression aérodynamique externe supersonique linéaire et non linéaire donnée par la théorie de Piston

et est capable :

- de faire l'analyse dynamique linéaire et non linéaire des coques vides et soumises à l'écoulement supersonique;
- de prédire le début du flottement et le comportement après le début de flottement;
- effet des contraintes initiales sur la stabilité linéaire et non linéaire aéroélastique.

Ce logiciel, résultat d'un travail analytique-numérique performant, précis et moins coûteux au sens du temps de calcul, est considéré plus efficace que des programmes couplés en MEF et CFD.

Les futurs travaux seront focalisés sur l'étude de l'effet de la température, qui est sûrement un paramètre très important au niveau du design des structures aérospatiales et qui entre dans la discipline d'ingénierie d'aérothermoélasticité. Les structures d'aujourd'hui font face à la température élevée qui peut influencer la stabilité de ces structures à travers la distribution de la

température dans l'épaisseur des parois et aussi sur l'étude des différentes géométries des panneaux utilisés dans l'industrie aérospatiale : les coniques, les plaques courbées,…afin d'aboutir à la modélisation et l'analyse aérothermoélastique d'un véhicule complet, soit dans le domaine fréquentiel ou temporel, soumise à un écoulement supersonique.

BIBLIOGRAPHIE

Bishlinghoff, R. L., Ashley, H. and Halfman R. L. (1955). *Aeroelasticity*, Addison-Wesley publishing Company, Inc.

Dowell, E. H. (1975). *Aeroelasticity of Plates and Shells*, *Noordhoff*, International Publishing, Lyden, The Netherlands.

Librescu, L. (1975). Elastostatics and Kinetics of anisotropic and Heterogeneous Shell-type Structures. Noordhoff International Publishing, Lyden.

Fung, Y. C. (1960). A summary of the theories and Experiments on Panel Flutter. AFSOR TN 60-224. Guggenheim Aeronautical Lab. California Institute of technology, Pasadena, CA.

Johns, D. J. (1961). The Present Status of Panel Flutter. AGARD Report 484. Advisory Group for Aeronautic Research and Development

Johns, D. J. (1965). A Survey on Panel Flutter, Advisory report 1, Advisory Group for Aeronautic& Research and Development

Dowell, E. H. (1970). Panel Flutter: A Review of the Aeroelastic stability of Plates and Shells. AIAA Journal, 8(3), 385-399.

Mei, C., Abdel-Motagaly, K., and Chen, R. (1999). Review of Nonlinear panel flutter at Supersonic and Hypersonic speeds. Applied Mechanics reviews, 52(10), 321-332.

Gray, C. E. And Mei, C. (1993). large Amplitude Finite element Flutter analysis of Composites panels in hypersonic Flow. AIAA Journal, 31(6), 1090-1099.

McIntosh, S. C., Reed, R. E. and Rodden, W. P. (1981). Experimental and theoretical study of nonlinear flutter. Journal of Aircraft, 18, 1057-1063.

Reed, W. H. (1967). Review of Propeller-Rotor Whirl Flutter, NASA TR R-264.

Bismarck-Naser. (1978).Finite element method applied to the supersonic flutter of circular cylindrical shells. International journal for numerical method in engineering, 10(4), 423-435.

Bismarck-Naser. (1977). Finite element method applied to the flutter of two parallel elastically coupled flat plates. International journal for numerical method in engineering, 11(7), 1977,1188-1193.

Zhou R C, Xue D Y, Mei C. (1994). A finite element time domain-modal formulation for nonlinear flutter of composite panels. AIAA J, 32(10), 2044–2052.

Hedgepeth, J. and Widmayer, E. (1963). Dynamic and Aeroelastic Problems of Lifting Re-Entry Bodies. Aerospace Engineering, pp.148-153.

Dugundji, J. (1958). Effect of Quasi-Steady Air Forces on Incompressible Bending–Torsion Flutter, Journal of the Aeronautical Sciences, 25(2), 119–121

Cunningham, H.J., Batina, J .T., and Yang, H.T. (1991). Aeroelastic Analysis of Wings Using the Euler Equations with a Deforming Mesh. Journal of Aircraft, 28, 778-788.

Timoshenko, S., Woinowsky-Krieger, S. (1959).Theory of Plates and Shells, New York: McGraw-Hill.

Eisley, J. G. (1956). The flutter of a Two- Dimensional Buckled Plate with Clamped edges in a supersonic flow, OSR-TN-56-296.

Houboult, J. C. (1958). A Study of several Aerothermoelastic problems of Aircraft structures in High-Speed Flight. Ph.D Thesis. The Swiss Federal Institute of Technology. Zurich: Eidenossischen technischen Hochschule.

Fung, Y.C. (1958). On Two-Dimensional panel flutter. Journal of the Aeronautical sciences, 25, 145-160.

Bolotin, V. V. (1963). Nonconservative Problems of the Theory of Elastic Stability. New York: McMillan Co, pp. 199-312.

Chu, H.N. And Herrmann, G. (1956). Influence of Large Amplitudes on Free Flexural Vibration of rectangular elastic Plates. Journal of applied Mechanics, 23, 532-540.

Ashley, H. And Zaratarian, G. (1965). Piston Theory - A New Aerodynamic Tool for the Aeroelastician. Journal of Aeronautical science, 23(10), 1109-1118.

Dowell, E. H., and Voss, H. M. (1965). Experimental and theoretical panel flutter Studies in mach Number range 1.0 to 5.0. AIAA Journal, 3(12), 2292-2304.

Dowell, E, H. (1966). Nonlinear Oscillation of a fluttering Plate I. AIAA Journal, 4(7), 1267-1275.

Dowell, E. H. (1967). Nonlinear Oscillation of a Fluttering Plate II. AIAA Journal, 5(10), 1856-1862.

Fralich, R. W. (1965). Postbuckling effects on the flutter of simply supported rectangular panels at Supersonic speed. NASA TN D-1615.

Ventres, C.S. (1970). Nonlinear flutter of Clamped Plates. Ph.D, Dissertation. Princeton University.

Librescu, L. (1965). Aeroelastic stability of orthotropic heterogeneous thin Plates in the Vicinity of flutter critical Boundary. Journal de Mecanique, 4(1), 51-76.

Kobayashi, S. (1962). Flutter of Simply Supported Rectangular Panels in a Supersonic Flow-Two- Dimensional Panel Flutter, I- Simply supported panel, II- Clamped Panel. Transaction of Japan Society of Aeronautical and Space Sciences, 5, 79-118.

Yuen, S. W., and Lau, S. L. (1991). Effect of in- Plane load on nonlinear Panel Flutter by Incremental Harmonic Balance Method. AIAA Journal, 29(9), 1472-1479.

Eslami, H. (1978). Nonlinear flutter and Forced Oscillations of Rectangular Symmetric Cross-Ply and Orthotropic Panels using harmonic balance and Perturbation Methods, Ph.D. Dissertation. Old Dominion University.

Morino, L. (1969). A Perturbation Method for Treating Nonlinear Panel Flutter problems. AIAA Journal, 7(3), 405-410.

Morino, L, and Kuo, C. C. (1971). Detailed extensions of perturbation Methods for Nonlinear Panel flutter. ASRL TR 164-2, M.I.T. Cambridge.

Kuo, C. C., Morino, L., and Dugundji, L. (1972). Perturbation and harmonic balance for Treating Nonlinear Panel Flutter. AIAA Journal, 10(11), 1479-1484.

Olson, M. D. (1967). Finite element Approach to Panel Flutter. AIAA Journal, 5(12), 226-227.

Appa, K. and Somashekar, B. R. (1969). Application of Matrix Displacement Methods in the study of Panel Flutter. AIAA Journal, 7(1), 50-53.

Sander, G., Bon, C. and Geradin, M. (1973). Finite element Analysis of supersonic Panel Flutter, International Journal for Numerical Methods in Engineering, 7(3), 379-394.

Yang, t. Y. and Sung, S H. (1977). Finite element in three- Dimensional supersonic Unsteady Potential Flow. AIAA Journal, 15(12), 1677-1683.

Mei, C. (1977). Finite Element in Approach for Nonlinear Panel Flutter. AIAA Journal, 15(8), 1107-1110.

Mei, C. and Rogers, J. L. (1976). Application of Nastran to large Deflexion supersonic Flutter of Panel. NASA TM X-3428, 67-98.

Rao, K. S. and Rao, G. V. (1980). Supersonic Flutter of Panels Elastically Restrained Against Rotation. Computer and Structures, 11, 197-201.

Mei, C. and Weidman, D. J. (1977). Nonlinear Panel Flutter – A finite element Approach, Computational Method for Fluid-Structure Interaction Problems, T.Belytsechke and T.L.Geers, ASME, New York, 26, 944-951.

Mei, C. and Wang, H. C. (1982). Finite Element Analysis of Large Amplitude Supersonic Flutter of Panels. Proceedings of international conference on Finite Element Methods. Shanghai, China, Gordon and Breach Science Publishers, Inc. 944-251.

Han, A. D. and Yang, T. Y. (1983). Nonlinear Panel Flutter using High Order Triangular Finite Element. AIAA Journal, 21(10), 1453-1461.

Green, P. D. and Killey, A. (1997), Time Domaine Dynamic Finite Element Modelling in Acoustic Fatigue Design, in Proc., 6th International Conference on Structural Dynamic, ISVR, 11, 1007-1026.

Robinson, J. H. (1990). Finite Element Formulation and Numerical Simulation of the large deflection Random Vibration of Laminated composite Plates. MS Thesis. Old Dominion University.

Chandiramani, N. K. and Plaut, R. H, and Librescu, L. L. (1995). Nonperiodic Flutter of a Buckled Shear deformable Composite Panel in a high-supersonic Flow. International Journal of Non-Linear Mechanics. 30(2), 149-167.